



NTNU – Trondheim
Norwegian University of
Science and Technology

Combined Effects of Perfluorooctane sulfonic acid (PFOS) and Carbon dioxide (CO₂) on oxidative stress responses in the gill of Atlantic cod (*Gadus morhua*)

Ivan Munyemera

Biotechnology (5 year)

Submission date: May 2014

Supervisor: Augustine Arukwe, IBI

Norwegian University of Science and Technology
Department of Biology

Combined Effects of Perfluorooctane sulfonic acid (PFOS) and Carbon dioxide (CO₂) on oxidative stress responses in the gill of Atlantic cod (*Gadus morhua*)

Ivan Munyemera

AKNOWLEDGEMENTS

This master thesis was carried out at the Norwegian University of Science and Technology (NTNU) at the department of biology 2013/2014. It is part of the project entitled “Climate change, emerging pollutants and reproduction dysfunction in fish: Linking quantifiable measures of climate change with pollution and biological consequences”- and it is funded by the Norwegian Research Council.

Firstly, I would like to thank my supervisor, Professor Augustine Arukwe for his help, patience and guidance throughout this project. His “open door” and frank feedback policy has kept me on track through this project. I would also like to thank my co-supervisor, Marianne Opsahl Olufsen for teaching me the necessary methods in the laboratory. I also extend a token of thanks to the senior engineer at Arukwe-Lab, Randi Røsbak for her patience with me and for teaching me some laboratory methods. I would like to thank Professor Francesco Regoli’s group at University of Ancona, Italy, for performing the enzyme activity assays presented in this thesis.

My appreciation also goes to my fellow student, Håkon Langberg for being a firm shoulder to lean on. Lastly, special thanks go to my lovely girlfriend, Camilla and my son, Erik for their love, support and understanding throughout this period. Appreciation also goes to my parents and siblings.

ABSTRACT

Increasing levels of anthropogenic CO₂ in atmosphere and aquatic environment have been regarded as significant force behind global climate changes. The aquatic environment is also a heavy recipient for pollutants embedded in among others municipal and industrial wastewater. Despite this, very little effort has currently been put in investigating the potential toxic effects of aquatic pollutants on aquatic organisms (fish) in a continuously changing aquatic environment driven by global climate change. In the present study, juvenile Atlantic cod (*gadus morhua*) were exposed to Perfluorooctane sulfonate (PFOS; 0, 100 and 200 µg/L) for 1 hour per day in a total of 5 days, and thereafter transferred to water tanks containing; 0%, 0.3% and 0.9% CO₂ for 3, 6 and 9 days. Oxidative stress responses in gills upon exposure to PFOS and elevated CO₂ levels, singly or in combination were evaluated. Real-time RT PCR was in gene expression analysis of; peroxisome proliferator-activated receptor β (*ppar-β*), *Acyl-CoA oxidase (acox)* and selected antioxidant genes. Enzyme activity levels of selected antioxidant enzymes and the total content of reduced glutathione and malondialdehyde were measured spectrophotometrically. Generally, single exposure to PFOS or elevated CO₂ levels had a weak effect on the transcription of peroxisomal β-oxidation related genes (*ppar-β* and *acox*). However, an increase in mRNA levels of these genes was observed upon combined exposure to both stressors (though not significantly). An apparently CO₂ dependent increase in mRNA levels for *gpx1* and *gpx3* at day 6, and SOD activity at day 9 was observed in fish exposed to a combination of high PFOS (200 µg/L) and CO₂-this indicated presence of high cytosolic ROS levels. An apparent time-dependent decrease in activity of all antioxidant enzymes was generally observed in most of the exposure groups at day 9. Overall, the alterations in gene expression and/or enzyme activities of both peroxisomal β-oxidation related genes and antioxidant defenses suggest that both PFOS and elevated CO₂ might induce oxidative stress, however, combined exposure to these stressors apparently enhances this effect. The apparent interactive effect between PFOS and elevated CO₂ observed in this study suggests that the toxicity of aquatic pollutants could be modified under environmental hypercapnia-and this could adversely affect aquatic organisms in numerous ways.

ABBREVIATIONS

ANOVA	Analysis of variance
ATP	Adenosine triphosphate
cDNA	Complementary deoxyribonucleic acid
CDNB	1-Chloro-2,4-dinitrobenzene
CoA	Coenzyme A
Ct	Cycle threshold
CYP19	Cytochrome P450 19
ddH ₂ O	Double-distilled water
dH ₂ O	Distilled water
DEPC	Diethylpyrocarbonate
Dil.	Dilution
DNA	Deoxyribonucleic acid
DTNB	Ellman's Reagent, 5,5'-Dithiobis-(2-Nitrobenzoic Acid)
DTT	Dithiothreitol
EDTA	Ethylenediaminetetraacetic acid
FA	Fatty acid
GP _x	Glutathione peroxidase
GR	Glutathione reductase
GSH	Glutathione
GSSG	Oxidized Glutathione
GST	Glutathione S-transferase
H ₂ O ₂	Hydrogen peroxide
KH ₂ PO ₄	Potassium phosphate (K-phosphate)
MDA	Malondialdehyde
mM	millimoles L ⁻¹
mRNA	Messenger ribonucleic acid
MS-222	Tricaine methanesulphonate
MQ-water	Milli-Q water
NaCl	Sodium Chloride
NADPH	Nicotinamide adenine dinucleotide phosphate

nm	Nano meters
$\cdot\text{O}_2$	Superoxide anion
OD	Optical density
$\cdot\text{OH}$	Hydroxyl radical
PCR	Polymerase chain reaction
PFAA	Perfluoroalkyl acid
PFC	Perfluorinated compounds
PFOS	Perfluorooctane sulfonate
PMSF	Phenylmethylsulfonyl fluoride
POP	Persistent organic pollutant
POSF	Perfluorooctanesulfonyl fluoride
PPAR	Peroxisome proliferator-activated receptor
PPRE	Peroxisome proliferator response element
R^2	Correlation coefficient
RNA	Ribonucleic acid
RNase	RNA nuclease
ROS	Reactive oxygen species
rRNA	Ribosomal ribonucleic acid
RT-PCR	Reverse transcriptase polymerase chain reaction
RXR	Retinoid X receptor
SOD	Superoxide dismutase
TCA	Tricarboxylic acid cycle (citric acid cycle)
T_m	Melting temperature
U	Unit
Vol.	Volume
w/v ratio	Weight/volume ratio

CONTENTS

1.0 INTRODUCTION	2
1.1 BACKGROUND.....	2
1.2 PERFLUORINATED COMPOUNDS (PFCS)	3
1.2.1 ENVIRONMENTAL DISTRIBUTION, BIOACCUMULATION AND BIOMAGNIFICATION.	5
1.2.2 TOXICOLOGICAL EFFECTS OF PFCS	6
1.3 PEROXISOME PROLIFERATOR-ACTIVATED RECEPTORS (PPARS)	7
1.4 FATTY ACIDS AND ENERGY METABOLISM	9
1.5 INTRACELLULAR OXIDATIVE STRESS	10
1.5.1 XENOBIOTIC-ENHANCEMENT OF ROS/RNS GENERATION.....	12
1.5.3 LIPID PEROXIDATION	14
1.6 ANTIOXIDANT DEFENSE SYSTEMS	15
1.6.1 ANTIOXIDANT ENZYMES	15
1.6.1 a Superoxide dismutase (SOD).....	15
1.6.1 b Catalase (Cat).....	15
1.6.1 c. Glutathione peroxidase-GPx.....	16
1.6.1 d. Glutathione-s-transferases (GST).....	16
1.6.2 NON-ENZYMATIC ANTIOXIDANTS	16
1.6.2 a. Glutathione (GSH).....	17
1.7 GLOBAL CLIMATE CHANGE	18
1.7.1 ANTHROPOGENIC CARBON AND OCEAN ACIDIFICATION.....	18
1.7.2 Hypercapnic challenges to aquatic organisms	19
1.8 ATLANTIC COD (<i>GADUS MORHUA</i>) AS A MODEL ORGANISM	20
1.8 A. FISH GILLS	20
1.9 AIMS OF THIS STUDY	21
2.0 MATERIALS AND METHODS	22
2.1 CHEMICALS AND REAGENTS.....	22
2.2 EXPERIMENTAL DESIGN	22
2.2.1 Model organism.....	22
2.2.2 PFOS exposure	23
2.2.3 CO ₂ exposure	23
2.2.4 Tissue collection and storage.....	24
2.3 GENE EXPRESSION ANALYSIS	25
2.3.1 RNA ISOLATION, AND QUALITY ASSESSMENT	25
2.3.2 Primer testing	28
2.3.3 cDNA synthesis	30
2.3.4 Real-Time Polymerase Chain Reaction (qPCR).....	32

2.3.5 Normalization of gene expression data.....	34
2.4 ENZYME ASSAYS	34
2.4.1 PREPARATION OF CYTOSOLIC FRACTION	34
2.4.2 DETERMINATION OF ENZYME ACTIVITY	34
2.4.3 DETERMINATION OF REDUCED GLUTATHIONE	38
2.4.4 DETERMINATION OF MALONDIALDEHYDE	39
2.5 STATISTICAL ANALYSIS.....	40
3.0 RESULTS.....	42
3.1 VALIDATION OF HYPERCAPNIA IN EXPERIMENTAL TANKS	42
3.2 BODY PFOS BURDEN.....	44
3.3 EFFECTS ON PHYSIOLOGICAL PARAMETERS	45
3.4 EFFECTS ON LIPID METABOLISM.....	46
3.4.1 PPAR-B.....	46
3.4.2 EFFECTS ON ACYL-CoA OXIDASE (<i>acox1</i>)	47
3.4.3 EFFECTS ON GENES INVOLVED IN MEMBRANE PHOSPHOLIPID HOMEOSTASIS	48
3.5 EFFECTS ON OXIDATIVE STRESS RESPONSES	50
3.5.1 SUPEROXIDE DISMUTASE (SOD).....	50
3.5.2 CATALASE (CAT).....	52
3.5.3 GLUTATHIONE PEROXIDASE (GPx)	54
3.5.6 GLUTATHIONE REDUCTASE (GR)	56
3.5.7 GLUTATHIONE S-TRANSFERASE (GST)	58
3.5.7 NON-ENZYMATIC ANTIOXIDANTS.....	59
REDUCED GLUTATHIONE (GSH).....	59
3.6 EFFECTS ON LIPID PEROXIDATION.....	60
3.6.1 MALONDIALDEHYDE (MDA).....	60
4.1 ANALYTICAL METHODS.....	62
4.1.1 EVALUATION OF REAL-TIME PCR PROCEDURES	62
4.1.2 NORMALIZATION OF qPCR DATA	64
4.1.3 MALONDIALDEHYDE AND THIOBARBITURIC ACID (TBARS)	64
4.1.4 EVALUATION OF STATISTICAL ANALYSIS.....	65
4.2 EXPERIMENTAL SETUP.....	66
4.2.1 PFOS EXPOSURE, UPTAKE AND BIOCONCENTRATION.....	66
4.2.2 DISSOLVED CO ₂ LEVELS IN EXPERIMENTAL TANKS	67
4.3 EFFECTS ON PEROXISOMAL-B OXIDATION	67
4.4 EFFECTS ON ANTIOXIDANT SYSTEMS	70
4.4.1 EFFECTS ON GLUTATHIONE BASED ANTIOXIDANT RESPONSES	75
4.5 EFFECTS ON MEMBRANE PHOSPHOLIPID HOMEOSTASIS	77
5.0 CONCLUSION	78

6 FUTURE PERSPECTIVES.....	78
REFERENCES	79
APPENDIX	89

1.0 INTRODUCTION

1.1 BACKGROUND.

The rapid growth of human population and the general propensity for humans to desire to lead modern (comfortable) lifestyles could explain the boom in technological advancements and changes in utilization of nature in the past couple of centuries (United Nations Statistics Division, 2010). New chemicals have been invented to be used in production of pharmaceuticals, household, industrial and warfare products, these include perfluorinated compounds (PFCs), brominated organic compounds, and nanoparticles. In addition to increased consumption of fossil fuels, land utilization patterns have also changed as more forests, wetlands and other compartments of nature are cleared for agriculture, mining and other human activities. Although, it has been known that periodically or permanently elevated CO₂ partial pressure (hypercapnia) in the atmosphere and different ecosystems is a natural phenomenon (Langenbuch and Pörtner, 2003), the role of human activities in global climate change is hard to ignore, due to increased human-driven emissions of greenhouse gases (CO₂, CH₄, and nitrous oxide). The increasing levels of anthropogenic CO₂ in atmosphere and ocean surface (Kleypas et al., 2006), coupled with the anticipated disposal of industrial CO₂ in deep sea (Rajnauth, 2013), imply that elevated CO₂ levels may be a serious stress factor in aquatic environments, and may potentially impact aquatic organisms in several ways.

The aquatic environment has also been reported to be a recipient of a variety of persistent organic pollutants (POPs) including PFCs that are embedded in municipal, hospital, industrial- and sewage treatment-plant effluent deposits (Renner, 2001, Paul et al., 2008). This means that aquatic organisms are exposed to a cock-tail of aquatic pollutants, but this is happening in a continuously changing environment-due to global climate change. Climate change not only affects contaminant exposure, it may also act in concert with the contaminants and subsequently alter their toxicities toward aquatic organisms (Doris et al., 2007). However, the scientific community has mainly focused on the interactive effects of combined exposure to aquatic pollutants and elevated ambient temperatures (as an aspect of global climate change) (Noyes et al., 2009, Doris et al., 2007), and surprisingly little attention has so far been given to the interactive role of environmental hypercapnia despite the huge amounts of anthropogenic CO₂ (over 30%) that have been absorbed by the aquatic

environment (Sabine, 2004, Khatiwala, 2013). There is a wide knowledge gap about the combined effects of PFCs and elevated CO₂ on aquatic organisms-hence highlighting the importance of this study.

1.2 PERFLUORINATED COMPOUNDS (PFCs)

Perfluorinated organic compounds are generally defined as organic compounds containing a fully fluorinated carbon backbone and a charged group at the opposite end (Renner, 2001). There are several species of PFCs, but considerable attention has recently been given to perfluorinated alkyl acids (PFAAs) such as perfluorooctane sulfonate (PFOS), perfluorooctanoic acid (PFOA) and their precursor compounds especially perfluoroalkyl sulfonamide alcohols and fluorotelomere alcohols (Lehmler, 2005, Zhang et al., 2009, Paul et al., 2008, Bijland et al., 2011).

PFCs have been produced and used for over 50 years. Between 1970s and 1989 there was a reported 5-fold increase in the production of PFCs particularly-perfluorooctane sulfonyl fluoride (POSF), a trend that remained constant throughout the 1990s (Paul et al., 2008, Renner, 2001). POSF was primarily produced by the 3-M company since 1949 and was mainly used as a starting material for the production of PFOS and other PFOS precursors such as N-methyl perfluorooctane sulfonamide (N-Me PFOSA) and N-ethyl perfluorooctane sulfonamide (N-Et PFOSA). However, 3M company discontinued the production of these chemicals in 2002 (Renner, 2001, Wåggbø et al., 2012). Despite this, considerable attention is being given to PFOS and its derivatives due to their ubiquitous distribution in the environment, as well as bioaccumulation in wildlife and humans (Kannan and John, 2001, Harada et al., 2007).

Sulfonyl-based fluorinated compounds including PFOS and its derivatives such as perfluorooctane sulfonyl-fluoride (POSF) and N-alkyl perfluorooctanesulfonamide alcohols can be synthesized by several methods including electrochemical fluorination (ECF), and telomerization (Renner, 2001, Lehmler, 2005). In the ECF method a hydrocarbon compound is dissolved in liquid hydrogenfluorine (HF) and an electric current is then passed through the medium resulting into total fluorination of the hydrocarbon compound, this reaction yields a complex of fluorinated compounds among others around 25% POSF- a starting material for

synthesis of PFOS and PFOS derivatives (Lehmler, 2005, Pabon and Corpart, 2002, Renner, 2001).

PFOS is an anion containing a fully fluorinated carbon tail with an adjacent sulfonic acid group (Figure 1). The fluorine-carbon bond in the alkyl tail is characterized as being thermodynamically very strong (Pabon and Corpart, 2002). The sulfonic acid group of PFOS confers a limited degree of activity with different charged substances including positively charged amino acid residues of polypeptides, indeed, it has been reported that PFOS is a blood-borne toxicant because of its ability to bind to plasma proteins-a mechanism through which its systemic distribution is achieved (Zhang et al., 2009). The above mentioned structural features of PFOS confer this toxicant with unique physicochemical properties such as; oil and water repellency, chemical inertness and thermal stability (hence the subsequent resistance to both environmental and biological degradation), low surface energy (surface activity), and very low vapor pressure (very poor volatility) (Martin et al., 2002, Lehmler, 2005, Houde et al., 2006, Mitchell et al., 2009, Pabon and Corpart, 2002, Paul et al., 2008, Hoff et al., 2003b, Renner, 2001).

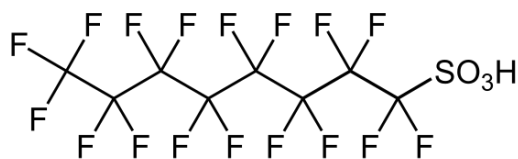


Figure 1: An image of the chemical structure of PFOS, showing the fluorinated carbon-tail and the adjacent sulfonic acid group.

Because of these properties, PFOS and its derivatives have extensively been used in the production of several industrial and household products such as coating treatments for carpets, fanishers and apparel, refrigerants, lubricants, adhesives, aqueous firefighting foams (AFFFs), and cosmetics (Abbott et al., 2009, Bijland et al., 2011, Kannan and John, 2001, Harada et al., 2007, Hoff et al., 2003b, Jeon et al., 2010, Lehmler, 2005, Houde et al., 2006).

1.2.1 Environmental distribution, bioaccumulation and biomagnification.

In wild-life species, PFOS is the most predominant of all PFCs species (Houde et al., 2006). This chemical is globally distributed, and has reportedly been found in highly populated urbanized areas in North America, Southeast Asia, and Europe as well as scarcely populated remote locations such as the Arctic, Antarctic and several pacific regions (Kannan and John, 2001, Kannan et al., 2002, Renner, 2001). It is unlikely that the global distribution of PFOS is attributed to water or air based transport due to its poor water-solubility and low volatility. Alternatively, it was hypothesized that particle-bound PFOS and volatile PFOS precursor compounds such as *N-ethyl* and *N-methyl* perfluorooctane sulfonamide (*N-Et-PFOSA* and *N-Me-PFOSA*) could explain the global distribution of PFOS via long-range atmospheric transport (Renner, 2001). This hypothesis was reinforced by the findings made by Martin et al, (2002) where *N-Et-PFOSA* and *N-Me-PFOSA* were detected in air samples collected in Southern Ontario, Canada. Consumption of PFOS-containing products and release of wastewater sludge containing PFOS precursors could be considered as an acceptable route for direct emission of PFOS into the aquatic environment (Paul et al., 2008). This indicates that long-range oceanic transport could be a possible dispersion route for PFOS from industrialized urban regions to remote rural locations (Wania, 2007).

The occurrence PFOS and its precursors in marine mammals, humans, fish and birds has been reported by several studies (Kannan and John, 2001, Kelly et al., 2009). Given the above mentioned physicochemical properties of PFOS, it has been found not only to be persistent in the environment, but also bioaccumulative in both aquatic and terrestrial food webs (Zhang et al., 2009). PFOS and its precursors enter aquatic-breathing organisms (fish) through the gills and/or intestines (ingested food), upon entry they bind to plasma proteins such as albumin and are distributed around the body. Once in the body, PFOS is poorly excreted since the compound has been reported to be subjected to extensive enterohepatic recirculation (Johnson et al., 1984), and this could partially explain its bioaccumulative properties. The body burden of Perfluoroalkyl sulfonamide alcohols such as *N-et-PFOSA* and *N-Me-PFOSA* could be a stable source for PFOS in different organisms. Laboratory studies have shown that PFOS could be generated *in vitro* via *N-Et-PFOSA* → *PFOSA* → PFOS degradation pathway (Kelly et al., 2009). Due to their neutral and lipophilic nature, these PFOS precursors can accumulate in fat tissue and therefore bioaccumulate in different organisms. Indeed, these compounds have been detected in several organisms such as fish, marine birds, marine mammals and

others (Tommy et al., 2004a), and may therefore act as stable internal sources of PFOS in both humans and wildlife. It can be hypothesized that biomagnification of PFOS in both aquatic and terrestrial food webs could to a given degree be attributed to the presence of these compounds (Kelly et al., 2009, Tommy et al., 2004a, Tommy et al., 2004b). High levels of PFOS have been found in several animals in the wildlife for example, 1100 ng/g ww and 3673 µg/L have been reported from liver tissue of tilapia *oreochromis niloticus* and mullet bile *mugil icilis*, respectively (Olivero-Verbel et al., 2006, Tseng et al., 2006). Biomagnification of PFOS has been shown to preferably occur in top predators such as polar bear, marine birds, marine mammals and other fish-eating species (OECD, 2002, Haukås et al., 2007).

1.2.2 TOXICOLOGICAL EFFECTS OF PFCs

There is growing evidence indicating the biological activity and subsequent toxicity of PFOS (Krøvel et al., 2008, Wågbø et al., 2012, Bjorka et al., 2011). Numerous *in vivo* and *in vitro* studies have demonstrated effects of PFOS on gap junction intercellular communication (Hu et al., 2002b), membrane fluidity and mitochondrial membrane potential (Hu et al., 2002a), peroxisome proliferation (in rodents and primates) (Issemann and Green, 1990a, Takacs and Abbott, 2007a, Starkov and Wallace, 2002), oxidative stress responses-and lipid metabolism (Jurgen et al., 1997, Arukwe and Mortensen, 2011). A number of studies have also indicated the potential developmental and reproductive toxicity, carcinogenicity, neurotoxicity, and immuno-toxicity of PFOS in mammals and low vertebrates such as fish (Zhang et al., 2009).

In vivo and *in vitro* studies have demonstrated that peroxisomal β -oxidation of fatty acids and activation of peroxisome proliferator-activated receptors (PPARs), and downstream responses, as one of the major metabolic pathways affected by PFOS. The activities of some of the enzymes involved in this pathway (especially ACOX) have been shown to be substantially increase upon exposure to PFOS (Hu et al., 2005, Oakes et al., 2005), consequently leading to generation hydrogen peroxide and intracellular oxidative stress. Indeed, several studies have demonstrated an increase in oxidative stress responses such as changes in expression of antioxidant genes, and lipid peroxidation following exposure to PFOS (Arukwe and Mortensen, 2011, Lorentzen, 2013, Hu et al., 2005) . Given its global distribution, persistence and bioaccumulative properties, PFOS will remain a contaminant of major concern to aquatic ecosystems for many years to come (Oakes et al., 2005, Wågbø et al., 2012).

1.3 PEROXISOME PROLIFERATOR-ACTIVATED RECEPTORS (PPARS)

Peroxisome proliferator-activated receptors (PPARs) are ligand-activated transcriptional factors that belong to the steroid/thyroid/retinoid nuclear hormone receptor superfamily (Desvergne and Wahli, 1999). So far, three related isoforms of PPARs (α , β and γ) have been identified in vertebrates (*Xenopus*, mouse and rats) (Issemann and Green, 1990b, Dreyer et al., 1992). PPARs are widely recognized for playing a central role in the transcriptional regulation a variety of genes involved in several pathways of lipid metabolism such as fatty acid transport, cellular uptake, intracellular activation, catabolism (via both beta and omega oxidation) and storage (Desvergne and Wahli, 1999).

In vitro and *in vivo* studies have shown that PPAR α , PPAR β and PPAR γ are expressed in a tissue specific manner and have distinct functions (Jurgen et al., 1997). PPAR α is generally expressed in tissues with high rate of lipid catabolism such as liver, kidney, and heart across several species, since this receptor has been reported to play a central role in the transcriptional modulation of genes encoding enzymes involved in lipid catabolic pathways such as peroxisomal and mitochondrial β -oxidation of fatty acids (Mandard et al., 2004).

PPAR γ is highly expressed in adipose tissue and is reported to promote lipid storage by upregulating genes involved in fatty acid and triglyceride biosynthesis, and adipogenesis (Vidal-Puig et al., 1996, Hotta et al., 1998, Mizukami and Taniguchi, 1997). PPAR β is ubiquitously expressed, with varying levels in different organs, but its physiological functions are yet to be fully clarified (Escher et al., 2001). However, research indicates that PPAR β is ubiquitously expressed and is involved in global regulation of lipid metabolism and adaptive thermogenesis (Vidal-Puig et al., 1996). PPAR β has also been suggested to play an important role in the control of cell differentiation, proliferation, and survival (Tanaka et al., 2003, Tachibana et al., 2005, Michalik et al., 2006).

PPARs bind different types of ligands both natural and synthetic. Some of the *bona fide* natural PPAR ligands include unsaturated fatty acids and their metabolic derivatives such as eicosanoids (Barry et al., 1997). It has been observed that poly-unsaturated fatty acids (PUFA) such as decosahexaenoic acid (DHA), eicosapentaenoic acid (EPA), and linoleic acid

are more potent PPAR agonists than mono-unsaturated fatty acids (Jurgen et al., 1997, Desvergne and Wahli, 1999). Several synthetic PPAR ligands have also been identified, these include several hypolipidemic agents such as fibrates and insulin sensitizers such as Thiazolidinediones (TZDs) (Desvergne and Wahli, 1999). Several *in vivo* and *in vitro* studies have shown that PFOS and other perfluoroalkyl acids (PFAAs) species can activate PPARs in different organisms (James A. Bjork, 2009). This could partially be explained by the fact that PFOS is a structural analogue to some of the endogenous ligands of PPARs such as fatty acids. Indeed, PFOS and other PFAAs have sometimes been referred to as “perfluorinated fatty acids” (Hu et al., 2005).

Ligand-bound PPAR forms heterodimers with *9-cis* retinoic acid receptor (RXR/ NR2B) after which the PPAR:RXR receptor complex binds to PPAR response elements (PPREs) of the direct repeat 1 (DR1) type found in the promoter region of target genes, followed by transcription the genes (Jonathan et al., 1992, Issemann and Green, 1990b, Mangelsdorf et al., 1995).

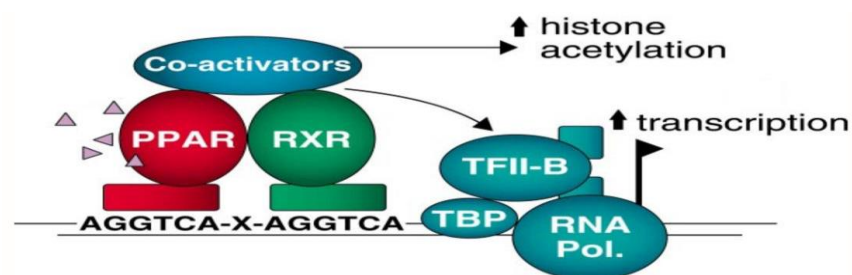


Figure 2. PPARs bind DNA only after forming heterodimers with *9-cis*-retinoic acid receptor (PPAR:RXR). After ligand binding, the PPAR undergoes conformational changes which allows the recruitment of cofactors such as cAMP response element-binding protein (CBP), which in turn promote the recruitment of chromatin modifying elements such as coactivator acetyl-transferase complex, hence the subsequent assembly of components of specific and basal transcription initiation complex.

According to Lehmann et al (1997), PPARs appear to promiscuously interact with a variety of compounds, and can potentially be activated by different endogenous and exogenous compounds.

1.4 FATTY ACIDS AND ENERGY METABOLISM

In addition to serving as metabolic regulators, and important components of cell membranes- fatty acids (FAs) also serve as essential metabolic fuels (Forman et al., 1997). The breakdown of FAs occurs via peroxisomal or mitochondrial β -oxidation pathway depending on the physical characteristics of the fatty acids. Catabolism of short, medium, and long straight-FAs occurs in the mitochondria, while that of very long straight and branched-FAs occur in peroxisomes (Clark, 2010, Kim and Miura, 2004). The differences in FA substrates of the two β -oxidation systems is attributed to the differences in the substrate preferences of the enzymes that catalyze the rate limiting steps in these systems. Acyl-CoA dehydrogenase (ACOD) catalyzes the first and rate-limiting step of mitochondrial β -oxidation and prefers short-and medium straight fatty acids as substrates. On the contrary, short-chain fatty acids are poor substrates of acyl-CoA oxidase (ACOX), the enzyme which catalyzes the first and rate-limiting step of peroxisomal β -oxidation which preferentially binds to long straight and branched fatty acids. Complete β -oxidation of fatty acids does not occur via peroxisomal β -oxidation, therefore this system of fatty acid β -oxidation- is widely considered as a chain shortening step, whose output (short-chain acyl-CoA) are subjected to further (complete) oxidation in mitochondria (Crockett and Sidell, 1993, Osmundsen et al., 1991).

Both ACOD and ACOX are flavoproteins, containing a Flavin adenine dinucleotide (FAD) prosthetic group that serves as an electron-accepting group during the oxidation of activated fatty acids (fatty acyl-CoA). Peroxisomal β -oxidation is not directly coupled to the electron transport chain and oxidative phosphorylation. In the first of the four steps of β -oxidation hydrogen peroxide (H_2O_2) is produced (Nelson and Cox, 2008). This is because after oxidation of fatty acyl-CoA, the FAD subunit of ACOX is re-oxidized by transfer of electrons to molecular oxygen (Mannaerts and Van Veldhoven, 1993). In contrast, mitochondrial β -oxidation is directly coupled to the electron transport chain and therefore substantially contributes to energy production via oxidative phosphorylation (Gulick et al., 1994). This is because FAD subunit of ACOD is re-oxidized by transfer of electrons to the electron transfer flavoprotein (ETF) which delivers the electrons to the electron transfer chain apparatus in the

inner mitochondrial membrane, followed by ATP synthesis via oxidative phosphorylation (Mannaerts and Van Veldhoven, 1993, Gulick et al., 1994). However, any perturbation of this electron transfer process can lead to generation of superoxide anions ($\cdot\text{O}_2^-$) (Gary, 1990). It can be argued that hydrogen peroxide and superoxide anions are by-products of peroxisomal or mitochondrial β -oxidation of fatty acids. H_2O_2 and $\cdot\text{O}_2^-$ are reactive oxygen species (ROS) which can react and damage several biological macromolecules such as proteins, nucleic acids and lipids and hence inducing different oxidative stress responses (Doull and Casarett, 2013).

1.5 INTRACELLULAR OXIDATIVE STRESS

Free radicals are defined as chemical species capable of independent existence and containing one or more unpaired electrons in their outer orbital (Barry and Susanna, 1993, Doull and Casarett, 2013, Gutteridge, 1995). There are several types of free radicals including oxygen-centered radicals (reactive oxygen species), sulfur-centered radicals (thyl), carbon-centered radicals (trichloromethyl) and reactive nitrogen species (RNS). In this thesis the emphasis will be put on reactive species of oxygen and nitrogen since they are not only reported to be mediators of toxicity of various environmental pollutants, they have also been reported to play several biologically important roles such as signal transduction (redox signaling) (Forman et al., 2004), and immune-defense responses (respiratory burst by macrophages) (Doull and Casarett, 2013).

Reactive oxygen species (ROS) is a collective term used on oxygen-centered radicals such as superoxide anions (O_2^-) and hydroxyl radicals ($\cdot\text{OH}$), as well as non-radical derivatives of oxygen such as singlet oxygen, hydrogen peroxide (HOOH) and hypochlorous acids (HOCl) (Barry and Susanna, 1993). ROS are generated *in vivo* during normal utilization of oxygen by aerobic unicellular and multicellular organisms, but can also be generated at relatively high rates under pathophysiological conditions (Gary, 1990, Oakes et al., 2005, Sies, 1997). Although O_2^- is less reactive than $\cdot\text{OH}$, it is of high toxicological importance because it serves as starting material for production of other types of ROS including hydrogen peroxide (HOOH) and hydroxyl radical ($\cdot\text{OH}$) (Winston and Di Giulio, 1991). There are a number of endogenous sources of intracellular O_2^- in aerobic organisms, but autoxidation reactions, mitochondrial electron transport chain and oxidative biotransformation of both endogenous

and exogenous compounds by microsomal cytochrome P450 (CYP) appear to be of particular interest. During aerobic respiration four electrons are required for complete reduction of molecular oxygen to water (Gary, 1990). One electron reduction of molecular oxygen produces O₂^{•-}, further reduction of O₂^{•-} with a single electron produces HOOH, and when further reduced with a single electron HOOH is converted into [•]OH (Figure 3). Any perturbation of the electron transport chain (inner mitochondrial membrane) may result into a leakage of partially reduced oxygen species (Gary, 1990).

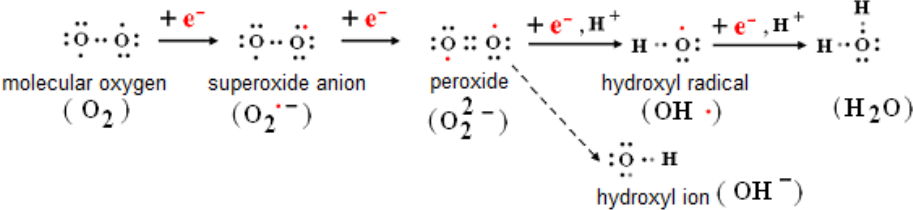


Figure 3: A schematic illustration of how reactive oxygen species are generated via single electron-reduction pathway (the red dots represent unpaired electrons).

Excessive production of intracellular HOOH is generally considered toxic. It is not the toxicity of HOOH *per se* that is of major concern, but rather its ability to serve as a starting material for the production of the extremely strong oxidant [•]OH via Haber-Weiss/Fenton reaction (Parihar et al., 1996). In the presence of transition-metal ions such as Fe²⁺, Cu⁺, Mn²⁺ and Ni²⁺ intracellular HOOH undergoes reductive homolytic fission to yield [•]OH, a process also known as Fenton reaction (Figure 4).

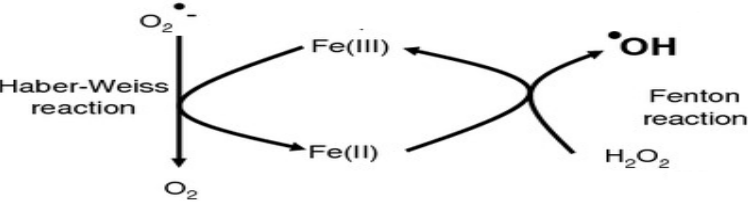


Figure 4: Transitional metal ions such as ferrous iron (Fe²⁺) catalyse Fenton reaction whereby HOOH is reduced to [•]OH and OH⁻, while ferrous iron is oxidized to ferric iron (Fe³⁺). In the presence of electron-rich molecules such as O₂^{•-}, Fe³⁺ is reduced back to Fe²⁺ ready for a new round of Fenton reduction, hence O₂^{•-} can stimulate transition-metal-ion dependent generation of [•]OH from HOOH (Barry and Susanna, 1993).

Hydroxyl radicals are of high toxicological relevance because they are extremely reactive to all biomolecules (membrane phospholipids, proteins, nucleic acids and organelles) (Storey, 1996). With a very short half-life (10^{-9} seconds) hydroxyl radicals are poorly detoxified by non-enzymatic antioxidants such as glutathione, ascorbate and uric acid (Lopez-Torres et al., 1993), additionally, no antioxidant enzymes are known to eliminate $\cdot\text{OH}$. This means that these radicals can exert their toxicity without being intercepted (Doull and Casarett, 2013).

Superoxide anion ($\text{O}_2\cdot^-$) plays a central role not only in the production of HOOH, but also in the production of reactive nitrogen species. This is because it avidly reacts with nitric oxide ($\cdot\text{ON}$), the product of nitric oxide synthase (NOS), to form peroxynitrite (ONOO^-) that spontaneously reacts with CO_2 to yield nitrosoperoxy-carboxylate (ONOOCO_2^-). The products of homolytic fission of this intermediate are two radicals; nitrogen dioxide ($\cdot\text{NO}_2$) (a reactive nitrogen species) and carbonate anion radical ($\text{CO}_2\cdot^-$) (Denicola and Rafael, 2005). The mitochondria are a predominant intracellular site for production of peroxynitrite, $\cdot\text{NO}_2$ and $\text{CO}_2\cdot^-$. This is because nitric oxide ($\cdot\text{ON}$) is lipophilic and could readily diffuse into mitochondrial matrix where there is a steady supply of $\text{O}_2\cdot^-$ and CO_2 from electron transport chain and citric acid cycle, respectively (Denicola and Rafael, 2005, Squadrito and Pryor, 1998).

1.5.1 Xenobiotic-enhancement of ROS/RNS generation

Oxidative stress is defined as the occurrence of an imbalance between production of pro-oxidants such as ROS and RNS and antioxidant defense systems in favor of pro-oxidants (Gary, 1990, Barry and Susanna, 1993). Organic xenobiotic compounds can directly or indirectly induce oxidative stress in several organisms. The direct induction of ROS generation by xenobiotic compounds may occur via several pathways including;

a) Redox cycling, in which organic xenobiotic compounds are reduced with electrons derived from NADPH, and the unstable intermediates rapidly lose electrons to molecular oxygen, thereby forming superoxide radicals (Sies, 1997). In addition to ROS generation, redox cycling involving xenobiotic compounds also disrupts cellular energy and redox status due to consumption of NADPH (Figure 5).

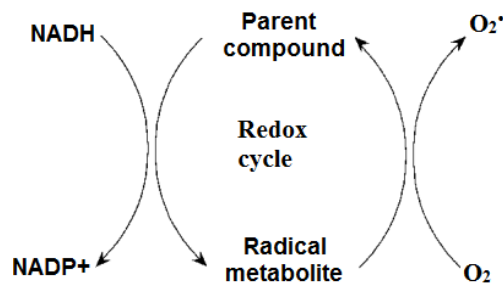


Figure 5: An illustration of ROS generation via redox cycling of xenobiotic compounds.

b) Redox reactivity, in which xenobiotic compounds can directly induce oxidative stress by behaving like free reactive radicals.

Xenobiotic compounds could indirectly induce oxidative stress via perturbation of several metabolic processes. Generally, exposure to contaminants has been associated with a concomitant increase in metabolism in order to cover the energy costs related to stress responses that are provoked during chemical insult (Heugens et al., 2001). PFOS has been associated with induction of oxidative stress in fish (Krøvel et al., 2008, Liu et al., 2007, Wei et al., 2010). This effect has been proposed to be mediated by PPARs-which when bound to and activated by PFOS lead to increased transcription of fatty acid β -oxidation related genes; *Acyl-CoA oxidase (acox)* and *Acyl-CoA dehydrogenase (acod)*, and increased activity of these enzymes generates ROS (Bjorka et al., 2011, Bjork and Wallace, 2009, Desvergne and Wahli, 1999).

Another way in which xenobiotic compounds may indirectly induce oxidative stress is via their oxidative biotransformation by microsomal cytochrome P450 enzymes (CYP). CYP mediates biotransformation of its substrates (endogenous, as well as xenobiotics) by incorporating one oxygen atom into them ($RH \rightarrow ROH$). The catalytic cycle of this process consists of multiple sub-steps and disruption at one or several of these steps could cause leakage of partially reduced oxygen species including superoxide anions, hydrogen peroxide and hydroxyl radical (Bernard et al., 2004). However, generation of ROS via this pathway may not be relevant for PFOS since biotransformation of this compound has not been yet demonstrated in any biological system, so far. When excessive production of ROS such as $\cdot OH$ or RNS ($\cdot NO_2$) is not outbalanced by antioxidant systems, high intracellular concentrations of these radicals may be reached (Dongmei et al., 2013). These radicals are a constant threat to the functional and physical integrity of affected cells since they indiscriminately react with all intracellular macromolecules including DNA, several

membrane components, proteins and organelles. Some of the pathophysiological outcomes of oxidative stress are; apoptosis, necrosis, genotoxicity, carcinogenicity, atherosclerosis (Barry and Susanna, 1993)

1.5.3 Lipid peroxidation

Lipid peroxidation is initiated when free radicals such as hydroxyl radicals, trichloromethyl radicals ($\text{CCl}_3\cdot$) or trichloromethylperoxy radicals ($\text{CCl}_3\text{OO}\cdot$) abstract a hydrogen atom from methylene group ($-\text{CH}_2-$) of fatty acids converting them into carbon-centered lipid radicals ($\text{L}\cdot$). Polyunsaturated fatty acids which are crucial lipid components of biological membranes, are major targets for initiation of lipid peroxidation (Barry and Susanna, 1993, Parihar et al., 1996, Gutteridge, 1995). In aerobic organisms, $\text{L}\cdot$ undergo molecular rearrangement, followed by oxygen fixation leading to their conversion to lipid peroxy radicals ($\text{LOO}\cdot$). $\text{LOO}\cdot$ can have different fates including reacting with other $\text{LOO}\cdot$ molecules, attacking membrane proteins or abstracting hydrogen atoms from adjacent fatty acids, hence propagating lipid peroxidation chain reaction. The length of the propagation chain is determined by factors such as membrane lipid composition, membrane lipid-protein ratio, oxygen levels and presence of chain-breaking antioxidant molecules such as α -tocopherol within the membrane (Esterbauer et al., 1989). After the removal of hydrogen atom, the resultant $\text{LOO}\cdot$ is converted into lipid hydroperoxides (LOOH). Reduced metal complexes such as Fe^{2+} and Cu^+ facilitate the decomposition of LOOH to lipid alkoxyl radicals ($\text{LO}\cdot$) via Fe^{2+} -mediated Fenton reaction (Gutteridge, 1995). Subsequent fragmentation of $\text{LO}\cdot$ yields hydrocarbons including ethane and cytotoxic aldehydes such as 4-hydroxynon-2-enal and malondialdehyde (Arukwe and Mortensen, 2011, Gutteridge, 1995, Barry and Susanna, 1993).

Deleterious consequences of lipid peroxidation in biological membranes include changes in membrane fluidity, a general compromise of membrane functionality, inactivation of membrane-bound proteins such as ion channels, signal receptors and several enzymes, and increased membrane permeability to ions such as Ca^{2+} (Barry and Susanna, 1993, Boelsterli, 2009, Gutteridge, 1995).

1.6 ANTIOXIDANT DEFENSE SYSTEMS

Antioxidants are defined as any substance that when present at low concentrations compared with the oxidizable substrate, considerably delays or inhibits oxidation of the substrate (Gutteridge, 1995). Aerobic organisms have developed both enzymatic and non-enzymatic antioxidant defense systems for keeping several reactive species in the cell at steady-state (non-toxic) concentrations. Protection from oxidative stress is carried out by antioxidants at different levels; prevention of radical formation, interception and subsequent detoxification of radicals or oxidized products, and repairing oxidative damage (Gutteridge, 1995, Parihar et al., 1996, Sies, 1997).

1.6.1 Antioxidant enzymes

Typical to the nature of radicals is the propensity towards chain reactions therefore, scavenging, interception and subsequent detoxification of radicals is an important strategy against oxidative stress (Sies, 1997, Parihar et al., 1996). These are achieved through a concerted effort from both enzymatic and non-enzymatic antioxidants.

1.6.1 a Superoxide dismutase (SOD)

Superoxide anion radicals can be eliminated by their conversion (dismutation) to hydrogen peroxide (HOOH) a reaction catalyzed by SOD. SOD (E.C.1.15.1.1) exists as different forms of metallo-proteins with different intracellular distribution. In eukaryotes such as animals and higher plants copper/zinc (Cu/Zn) SOD is basically located in the cytoplasm, but it is also present in peroxisomes and chloroplast, the manganese (Mn) form of SOD is principally found in the mitochondria, while Iron (Fe)-SOD is extracellular (Lesser, 2006, Boelsterli, 2009). The half-life of O_2^{\bullet} is significantly reduced by SOD, this ensures maintenance of steady-state concentration of O_2^{\bullet} at approximately 10^{-10} mol/L (Lesser, 2006).

1.6.1 b Catalase (Cat)

Catalase (EC.1.11.1.6) plays a crucial role in conversion of HOOH to H_2O and O_2 in peroxisomes-the compartment where high levels of HOOH are generated during fatty acid catabolism (Hashimoto and Hidenori, 1987). Catalase is a heme-containing tetrameric enzyme with a molecular weight of 220 kD. Its high affinity to HOOH renders it the most efficient scavenger of HOOH. This antioxidant enzyme has some unique features; sensitivity to light

and rapid turnover that may be attributed to absorption of light by the heme-group. Catalase activity is susceptible to several conditions that reduce the rate of protein turnover such as perturbation of local environment caused by different forms of stress including heat, cold, pH and others (Parihar et al., 1996).

1.6.1 c. Glutathione peroxidase-GPx

Extra-peroxisomal HOOH is scavenged by glutathione peroxidases, GPXs (EC.1.11.1.9).(Raes et al., 1987). Like catalase, GPx enzymes catalyze the conversion of HOOH to H₂O and O₂. There are two main categories of GPx enzymes; selenium-dependent GPXs and selenium-independent GPXs. Four isoenzymes of selenium-dependent GPXs have been identified; Gpx1, GPx2, GPx3-each with different intracellular locations and GPx4 (extracellular) (Arthur, 2000). GPx catalyzed reduction of HOOH to H₂O and O₂ requires reduced glutathione (GSH) as a source of electrons (Figure 4)

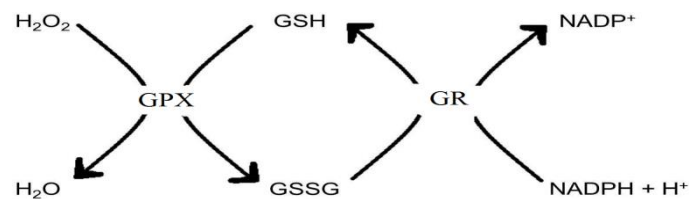


Figure 6: Consumption and regeneration of glutathione by glutathione peroxidases (GPx) and glutathione reductase (GR), respectively.

1.6.1 d. Glutathione-s-transferases (GST)

Glutathione-S-transferases (GSTs) is a superfamily of selenium-independent peroxidases (Storey, 1996). They catalyze the conjugation of reduced glutathione with electrophilic substrates such as organic xenobiotic compounds and ROS-damaged cellular components including organic hydroperoxides such as lipid and nucleotide hydroperoxides (Storey, 1996, Doull and Casarett, 2013). Due to GST activity, a gradual accumulation of potential cytotoxic products under oxidative stress is kept under control.

1.6.2 Non-enzymatic antioxidants

Breaking free radical initiated reaction-chain requires a combination of two processes; a) deactivation of radicals to non-reactive/non-radical end products and b) transfer of radicals

from highly sensitive site such as lipid membranes to sites where minimal damage may be inflicted (aqueous environment) (Sies, 1997). Several non-enzymatic antioxidants are reported to be effective chain-breakers and these include glutathione (GSH), α -tocopherol (vitamin E), carotenoids, and others (Storey, 1996, Sies, 1997, Parihar et al., 1996).

1.6.2 a. Glutathione (GSH)

Glutathione is tripeptide made up of glutamic acid, cysteine, and glycine and is abundantly present in animals and plant tissues (Lesser, 2006). Glutathione plays a direct role in antioxidant defense by acting as a chain-breaker of free radical reactions as it has been reported to spontaneously react with free radicals such as singlet oxygen, hydroxyl radicals and reactive metabolites such as organic hydroperoxides (Parihar et al., 1996). The role of glutathione in antioxidant defense comes from its function as a substrate for antioxidant enzymes (GPx and GST), regeneration of non-enzymatic antioxidants such as vitamin E and reactivation of enzymes inhibited under oxidizing conditions (Storey, 1996). In these processes GSH serves as a hydrogen donor and is oxidized to thyl radicals (GS \cdot) that are further dismutated to their disulfide form (GSSG). GSH is replenished via a NADP(H)-dependent reaction catalyzed by glutathione reductase (GR) (Figure 4). The intracellular ratio of reduced to oxidized glutathione (GSH/GSSG) is considered as a good indicator of oxidative stress (Boelsterli, 2009, Lesser, 2006, Storey, 1996, Arthur, 2000).

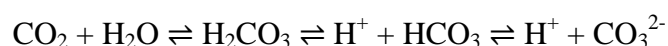
Due to the fact that antioxidant protection against oxidative stress is rarely 100% effective, repair of the damage caused during oxidative stress is crucial for survival of affected cells. This may include various repair mechanisms of oxidative lesions inflicted on DNA, proteins, biological membranes and organelles (Gutteridge, 1995).

1.7 GLOBAL CLIMATE CHANGE

During the pre-industrial revolution era, temperature on planet Earth has been stable mainly because the radiation energy budget (incoming solar radiation versus outgoing radiation) of the Earth has almost been in balance (IPCC, 2013). The Earth's radiation energy budget balance can be perturbed by several natural and/or anthropogenic-driven changes in atmosphere, biosphere, cryosphere, oceans and land. Changes in climate on a global scale have been noticed since the onset of the industrial revolution in the 1760's. This indicates that global climate change has an anthropogenic element to it (Kenneth et al., 2011). The changes in atmospheric constituents such as gases, clouds and aerosols, and the subsequent enhancement of the greenhouse effect is partly blamed on the increased emissions of greenhouse gases such as Carbon dioxide (CO₂), methane (CH₄), nitrous oxide (N₂O) and chlorofluoro carbons (CFCs) into the atmosphere due to human activities. Indicators of global climate change include changes in the following environmental parameters; surface temperature, ice/snow cover, sea levels, and ocean pH.

1.7.1 Anthropogenic carbon and Ocean acidification

Rising atmospheric CO₂ concentrations resulting from human activities is playing a central role in anthropogenic ocean acidification (IPCC, 2011). Global atmospheric CO₂ concentrations have increased by 40% from 278 to 390.5 ppm in a time period stretching from 1750's to 2011 (Ballantyne et al., 2012). Basically, this development has been paralleled with human activities such as industrialization, fossil fuel combustion and agricultural activities. About 30% (155 ± 30 PgC) of this anthropogenic CO₂ in the atmosphere has been reported to be taken up by oceans, consequently causing a reduction of pH especially in the ocean surface by 0.1 units from 8.2 to 8.1 (Sabine, 2004, Khatiwala, 2013). After absorption CO₂ reacts with seawater to form carbonic acid (H₂CO₃) which dissociates to H⁺ and CO₃²⁻ via bicarbonate as shown in the reaction below.



The hydrogen ions produced by these reactions account for the increased H^+ concentration and the corresponding fall in pH in oceans. Indeed, the hydrogen ion concentration has been reported to be more than 30% higher than it was for 200 years ago (Potera, 2010), and ocean pH has been projected to fall by 0.3-0.5 units within the next century (Caldeira and Wickett, 2005).

1.7.2 Hypercapnic challenges to aquatic organisms

Acid-base status influences several physiological and biochemical processes in both vertebrates and invertebrates, for example acid-base parameters such as pH plays a regulatory role in metabolic processes and overall rate of energy turnover (Reipschlager and Pörtner, 1996). This explains why maintenance of acid-base steady state is important for normal functionality and survival.

Elevated environmental CO_2 may compromise the aquatic-breather's (fish) ability to maintain physiological pH mainly by weakening the organism's gas-exchange capacities. One mode of regulation of extracellular/plasma pH is through delivery of metabolic CO_2 to gills by plasma respiratory protein, followed by the diffusion of CO_2 to the external medium (Campbell et al., 2008). Plasma respiratory proteins are highly sensitive to plasma pH and their functional capacity is compromised with decreasing plasma pH (Claiborne et al., 2002). High environmental CO_2 is followed by diffusion of CO_2 into the plasma via the gills. CO_2 reacts with H_2O to form H^+ and HCO_3^- , a reaction catalyzed by erythrocytic carbonic anhydrase (CA), subsequently causing a drop in plasma pH. At lower plasma pH values, plasma respiratory proteins have low affinity to CO_2 , hence poor delivery of CO_2 to gills for excretion (Claiborne et al., 2002).

Alternatively, fish mainly maintain physiological pH via direct trans-epithelial exchange of acid-base relevant ions such as H^+ , Na^+ , Cl^- , and HCO_3^- with their environment (Campbell et al., 2008, Claiborne et al., 2002). This task is performed by several ion-exchanger membrane proteins including Na^+/H^+ -exchangers (NHE), Cl^-/HCO_3^- exchangers, H^+ -ATPases, and Na^+/K^+ -ATPase (Claiborne et al., 2002). Several of the genes encoding the ion-exchangers have been shown to be induced under acid-base stress conditions such as hypercapnia (Claiborne et al., 2002, Portner et al., 2004, Portner et al., 1998, Portner et al., 2001, Reipschlager and Pörtner, 1996). Several effects of hypercapnia-induced acidosis have been demonstrated in vertebrates and invertebrates including metabolic depression and decreased

biosynthesis of protein (Langenbuch and Pörtner, 2003, Claiborne et al., 2002, Portner et al., 2004, Portner et al., 1998).

1.8 ATLANTIC COD (*Gadus morhua*) AS A MODEL ORGANISM

Investigation of how aquatic organisms are being impacted by combined exposure to aquatic pollutants and different aspects of climate change is increasingly becoming important. Atlantic cod is commonly used as model organism in toxicological studies on marine organisms because of the following reasons; Cod is not only a key ecological species in marine ecosystems, but is also one of the major commercial fish species (Olsvik et al., 2009), there is also relatively good knowledge about cods life history, genome and responses to ocean climate variability (Cohen et al., 1990, Drinkwater, 2005).

1.8 a. Fish gills

Gills perform critical physiological functions in fish including maintenance of acid-base homeostasis, ion regulation and exchange of respiratory gases. Basically, the structure of fish gills comprises of branchial arches from which large numbers of filaments extend; from the filaments extend lamella which are covered by layers of respiratory cells (Evans, 1987). Gills have a large surface area derived from the large respiratory surface of the lamella and the extensive epithelial lining the filaments. Although this extensive surface area allows for efficient gill functionality, it also forms an expanded and fragile target area for water-borne toxicants (Wendelaar and Lock, 2008), and as a result, gills are strongly affected by aquatic pollutants (Ahmad et al., 2000, Fatima et al., 2000, Pawert et al., 1998). A variety of aquatic pollutants-both POPs and non-POPs, as well as acidification have been reported to have negative impacts on fish gills both morphologically and physiologically (Wendelaar and Lock, 2008, Dortsas et al., 2011, Evans, 1987)-hence highlighting the relevance of gills in toxicology studies.

1.9 AIMS OF THIS STUDY

Several studies have previously demonstrated that PFOS could induce ROS generation, alterations in expression of antioxidant enzymes and subsequent oxidative stress (Oakes et al., 2005, Liu et al., 2007, Dortsa et al., 2011). These PFOS-related oxidative stress responses have been suggested to be mediated by PPARs (Arukwe and Mortensen, 2011). The role of CO₂-mediated acidification in generation of oxidative stress has also been reported, implying that hypercapnia may potentially enhance oxidative stress. Despite the global distribution of PFOS in aquatic environment, as well as the steady acidification of oceans, only few studies have investigated the effects of combined exposure to water-borne PFOS and environmental hypercapnia-and these studies have mainly focused on other test tissues (especially the liver) rather than the gills.

The purpose of this thesis is therefore to investigate the combined effects of PFOS as an emerging POP and increased CO₂ (hypercapnia), as a quantifiable measure of climate change on oxidative stress responses in the gills of an ecologically and economically important fish species-Atlantic cod (*gadus morhua*).

The hypothesis is that PFOS would induce oxidative stress in gills via activation of the ubiquitously distributed PPAR-isoform (PPAR β) and subsequent downstream target genes (*acox1* or *acod*), and that the presence of hypercapnia would influence this response either via; direct interactive pathways, or indirectly- via compromising antioxidant defenses (increased susceptibility to PFOS-related oxidative stress).

2.0 MATERIALS AND METHODS

2.1 CHEMICALS AND REAGENTS

PFOS (linear, technical grade) was purchased from AlfaAesar (Karlsruhe, Germany). TRIzol® reagent was purchased from Invitrogen Life Technologies (Carlsbad, CA, USA). Tricaine methane sulfonate (MS-222) was purchased from Norsk Medisinaldepot AS. iScript™ cDNA Synthesis Kit, dNTP mix, iTaq DNA polymerase, EZ Load 100 bp Molecular Ruler, and iTaq™ SYBR® Green Supermix with ROX were purchased from BioRad Laboratories (Hercules, CA, USA). Dimethyl sulfoxide (DMSO) and ethylenediaminetetraacetic acid disodium salt dihydrate (EDTA) were purchased from Sigma-Aldrich Chemie GmbH (Munich, Germany). Clinical grade Absolute Ethanol and Agarose were purchased from Sigma-Aldrich Co., MO, USA. Chloroform was purchased from Labscan Ltd. (Dublin, Ireland). GelRed™ nucleic acid stain was purchased from Biothium (Hayward, CA, USA). Clinical grade Isopropanol was purchased from Arcus produkter AS, Norway. Information about the reagents used in procedures for determination of content of malondialdehyde (MDA), and reduced glutathione (GSH) and enzyme assays is lacking. This is because these procedures were performed elsewhere (University of Ancona, Italy).

2.2 EXPERIMENTAL DESIGN

2.2.1 Model organism

Juvenile, sexually immature Atlantic cod (*Gadus morhua*) were supplied by Atlantic cod Juveniles AS (Rissa, Norway). The fish were of equal age and had a body weight of 4.5 ± 0.4 g and an average length of 8.7 ± 0.2 cm. They were kept at the Centre of Fisheries and Aquaculture (Sealab) at NTNU, Trondheim, in circulating seawater with a flow-through of 0,3 L/minute/kg fish. Prior to experiment the fish were acclimatized for 9 days to water temperature of 10 °C and a light:dark photoperiod of 12:12 hours. The fish were starved throughout the acclimatization and exposure periods.

2.2.2 PFOS exposure

Fish were equally distributed in three large tanks containing clean sea water. The three tanks represented the different PFOS exposure regimes, namely; no-PFOS, 100µg and 200µg PFOS/L (Table 1). Two stock solutions (SS) at 150mg/L (SS1) and 300mg/L (SS2) were made by dissolving PFOS into Milli-Q (MQ) water. To achieve a PFOS concentration of 100µg/L (moderate), three different 6 L tanks with sea water received 4 mL of SS1 each. To achieve a PFOS concentration of 200µg/L (high), three different 6 L tanks with sea water received 4 mL of SS2 each, three separate tanks received 4 mL of MQ-water (control). All the nine tanks were equipped with fresh air through an aquarium pump and an air stone, since air bubbles were used for homogenous mixing of the solutions inside the tanks. Fish were transferred from the three large tanks containing clean sea water to the different tanks with low, high or no PFOS for a duration of 1 hour, and then returned back to the respective large tanks with clean sea water. This event was performed daily for a time period of 5 days.

2.2.3 CO₂ exposure

Each of the three CO₂ exposure groups (0% (normal), 0,3% (moderate) and 0,9% (high)) were represented by three 6 L tanks with a continuous flow of water. To achieve the different levels of CO₂, air mixed with either normal CO₂ saturation, 0.3% CO₂ (low CO₂ saturation) or 0.9% CO₂ (high CO₂ saturation) was bubbled through the sea water. The CO₂-containing air was introduced into the water via a specific air pump system. Fish from each PFOS exposure group were distributed among each of the three CO₂ exposure groups, making a total of nine exposure regimens (Table 1). Calculation of water CO₂ levels were done based on measured pH values.

Table 1: An overview of the experimental PFOS and CO₂ exposure regimens. Fish were initially exposed to different concentrations of PFOS and thereafter exposed to increasing levels of CO₂.

<i>Group number</i>	<i>PFOS exposure</i>	<i>CO₂ exposure</i>
1		Control (normal sea water)
2	No (0µg PFOS/L)	Low (0,3% CO ₂)
3		High (0,9% CO ₂)
4		Control (normal sea water)
5	Low (100µg PFOS/L)	Low (0,3% CO ₂)
6		High (0,9% CO ₂)
7		Control (normal sea water)
8	High (200µg PFOS/L)	Low (0,3% CO ₂)
9		High (0,9% CO ₂)

2.2.4 Tissue collection and storage

Ten individuals from each of the exposure groups (Table 1) were anaesthetized using tricaine methanesulfonate (MS-222) and sacrificed (by snapping of the head). Organs and tissue from 5 individuals that were used in gene expression assays were embedded in TRIzol® reagent followed by snap-freezing in liquid nitrogen. Organs from the remaining fish were directly snap-frozen, these were used for biochemical analyses such as enzyme assays and others.

2.3 GENE EXPRESSION ANALYSIS

2.3.1 RNA isolation, and quality assessment

The success of all gene expression evaluations is highly dependent on the quality and quantity of RNA. For achievement of high performance, RNA-based analyses such as real time quantitative reverse transcriptase polymerase chain reaction (qRT-PCR) and micro-array require total RNA that is of high purity and integrity (Fleige and Pfaffl, 2006). Proper extraction of RNA from various biological sources is an important step in the aquirement of high quality total RNA-RNA free of contaminants such as genomic DNA, proteins, nucleases (RNases), and residues from upstream processes). There are several RNA isolation methods, but among the most commonly used are; phenol-based RNA isoalation methods and the guanidinium thiocyanate prosedures (Chirgwin et al., 1979, Cox, 1968).

RNA isolation procedure. In the current experiment, RNA isolation was based on TRIzol® reagent procedure. The procedure was conducted based on descriptions issued by the manufacturer (Invitogen). Gill samples of approximately 50-100 mg embedded in 300µL TRIzol thawed on ice. 500µL were added, and the tissue was homogenized using the Polytron® PT3000 machine homogenizer Kinematica AG. The pistil of the homogenizer was sequentially washed with distilled water, 70% ethanol, and DEPC-treated water immediately after each round of homogenization. 200µL TRIzol added to a total of 1mL and mixed by pipetting. The homogenate was incubated at room temperature for 5 minutes safter which 200µL of chloroform were added. After vigorous shaking for about 15 seconds, samples were incubated at room temperature for about 3 minutes, and thereafter centrifuged at 4°C, 12000 for 15 minutes using Allegra™ X-22R centrifuge from Beckman Coulter.

After centrifugation, the different substances in the sample were partitioned into three phases (aqueous, interphase, and phenol) depending on their chemical properties. The upper aqueous phase contains RNA, while the phenol phase contains DNA and proteins (chomzynski and sacchi 1987). The supernatant was transferred to a new tube and 500µL 100% isopropyl alcohol was added. For precipitation of RNA, the solution was mixed by inversion (4-5 times) followed by incubation at room temperature for 10 minutes. After centrifugation (4 °C, 15,000g for 10 minutes) precipitated RNA formed a pellet either at the bottom or on the walls

of the tube. Isopropyl was removed from the tube after which the RNA pellet was washed in 1mL 75% ethanol and vortexed until it loosened from the bottom and/or walls of the tube. This was followed by centrifugation (4 °C, 75000g for 5 minutes), and removal of ethanol by suction. The pellet was then dissolved in 150µL RNase-free diethylpyrocarbonate (DEPC) water, incubated at 60 °C for 10 minutes and thereafter stored at -80°C.

Determination of quantity and quality of RNA can be achieved various methods among others, by measurement of optical density (OD) via nanodrop (Fleige and Pfaffl, 2006). The nanodrop provides spectrophotometric readings for specific biological molecules at different wavelengths. OD deflection at 260nm and 280nm is specific for nucleic acids and proteins, respectively, while OD deflection at 240nm is specific for various chemical reagents and salts used in RNA isolation processes (BioTekInstrumentsInc, 2006). A spectrophotometric reading at 260nm facilitates the calculation of the concentration of RNA in a sample based on the fact that an optical density of 1 corresponds to 40µg/nl of single-stranded RNA, while the OD ratio at 260nm and 280nm (OD_{260}/OD_{280}) gives an estimate of purity of RNA. (Chomczynski and Sacchi, 2006). An OD 260/280 ratio greater than 1.8 is generally considered as a good indicator of high quality RNA (substantially pure RNA)(Fleige and Pfaffl, 2006).

Having an $OD_{260}/280$ ratio value greater than 1.8 does not automatically qualify the RNA sample as high quality RNA, it is also important to verify the integrity RNA for proper validation of RNA quality. This is because non-intact RNA may compromise the performance of several downstream procedures and assays such as complementary (c) DNA synthesis, qRT-PCR, etc (Fleige and Pfaffl, 2006). Since ribosomal RNA (18S and 28S rRNA) represents approximately 80% of the cells` total RNA, it expected that non-degraded RNA forms two clear bands on a gel (Blobel and Potter, 1967), while fragmented RNA would form clouds at the end of the gel.

RNA quantification and verification of RNA quality. In the current experiment, the nanodrop was used to determine the concentration of RNA (at 260nm). Samples with RNA concentration above 1000ng/µL were diluted with DEPC-treated water until concentrations below this limit were achieved. The measured RNA concentration for most of the samples

ranged between 500 and 2500 ng/ μ L, while the OD_{260/280} ratio was between 1.8 and 2.0. RNA integrity was evaluated by separating 1 μ g RNA from randomly selected samples using formaldehyde gel electrophoresis at 75 V for 1.5 hours. Two clear bands for 18S and 28S rRNA were observed from the resultant gel (Figure 7). Based on this observation, coupled with the absorbance ratio value greater than 1.8, it was concluded that the RNA was of an acceptable quality, and could therefore be used for cDNA synthesis.

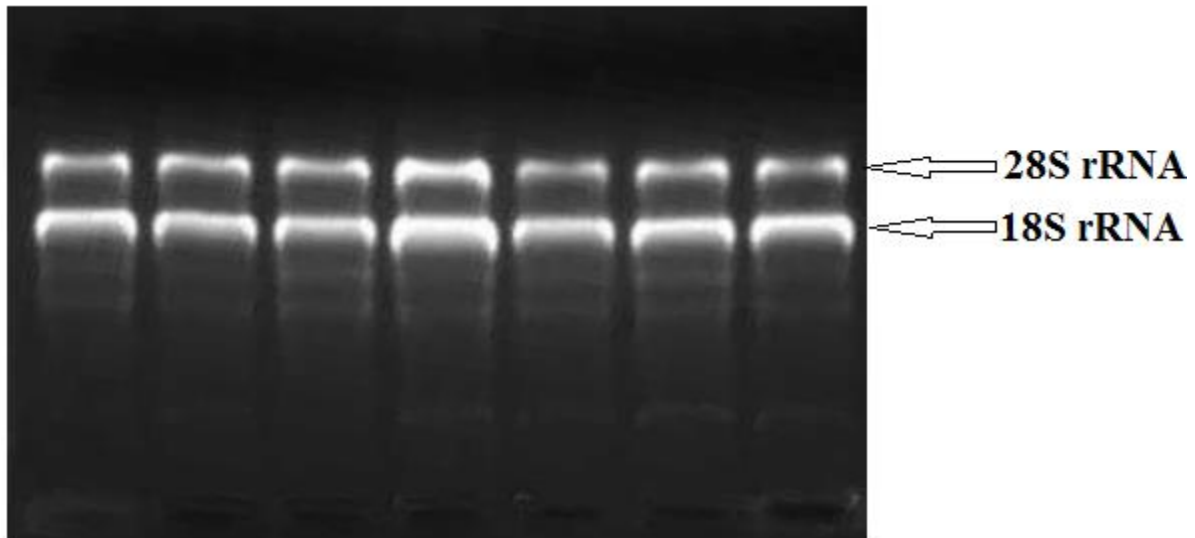


Figure 7: For validation of integrity of isolated RNA, total RNA in randomly chosen samples was separated by formaldehyde gel electrophoresis. The observation of two prominent bands of 18S rRNA and 28S rRNA (constitute approximately 80% of cellular RNA) shows the presence of intact RNA.

2.3.2 Primer testing

Gene specific Atlantic cod primer pairs used for gene expression analysis of target genes (table x) have been successfully used in prior experiments on Atlantic cod (Lorentzen, 2013). In order to test primer pairs for their sequence specificity and general functionality, they were used in PCR amplification of specific sequences from pooled cDNA samples using iTaq DNA Polymerase kit and dNTP mix from Bio-Rad, and PCR program shown in table 3. This was followed by separation of the amplification product using gel (1% agarose) electrophoresis (see Appendix A for reagents and protocol for DNA gel electrophoresis). Highly functional, sequence specific primer pairs were expected to yield a single amplification product that is shown in the gel as single, clear bands of a given size. Primer pairs yielding either nonspecific products or primer dimers are detected by the presence of multiple bands of incorrect size on the gel. Single bands of appropriate amplicon size were seen on gel after separation of the amplification product, an indication of specific primer binding and successful amplification of the target sequence. The primer pairs were ready for use in downstream processes such as qPCR.

Table 2: Gene specific primer pairs used in real-time PCR

Target gene	Primer sequence (5'-3')		Annealing temperature	Amplicon size (bp)
	Forward	Reverse		
<i>Catalase.</i> (<i>cat</i>)	GCCAAGTTGTTTGAGCACGTT	CTGGGATCACGCACCGTA	60°C	101
<i>Acyl-CoA oxidase.</i> (<i>acox</i>)	GCG TTCGTAGTGGAGAGGAG	GCGCACGTTCTCAAAGTA	60°C	108
Peroxisome proliferator-activated beta. (<i>ppar-β</i>)	GGCTTCGTGGACCTCTTCT	TCACAAATCCTTTGCCAT	60°C	133
<i>Mn-superoxide dismutase.</i> (<i>mn-sod</i>)	ATGTGGCCTCCTCCATTGAA	GCATCACGCCACCTATGT	60°C	129
<i>CuZn-superoxide dismutase.</i> (<i>cuzn-sod</i>)	CATGGCTTCCACGTCCATG	CGTTTCCCAGGTCTCCAA	60°C	133
<i>Glutathione peroxidase 1.</i> (<i>gpx1</i>)	GTAGGATGGCCAAAAATGTGT	GGCCCCAGTCATCTGAGC	60°C	116
<i>Glutathione peroxidase 3.</i> (<i>gpx3</i>)	CGTTCTCGGGTTTCCCTGTA	GCTCAAACAGCGGGAAC	60°C	125
<i>Glutathione reductase</i> (<i>gr</i>)	TCACGCTCACCACCAAGGA	GTGTGGAGGCCAGTCGTG	60°C	122
<i>Phosphatidylserine Decarboxylase.</i> (<i>psid</i>)	TCTGGACCTTTGGCGTCAAC	TTCAGCGGTCTCTGAAG	60°C	91

<i>Phosphatidylethanolam</i>				
<i>ine-N-methyltransferase</i>	GGTCTCCGTCAGGCTGAAAG	CGGCGACTACTTTGGGAT	60°C	68
(pent)				
<i>Aromatase</i>	GAGGAGACGCTCATCCTCAG	TAGCTGCGTGTCTTCTTCC	60°C	167
(cyp19)				

2.3.3 cDNA synthesis

Complementary DNA (cDNA) is essential for RNA-based gene expression analyses such as qRT-PCR. The assumption is that all mRNA is converted to cDNA, implying that a cDNA pool is representative of the original RNA profile (Pfaffl, 2004). Synthesis of cDNA and quantification of PCR product can be performed by one-step or two-step qRT-PCR. One-step qRT-PCR combines first-strand cDNA synthesis and qPCR reactions, while these reactions are separated in the two-step qPCR (Invitrogen, 2008). For high efficiency of cDNA synthesis processes there should be an optimal choice of primers, enzymes (RT and polymerase), and RNA free from contamination materials (salts, phenols and other chemicals used in the RNA isolation process) (Pfaffl, 2004). In the cDNA synthesis process, oligo (dT) primers anneal to the polyadenylated 3' tail present on most RNAs, and are extended across the length of mRNA molecules. The efficiency of Oligo (dT) primers is compromised by the presence of secondary structures in mRNA. This problem is overcome by the use of a blend of oligo(dT) primers and nonspecific hexamer primers. This ensures complete conversion of all mRNA to cDNA (Pfaffl, 2004).

cDNA synthesis procedure. Synthesis of cDNA was performed with the iScript cDNA synthesis kit from Bio-Rad and an Eppendorf Mastercycler gradient thermocycler (Brinkman instruments, Westbury, NY, USA). Synthesis of cDNA was based on the protocol provided by the manufacturer of the kit (Bio-Rad), with a reaction mastermix composition and PCR program given in table 3 and 4, respectively. The concentration of RNA extracts was determined with nanodrop, and samples with concentration above 1000ng/μL were diluted

with DEPC-treated water until a concentration below this limit was achieved (500-1000ng/ μ L). The measured RNA concentrations were used to calculate the volume of RNA needed to yield 1000ng. 1000ng was diluted in RNase free water to a volume of 5 μ L and used to produce a total volume of 20 μ L cDNA for each sample. A negative control (lacking template) was added to each cDNA well plate to check for contamination with exogenous nucleic acid in downstream processes, and the cDNA samples were stored at -20°C.

Table 3: Components for cDNA synthesis reaction.

Components	Volume per reaction (μL)
5x iScript reaction mix	4
iScript reverse transcriptase	1
Nuclease free water	10
RNA template(1000ug) diluted in RNase-free water	5
<i>Total</i>	20

Table 4: PCR program for cDNA synthesis.

Phase	Temperature ($^{\circ}$C)	Time (minutes)
Primer annealing	25	5
First strand synthesis	42	30
Termination	85	5
<i>Hold</i>	4	∞

2.3.4 Real-Time Polymerase Chain Reaction (qPCR)

The expression of 10 genes (Table 2) was analyzed by real-time PCR (Mx300P system and MxPro™ QPCR software) using SYBR® green for detection of amplified DNA sequences and ROX as reference dye. In contrast to the traditional (end-point) PCR, qPCR quantifies the PCR product at the end of each reaction cycle in real time (Invitrogen, 2008). SYBR® green is a molecular probe that indiscriminately binds to all double stranded (ds) DNA in a sample. After the intercalation of SYBR® green between ds DNA, the probe emits light at wavelength of 520nm (fluorescence) (Clark, 2010). Ideally, the strength of fluorescence signal is directly proportional to the amount of PCR product generated in the exponential phase of the PCR reaction (Invitrogen, 2008). As PCR proceeds, the amount of fluorescence increases exponentially until it's above the background fluorescence emitted by the reference dye. The number of cycles at which the target fluorescence signal crosses the threshold is called Cycle threshold (Ct). The input amount of the target in a sample can be derived from Ct value and a standard curve.

Real-time PCR protocol. Total cDNA from tissue collected at day 3 and day 6 was diluted to 1:10, and 1:6 for cDNA from tissue collected at day 9. A reaction mix containing 5 µL diluted cDNA, 12.5 µL 2x iTaq SYBR® Green supermix with ROX (from BioRad), 6.5 autoclaved water, 0.5 µL of each primer (forward and reverse) was made for each sample. The thermal cycling program was set as follows: hot-start polymerase activation at 95°C for 3 min, 40 cycles of; 30 s at 95°C (denaturation), 15 s at 60°C (annealing), 15 s at 72°C (extension), followed by melt curve stage; 1 min at 95°C, 30 s at 65°C, and 30 s at 95°C.

A quality check of the data generated by qPCR must be conducted. The disadvantage of using SYBR® green for amplification monitoring it nonspecifically binds to all PCR product molecules, both desired the amplicon, nonspecific products and primer dimers. The resultant fluorescence signal may provide misleading data, hence misinterpretation of expression of gene of interest. Post-amplification melt-curve analysis allows for the detection non-specific primer binding and primer dimers. Different PCR products can often be distinguished based on their sequence specific melting temperature. This is because the melting temperature of nucleic acids is influenced by physical and chemical characteristics of the nucleic acids such as length, GC content and others. Under post-amplification melt-curve analysis, a single qPCR product will give a single, narrow peak at a particular melting temperature, while

nonspecific products or primer dimers typically give additional peaks at different melting temperature than the target product (Invitrogen, 2008, Bustin, 2000, Bustin and Nolan, 2004). Post-amplification melt-curve analyses indicated successful qPCR amplification of all target genes, since a single peak at a given melting temperature was observed for all of the amplified genes (with the exception of GPx3).

For validation of existence of single qPCR product, a gel electrophoresis assay (1% agarose gel) was used to separate qPCR product taken from randomly chosen samples. Observation of a single bands expected amplicon size is often an acceptable validation of presence a single PCR product. Single bands of appropriate amplicon size were observed for all amplified genes (with the exception of GPx3), hence a verification of the successful amplification of target genes (Figure 8).

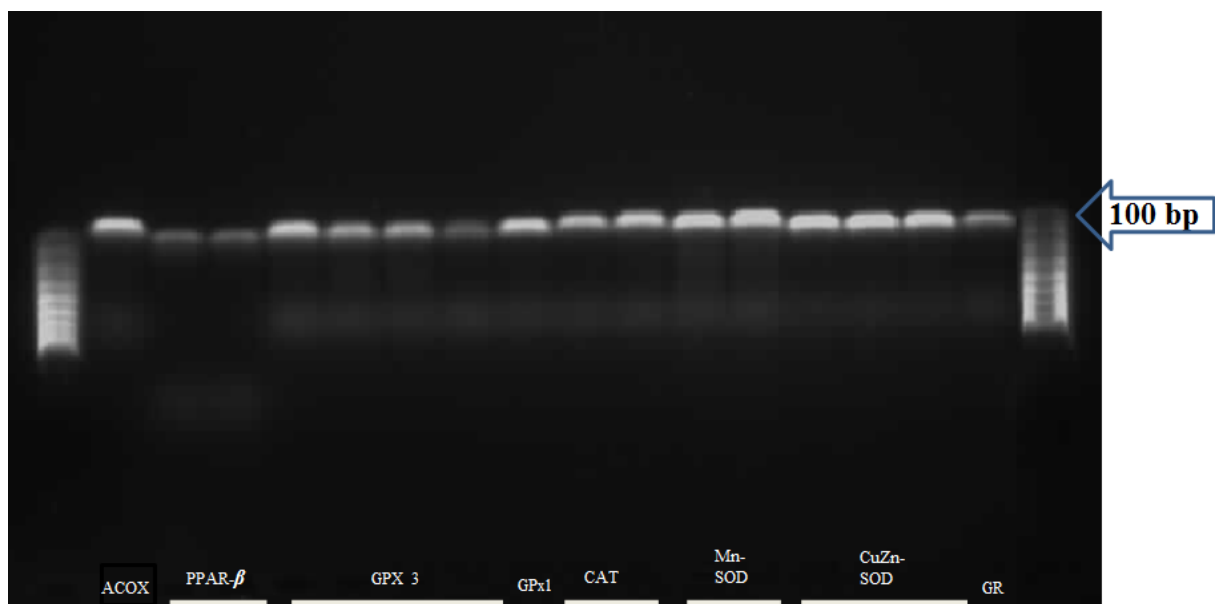


Figure 8: In order to validate the specificity of primer-pairs used in real-time PCR, amplification products chosen from random samples were separated gel electrophoresis. The presence of a single band in each well observed in the image is shows that only a single amplification product of appropriate size was produced after PCR procedure.

2.3.5 Normalization of gene expression data

A dilution series of known amount of plasmid containing *CYP19* (*aromatase*) gene was made and there after amplified using real-time PCR. The resultant Ct values were plotted against the logarithm of copy numbers to yield a standard plot (Appendix C, Figure C1). The linear equation obtained from this standard plot was used to normalize all gene expression data.

2.4 ENZYME ASSAYS

Enzyme activity levels of antioxidant enzymes; Glutathione reductase, Glutathione peroxidase, Superoxide dismutase, Glutathione-S-transferase, and Catalase, as well as total cellular content of malondialdehyde (MDA), and reduced Glutathione (GSH) were determined by using spectrophotometric methods. Table B1, in Appendix B contains the procedures for making the different reagents used in these assays.

2.4.1 Preparation of cytosolic fraction

Cytosolic fraction of gill tissue was prepared for enzyme activity assays. After pH of Tris-HCL buffer was adjusted to 7.5, samples were homogenized (1:4 w/v ratio) in homogenizing buffer, centrifuged at 110,000g for 1 hour and 10 minutes, and aliquots of supernatant were made and stored at -80 °C. 1 µL DTT (antioxidant) per 100 µL cytosolic fraction was added to aliquots that were to be used for GPx activity assays.

2.4.2 Determination of enzyme activity

Determination of Catalase activity

Due to the fact that Catalase functions as a scavenger for hydrogen peroxide (H₂O₂), its activity was determined by measuring the loss of absorbance due to consumption of H₂O₂ at 240 nm at a constant temperature of 18 °C. K-phosphate buffer was adjusted to pH=7 and then 980 µL 100 mM K-phosphate buffer, 10 µL H₂O₂ from 1.2 M stock and 10 mL sample

(cytosolic fraction) were added to a quartz spectrophotometer cuvette followed by the measurement of absorbance at 240 nm over time. Enzyme activity is expressed as a unit of activity relative to total protein content and is calculated via the following formula:

$$\text{Cat activity (units)} = \Delta_{240}/0.04 * \text{assay dil./proteins} = \mu\text{mol/mg proteins}$$

Where:

Δ_{240} = change in absorbance per minute

0.04 = extinction coefficient ($\text{M}^{-1} \text{cm}^{-1}$)

Proteins = concentration of (mg/mL)

Determination of Glutathione S-transferase activity

Glutathione S-transferase (GST) mediates the conjugation of reduced glutathione (GS^-) to electrophilic compounds. The conjugate produced absorbs light at 340 nm. The absorbance at 340nm was therefore used in the determination of GST activity. Working buffer solution (K-phosphate buffer + CDNB) was prepared by adding 1.5 mL 50 mM CDNB stock solution in 50 mL 50 mM K-phosphate buffer at pH 6.5. For measurement of enzyme activity: 965 μL working buffer solution, 15 μL 100 mM GSH, and 20 mL sample (cytosolic fraction) was added to a quartz spectrophotometer cuvette, and absorbance at 340 nm was measured over time. Enzyme activity is expressed as a unit of activity relative to total protein content and is calculated via the following formula:

$$\text{GST activity (units)} = \Delta_{340}/9.6 * \text{assay dil./proteins} * 1000 = \mu\text{mol/mg proteins}$$

Where:

Δ_{340} = change in absorbance per minute

9.6 = extinction coefficient ($\text{M}^{-1} \text{cm}^{-1}$)

Proteins = concentration of (mg/mL)

Determination of Glutathione reductase activity

Glutathione reductase (GR) uses NADPH as reduction equivalent as it mediates the reduction of oxidized glutathione (GSSG) back to its reduced state (GSH). GR activity can be determined by measuring consumption of NADPH at 340 nm at a constant temperature of 18 °C. 750 µL 100 mM K-phosphate buffer at pH 7, 100 µL 10 mM GSSG, 10 µL 100 mM EDTA, 100 µL 1 mg/L NADPH, and 40 µL sample (cytosolic fraction) was added to a quartz spectrophotometer cuvette, and absorbance at 340 nm was measured 5 times through a 3 minute period. Enzyme activity is expressed as a unit of activity relative to total protein content and is calculated via the following formula:

$$\text{GR activity (units)} = \Delta_{340}/6.22 * \text{assay dil./proteins} * 1000 = \mu\text{mol/mg proteins}$$

Where:

Δ_{340} = change in absorbance per minute

6.22 = extinction coefficient ($\text{M}^{-1} \text{cm}^{-1}$)

Proteins = concentration of (mg/mL)

Determination of Glutathione peroxidase activity

GPx uses reduced glutathione (GSH) as reduction equivalent as it catalyzes the reduction of H_2O_2 or organic peroxides to H_2O or ROH (reduced organic compound). The oxidized glutathione (GSSG) that is generated by GPx reactions is reduced by GR to regenerate GSH which is the biologically active form of glutathione. GR uses NADPH as reducing equivalent during the regeneration of GSH. GPx activity can be determined by measuring consumption of NADPH at 340 nm at a constant temperature of 18 °C. Stock solution of 100 U/mL GR was prepared from original stock solution (i.e. if stock solution is 1384 U/mL, take 72.25 µg/mL). 846 µL 100 mM K-phosphate buffer at pH 7.5, 10 µL 100 mM EDTA, 20 µL 100 mM GSH, 10 µL 100 U/mL GR, 100 µL sample or blank solution and 10 µL 20 mg/mL NADPH was added to a plastic spectrophotometer cuvette, and absorbance was measured at 340 nm. Several blank reactions were measured before measuring samples until a 0.10-0.15 $\Delta_{\text{min blank}}$ was achieved. After the volume of NADPH was modified to get an absorbance of 0.9-1.2, 15 µL 200 mM CHP was added. In order to get accurate absorbance values, absorbance of blank

reaction was subtracted from that of the sample reaction: $\Delta_{\text{min sample}} - \Delta_{\text{min blank}} = \Delta_{\text{min final sample}}$. Enzyme activity is expressed as a unit of activity relative to total protein content and is calculated via the following formula:

$$\text{GPx (CHP) activity} = \Delta_{340}/6.22 * \text{assay dil./proteins} * 1000 = \mu\text{mol/mg proteins}$$

Where:

Δ_{340} = change in absorbance per minute

6.22 = extinction coefficient ($\text{M}^{-1} \text{cm}^{-1}$)

Proteins = concentration of (mg/mL)

Determination of Superoxide dismutase activity

Determination of superoxide dismutase (SOD) activity was done by monitoring the diminishing reduction of cytochrome c by $\cdot\text{O}_2$ - by the xanthine oxidase/hypoxanthine system. One unit (U) of SOD is defined as the amount of enzyme inhibition by 50 % the reduction of cytochrome c. Different volumes of each sample were used to determine 50 % inhibition of the reaction rate. Xanthine oxidase 6mU/mL was prepared from available stock solution. Working buffer was prepared from 50 mL 100 mM K-phosphate buffer at pH 7.8, 0.006 g Hypoxanthine, 0.012 g Cytochrome c and 100 μL 100 mM EDTA, and absorbance at 550 nm was measured at 18 °C. Absorbance blank solution for; working buffer, K-phosphate buffer and Xantine oxidase was measured three times (Δ_{blank} should be \cong 0.08-0.1), and three absorbance values for different volumes of K-phosphate buffer and Xantine oxidase samples were also registered (Table 5). The percentage of inhibition in the blank samples for these three volumes should be; 70 % for Reading 1, 50 % for Reading 2, and 20 % for Reading 3. The results should fit on a semi logarithmic scale, yeilding $y = ax^2 + bx + c$ by second order regression. The x value is considered to represent 50 % variation of Δ_{blank} , and Volume (Vol.) necessary to reduce 50 % of blank reaction. Enzyme activity was calculated via the following formula:

$$\text{U.SOD/mg protein} = 1000/\text{Vol} * \text{sample dil./Proteins (mg/mL)}$$

Table 5: Overview of readings (at 55nm) taken during determination of SOD activity.

	Blank	Reading 1	Reading 2	Reading 3
Working buffer (µL)	500	500	500	500
K-phosphate buffer (µL)	470	460	450	430
Sample (µL)		10	20	40
Xanthine oxidase (µL)	30	30	30	30

2.4.3 Determination of reduced Glutathione

Conjugation of GSH with the dye DTNB at 412 nm was monitored for determination of total reduced GSH, the oxidized glutathione (GSSG) that is produced in this reaction is reduced back to GSH by GR (using NADPH as co-factor). Samples were homogenized (1:4 w/v ratio) in homogenizing buffer and kept on ice for 45 minutes, and thereafter centrifuged at 37,000g for 15 minutes at 4 °C. Aliquots of supernatants were made and stored at -80 °C. Preparation of working buffer was done by adding; 10 µL 100 mM EDTA to 1 mL 100 mM K-phosphate buffer at pH 7. The stock solution (100 mM GSH) from which standards were made was prepared by dissolving 0.0307 g GSH in 1 mL dH₂O, followed by dilution via the series given below:

GSH 100 mM → GSH 10 mM → GSH 1 mM → GSH 100 µM

GSH 100 µM → (GSH 10 µM, GSH 20 µM, and GSH 30 µM)

100 µM of each standard were used to obtain a 1 µM, 2 µM, and 3 µM final concentrations of GSH standards.

1 mL working buffer, 100 µL blank or standard, 5 µL 20 mM DTNB, 50 µL 4 mg/mL NADPH, and 10 µL 100 U/mL GR was added in cuvettes for blank and standard reactions.

1 mL working buffer, 5 μ L 20 mM DTNB, 100 μ L sample, 50 μ L 4 mg/mL NADPH, and 10 μ L 100 U/mL GR was added in cuvettes for sample reactions. Δ_{min} of blank and standards were used to obtain the linear equation between absorbance and concentration ($y=ax+b$). This equation was used to convert Δ_{sample} to concentration in $\mu\text{mol/L}$, thereafter total Glutathione levels were calculated via the following equation:

$$\text{GSH}+2\text{GSSG } (\mu\text{mol/g tissue}) = (\text{concentration}/1000) * \text{sample dilution} * \text{w/v ratio} * 1$$

2.4.4 Determination of Malondialdehyde

For determination of changes in lipid peroxidation MDA was measured. After gill tissue was washed in ice-cold 0.9 % NaCl, and blotted on blotting paper, approximately 0.1 g of tissue was minced, and diluted (1:3) in ice-cold Tris-HCL buffer at pH 7.4. Samples were homogenized and centrifuged for 20 minutes at 3,000g in 650 μ L of reagent 1-R1 (Table 6), thereafter, 100 μ L H₂O, 100 μ L sample and 150 μ L of R2 were added to microcentrifuge tube, vortexed and incubating at 45 °C for 40 minutes. Samples were thereafter cooled on ice and centrifuged for 10 min at 15,000g. This was followed by measurement of absorbance at 586 nm using Helma quartz cell and compared to a standard curve (Table 6).

Table 6: Reagents used for determination of malondialdehyde (MDA).

Reagent 1 (R1)	0.064 g 10.3 mM 1-methyl-2-phenylindole 30 mL acetonitrile 10 mL methanol
Reagent 2 (R2)	HCL 37 %
Reagent 3 (R3)	0.0165 mL 10 mM 1,1,3,3-tetramethoxypropane 10 mL 20 mM Tris-HCL

A standard curve was generated by diluting S2 in ddH₂O (Table 7). After addition of 150 μ L of R2 the solutions were; vortexed, incubated at 45 °C for 40 minutes and thereafter cooled on ice and centrifuged at 15,000g for 10 minutes. This was followed by measurement of absorbance at 586 nm.

Table 7: Volume of S2 and ddH₂O in standard curve used for determination of MDA levels

	Concentration μ M									
	0	0.2	0.5	0.8	1.0	2.0	3.0	4.0	6.0	8.0
S2 volume (μ L)	0	2	5	8	10	20	30	40	60	80
ddH₂O volume (μ L)	200	198	195	192	190	180	170	160	140	120

2.5 Statistical analysis

Statistical analysis was performed using IBM SPSS® statistical software (version 20). The Shapiro-Wilk test was used to test for normality. Non-normally distributed data was converted to normal distribution using natural logarithm (ln) or square root transformations. Potential outliers were identified by observation of the box-plot coupled with Grubbs tests. Datasets with adequate normality were further tested for homogeneity of variance using parametric Levene's test. Data found to be normally distributed and with homogenous variance was analysed for significant differences between groups using one-way ANOVA followed by Tukey's post hoc multiple comparison test. However, data found to be normally distributed,

but lacking homogeneity of variance (and/or equal sample size) was analyzed using one-way ANOVA followed by robust Welch test and Games-Howell post hoc multiple comparison test. Non-normally distributed data was tested for homogeneity of variance by nonparametric Levene's test and analyzed for significance by a Kruskal-Wallis one-way analysis of variance followed by Dunn's nonparametric post hoc test. Level of significance was set to $\alpha = 0.05$. Further analysis of biometric data was performed with Umetrics SIMCA-P⁺ 21.0 ($\alpha = 0.05$).

3.0 RESULTS

3.1 Validation of hypercapnia in experimental tanks

The relatively high permeability of CO₂ and carbonic acid across biological membranes compared to H⁺ could partly explain the reportedly higher toxicity of CO₂ in aquatic organisms compared to strong acids that yield the same pH (Kikkawa and Kita, 2004). It is therefore important to ensure that addition of CO₂ to experimental tanks actually caused an increase of partial pressure of CO₂ (P_{CO2}) (hypercapnia). In this study, verification of hypercapnia was done by daily measurement of experimental tanks pH values (Figure 9), which were in turn used to calculate P_{CO2} in the experimental tanks tanks (Figure 10) (with salinity of 33.8ppm, total alkalinity of 2223 μmol kg⁻¹, temperature of 10°C and atmospheric pressure of 10 dbar). In the tanks containing normal seawater, pH values ranging from 7.60 to 7.83 and P_{CO2} levels of 596-1136 were registered. In the 0.3% CO₂ experimental tanks pH values of 7.08-7.45 and P_{CO2} levels at 1714 and 3745 were registered, while in the 0.9% CO₂ experimental tanks, pH values of 6.63-6.96 and P_{CO2} at 4844-11455 were registered. An increase in P_{CO2} and a concomitant drop in pH was observed after fish were added to the experimental tanks, this was due to additional respiratory CO₂ from the fish (Figures 9 and 10).

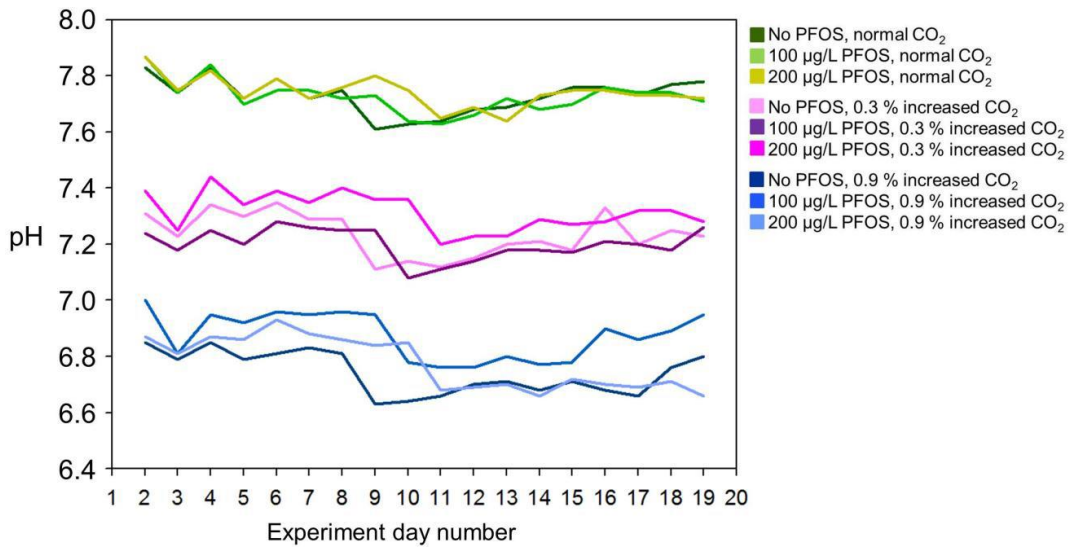


Figure 9: Saturation of CO₂ in the experimental tanks was achieved by the introduction of a mixture of air containing normal (green lines), 0.3% (purple lines) or 0.9% CO₂ (blue lines) to the appropriate experimental tanks. The pH in the various CO₂ exposure tanks was monitored throughout the experiment.

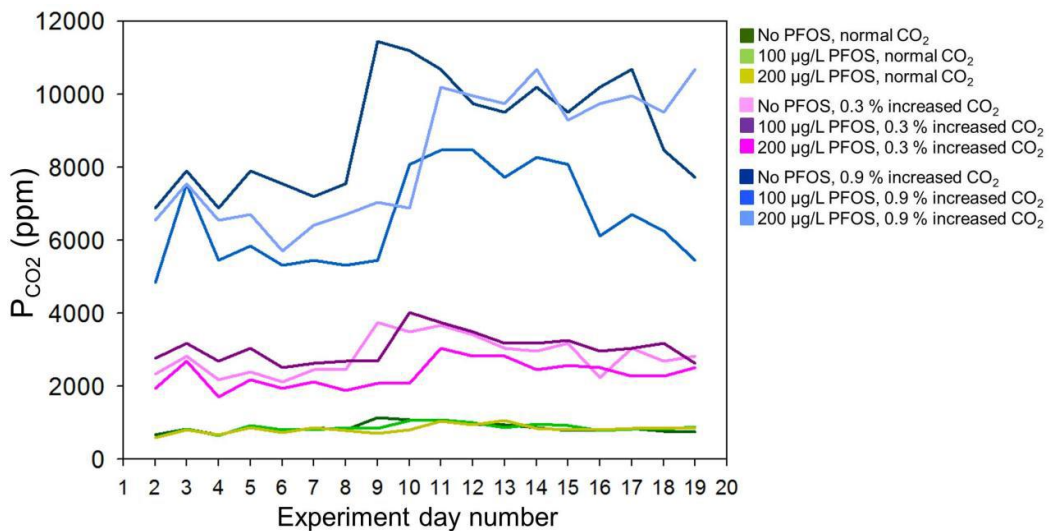


Figure 10: Saturation of CO₂ in the experimental tanks was achieved by the introduction of a mixture of air containing normal (green lines), 0.3% (purple lines) or 0.9% CO₂ (blue lines) to the appropriate experimental tanks. The levels of P_{CO2} in the different experimental tanks were calculated based on the measured pH values in the respective tanks.

3.2 Body PFOS burden

Carcasses (excluding the head, and internal organs) of fish from normocapnia exposure groups were analyzed for accumulated PFOS levels. High-performance liquid chromatography coupled with tandem mass spectrometry (HPLC/MS/MS) was used in the determination of PFOS body burden. For quantitative analysis, the isotope dilution method was performed with MPFOS as internal standard, a five-point calibration curve (0-400 ng/mL) for the analyte (PFOS) and a fixed concentration (20ng/mL) of internal standard. The performance of the above mentioned analysis was based on the procedures used in previous studies (Mortensen et al., 2011).

Table 9: Measured concentrations of PFOS body burden in carcasses of fish from normocapnia exposure groups.

Nominal concentration. ($\mu\text{g PFOS L}^{-1}$ water)	Measured concentration. (ng PFOS g^{-1} weight wet, mean \pm SEM)			
	<i>Day 3</i>	<i>Day 6</i>	<i>Day9</i>	<i>Total</i>
0	2.6 \pm 0.1	2.5 \pm 0.2	2.8 \pm 0.2*	2.6 \pm 0.1
100	1013 \pm 122.7	736.3 \pm 102.9	769.9 \pm 63.1	840.0 \pm 62.6
200	1693.4 \pm 154.2	1754.2 \pm 170.1	1425.7 \pm 401.8**	1674.1 \pm 93.5

3.3 Effects on physiological parameters

The effects of single or combined exposure to CO₂ or PFOS on the weight, and length of individual fish were measured. Based on the measurements of the weight and length of fish in the different exposure scenarios (Table 10), there were no significant changes in fish size. These observations indicated that stress related to experimental conditions (starvation and exposure to stressors), had a minimal (negligible) effect on biometric data of the individuals.

Table 10: Alterations in average length and weight following single or combined exposure of PFOS and elevated CO₂ levels to juvenile Atlantic cod. The measurements were done after the fish were sacrificed and are given in grams (g) and centimeters (cm), with SEM.

	Length (cm)		Weight (g)	
	Average	SEM	Average	SEM
No PFOS, normal CO₂ (control)	8.85	0.17	4.51	0.32
No PFOS + 0.3% (low) CO₂	8.73	0.14	4.30	0.25
No PFOS + 0.9% (high) CO₂	8.76	0.16	4.41	0.30
100µg PFOS + normal CO₂	8.68	0.21	4.19	0.35
100µg PFOS + 0.3 (low) CO₂	8.92	0.24	4.67	0.40
100µg PFOS + 0.9 (high) CO₂	8.74	0.22	4.21	0.28
200µg PFOS + normal CO₂	8.33	0.16	3.80	0.08
200µg PFOS + 0.3 (low) CO₂	8.61	0.17	4.11	0.18
200µg PFOS + 0.9 (high) CO₂	8.76	0.23	4.16	0.32

3.4 EFFECTS ON LIPID METABOLISM

3.4.1 PPAR- β

Generally, single exposure to PFOS or elevated CO₂ resulted to weak changes in the expression of *ppar- β* (Figure 11). Combined exposure to PFOS and elevated CO₂ caused differential changes in mRNA levels for *ppar- β* . Nonetheless, an insignificant increase of *ppar- β* transcript above control, occurred in several combined exposure groups; 200 μ g PFOS/L+ 0.3% CO₂ and 200 μ g PFOS/L+0.9CO₂ (day 3), 0.9%CO₂+PFOS (day 6) and 0.3%CO₂+PFOS (day 9) (Figure 11).

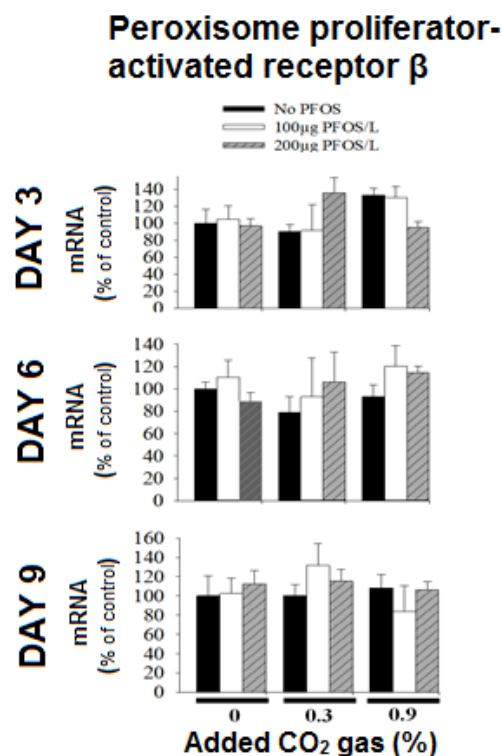


FIGURE 11: Changes in mRNA levels for *Peroxisome proliferator-activated receptor-beta* (*ppar- β*) in gills of juvenile Atlantic cod (*Gadus morhua*) exposed to PFOS and elevated levels of dissolved CO₂, singly or in combination. The mRNA levels were analyzed with quantitative RT-PCR using gene specific primer pairs. Data are presented as mean percentage of control (n=4/5) \pm standard mean of error (SEM), with the non-treated group (No PFOS/ 0% CO₂ group) referred to as the control. Asterisks denote significant differences between exposure groups and control, while different letters indicate significant differences between exposure groups (one-way ANOVA with Tukey's post-hoc test ($p < 0.05$) for *ppar- β* day 9, and Games-Howell post hoc test ($p < 0.05$) for *ppar- β* day3+ 6)

3.4.2 EFFECTS ON ACYL-CoA OXIDASE (*acox1*)

With the exception of the insignificant increase at day 6, minimal changes from control levels were observed in transcript levels for *acox1* upon single exposure to PFOS as seen at day 3 and 9, respectively (Figure 12). Apparently, an overall slight reduction in transcriptional regulation of *acox1* to levels below control was observed following exposure to elevated CO₂ alone (0.3% and 0.9%) (Although not significant) (Figure 12). An insignificant increase in *acox1* transcription above control levels was observed following combined exposure to high CO₂ levels (0.9% CO₂) and PFOS as seen at day 3 and 6, respectively.

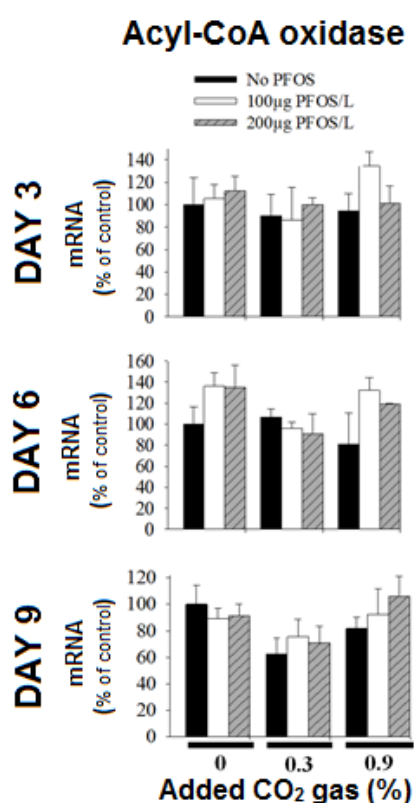


FIGURE 12: Changes in mRNA levels for *Acyl-CoA Oxidase (acox1)* in gills of juvenile Atlantic cod (*Gadus morhua*) exposed to PFOS and elevated levels of dissolved CO₂, singly or in combination. Messenger RNA (mRNA) levels were analyzed with quantitative RT-PCR using gene specific primer pairs. Data are presented as mean percentage of control (n=4/5) ± standard mean of error (SEM), with the non-treated group (no PFOS/ 0% CO₂ group) referred to as the control. Asterisks denote significant differences between exposure groups and control, while different letters indicate significant differences between exposure groups (one-way ANOVA with Tukey's post-hoc test (p < 0.05) for *acox1* day 3+9, and Games-Howell post hoc test (p < 0.05) for *acox1* day 6).

3.4.3 EFFECTS ON GENES INVOLVED IN MEMBRANE PHOSPHOLIPID HOMEOSTASIS

Generally, single exposure to PFOS or elevated CO₂ levels (0.3% or 0.9%) caused weak differential changes of both *pisd* and *pemt* mRNA levels from control levels (Figure 13). However, an increase in transcript levels for *pemt* was observed only after exposure to high CO₂ (0.9%) as seen at day 3 and 9, respectively (though not significant). A similar increase in transcriptional levels for *pemt* was also observed following combined exposure to high CO₂ and PFOS (0.9%CO₂+PFOS), though not statistically significant (Figure 13B). Apparently, combined exposure to low CO₂ levels and PFOS generally caused minimal changes in expression of both *pemt* and *pisd* from control levels. Of the two genes- *pemt* responded more clearly under the different exposure conditions, but this occurred predominately after exposure to high CO₂ levels alone or in combination with PFOS.

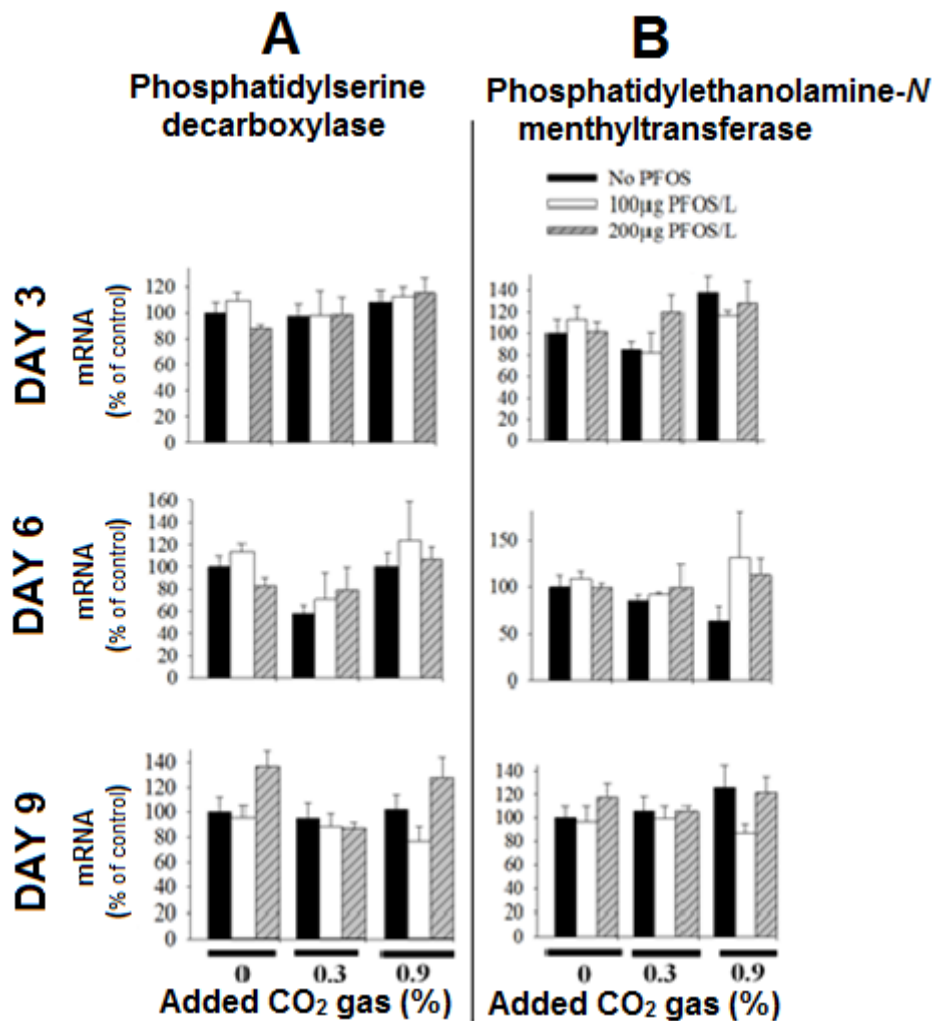


FIGURE 13: Changes in messenger RNA (mRNA) levels for **A:** *Phosphatidylserine decarboxylase* (*psid*) and **B:** *Phosphatidylethanolamine-N-methyltransferase* (*pemt*) expressed as percentage of control (n=3/4/5) ± standard mean of error (SEM). Juvenile Atlantic cod (*Gadus morhua*) were exposed to PFOS and elevated levels of dissolved CO₂, singly or in combination and transcriptional changes were analyzed with quantitative RT-PCR using gene specific primer pairs. Asterisks denote significant differences between exposure groups and control, while different letters indicate significant differences between exposure groups (one-way ANOVA with Tukey's post-hoc test (p < 0.05) for *psid* day 3+6+9, and for *pemt* day 9 and Kruskal-Wallis nonparametric one-way ANOVA (p < 0.05), followed by Dunn's nonparametric post hoc test for *pemt* day 3+6).

3.5 EFFECTS ON OXIDATIVE STRESS RESPONSES

3.5.1 SUPEROXIDE DISMUTASE (SOD)

Exposure to PFOS alone apparently led to differential transcriptional regulation of both isoforms of superoxide dismutase (*sod*) (Figure 14A and B, respectively). Differential regulation of both *CuZn* and *Mn-sod* was also observed after exposure to low CO₂ levels (0.3%) alone as seen at day 3 and 6, however, prolonged exposure to low CO₂ levels was followed by reduction in mRNA levels below control for both isoforms as seen at day 9. On the other hand, exposure to high CO₂ levels (0.9%) alone only resulted to minimal changes in *sod* mRNA levels from control levels (Figure 14A and B, respectively). Although differential regulation of both *CuZn* and *Mn-sod* transcription was generally observed upon combined exposure to elevated CO₂ and PFOS, a significant drop in mRNA levels for *Mn-sod* well below control levels at day 9 following combined exposure to low CO₂ levels and high PFOS concentration (0.3%CO₂+200µgPFOS/L) and high CO₂ levels and low PFOS concentrations (0.9% CO₂+100µgPFOS/L) was noteworthy (Figure 14B).

In fish exposed to PFOS alone (PFOS+ 0% CO₂), an apparent PFOS concentration dependent decline in SOD activity below control levels was observed at day 3 (though not significant). Additionally, an apparent decline in enzyme activity was also observed after single exposure to high PFOS alone (200µg PFOS/L) at day 9 (Figure 14C). Generally, insignificant reduction in SOD activity to levels below control occurred in elevated CO₂-alone exposure groups as seen at day 3 and 9, respectively (Figure 14C). At day 9, an apparent CO₂-level dependent increase (not significant) in SOD activity above control was observed in exposure groups treated with a combination of high PFOS concentration (200µg PFOS/L) and elevated CO₂ levels (Figure 14C).

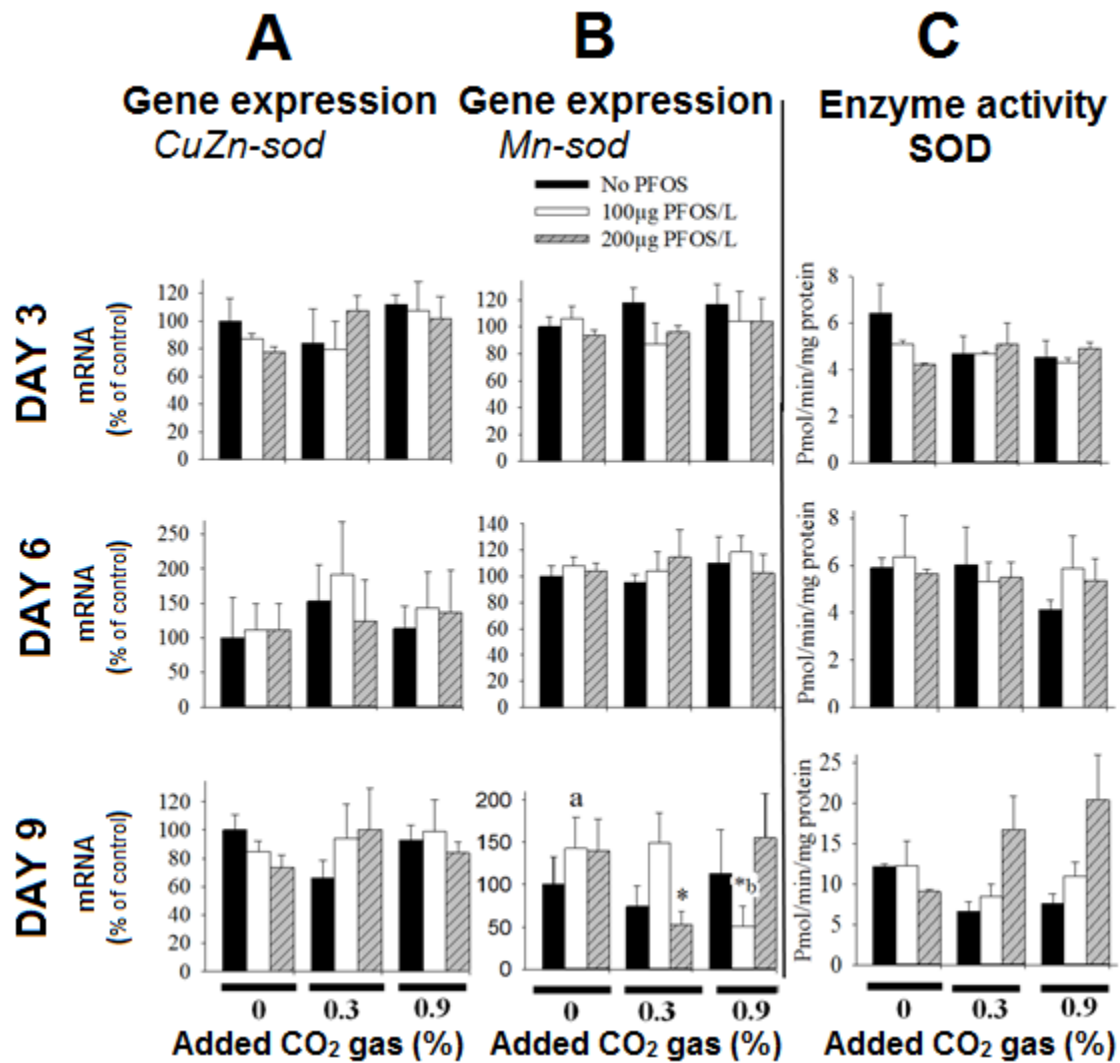


FIGURE 14: Changes in messenger RNA (mRNA) levels for **A:** *CuZn Superoxide dismutase* (*CuZn-sod*) and **B:** *Mn-superoxide dismutase* (*Mn-sod*) expressed as percentage of control (n=3/4/5) ± standard mean of error (SEM). Changes in enzyme activity for SOD (Figure 4C) are expressed as pmol/minute/mg protein, with SEM (n=2/3). Juvenile Atlantic cod (*Gadus morhua*) were exposed to PFOS and elevated levels of dissolved CO₂, singly or in combination. Transcriptional changes were analyzed with quantitative RT-PCR using gene specific primer pairs, and enzyme activity was measured spectrophotometrically. Asterisks denote significant differences between exposure groups and control, while different letters indicate significant differences between exposure groups (one-way ANOVA with Tukey's post-hoc test (p < 0.05) for *Mn-sod* day 9+3, and Games-Howell post hoc test (p < 0.05) for *CuZn-sod* day 9 and Kruskal-Wallis nonparametric one-way ANOVA (p < 0.05) followed by Dunn's nonparametric post hoc test for *CuZn-sod*+*Mn-sod* day 6 and enzyme assays).

3.5.2 CATALASE (CAT)

Generally, *cat* mRNA levels only slightly changed from control levels after exposure to PFOS alone (Figure 15A). A time-dependent reduction in *cat* mRNA levels below control levels occurred upon exposure to low levels of CO₂ (0.3% CO₂) alone, as observed from the significant drop at day 9 (Figure 15A). However, this effect was reversed after exposure to high CO₂ levels, since exposure to 0.9% CO₂ alone resulted either to restoration back to control levels or an apparent increase over control levels as seen at day 3 and 9, respectively (Figure 15A). It was observed that combined exposure to PFOS and elevated CO₂ resulted to differential regulation of expression of *cat*. Nevertheless, this effect was apparently characterized by noticeable increase in mRNA levels to levels above control after combined exposure elevated CO₂ levels and PFOS, as seen at day 3 in the 0.3% CO₂+200µg PFOS/L and 0.9% CO₂+100µg PFOS/L exposure groups, and at day 6 in the 0.9% CO₂+PFOS exposure groups (Figure 15A).

Apparently, weak differential changes from control levels were observed in CAT activity following exposure to PFOS alone (Figure 15B). Exposure to elevated CO₂ levels alone (0.3% or 0.9%) resulted to a general reduction in the enzyme activity below control levels, with an apparent CO₂-level dependent decline observed at day 6 (though not significant). This apparently negative impact of hypercapnia on CAT activity was clearer at day 9 where exposure to 0.3% CO₂ alone caused a significant reduction in enzyme activity well below control, while exposure to 0.9% CO₂ alone resulted to insignificant but noticeable reduction in enzyme activity (Figure 15B). Combined exposure to PFOS and elevated CO₂ caused differential changes in CAT activity as seen at day 3 and 6. However, a reduction in CAT activity was observed after relatively prolonged exposure to a combination of both stressors as seen at day 9, with a significant drop in the 0.3% CO₂+100µg PFOS/L exposure group (Figure 15B).

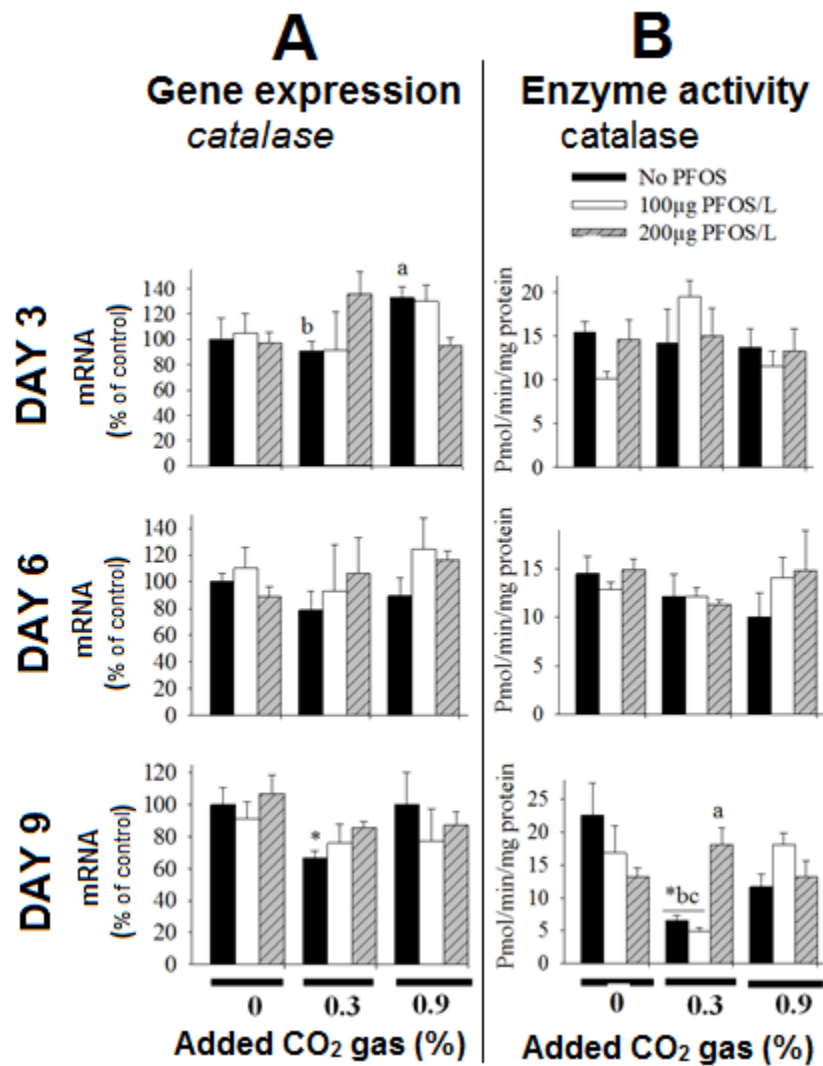


FIGURE 15: Changes in messenger RNA (mRNA) levels for **A:** *Catalase* (*cat*) expressed as percentage of control (n=4/5) ± standard mean of error (SEM), and **B:** enzyme activity for catalase (*CAT*) expressed as pmol/minute/mg protein, with SEM (n=2/3). Juvenile Atlantic cod (*Gadus morhua*) were exposed to PFOS and elevated levels of dissolved CO₂, singly or in combination. Transcriptional changes were analyzed with quantitative RT-PCR using gene specific primer pairs, and enzyme activity was measured spectrophotometrically. Asterisks denote significant differences between exposure groups and control, while different letters indicate significant differences between exposure groups (one-way ANOVA with Tukey's post-hoc test (p < 0.05) for *cat* day 6, and Games-Howell post hoc test (p < 0.05) for *cat* day 9 and Kruskal-Wallis nonparametric one-way ANOVA (p < 0.05) followed by Dunn's nonparametric post hoc test for *cat* day 3 and enzyme assays).

3.5.3 GLUTATHIONE PEROXIDASE (GPx)

A significant fall in *gpx3* mRNA levels to levels clearly below control was observed after treatment with low concentrations of PFOS alone (100µgPFOS/L) at day 3 and 9, while exposure to high concentrations of PFOS alone (200µgPFOS/L) generally resulted to differential changes in *gpx3* transcript levels (Figure 16B). When compared with the unexposed group, exposure to low levels of CO₂ caused an overall decrease in transcriptional expression of both *gpx1* and *gpx3* (Figure 16 A and B, respectively). However, this negative response was observed more clearly for *gpx3* compared to *gpx1*, as observed from the significant drop in mRNA levels for *gpx3* at day 3 and 9 following single exposure to 0.3% CO₂ compared to control (Figure 16B). Exposure to high levels of CO₂ (0.9%) led to differential regulation of both *gpx1* and *gpx3*.

Combined exposure to PFOS and elevated CO₂ levels had unclear effects on transcription levels of both *gpx1* and *gpx3* since both isoforms were regulated differentially (Figure 16 A and B). Nevertheless, some observations are noteworthy: a CO₂-level dependent increase in the amount of transcript for *gpx3* at day 6 following combined exposure to elevated CO₂ and high PFOS (elevated CO₂+ 200µg PFOS/L), and a similar but insignificant effect on *gpx1* in the same exposure groups (elevated CO₂+high PFOS) (Figure 16B)

After exposure to elevated levels of CO₂ alone (0.3% and 0.9%), a general decline in enzyme activity below control levels was observed at day 6 and 9, with a significant drop observed only in the 0.3% CO₂ group at day 6 (Figure 16C). Only minimal differences were found between enzyme activity observed after exposure to PFOS alone and that observed in the untreated group as seen at day 3 and 6. This was however followed by an apparent reduction in GPx activity in the same exposure groups to levels well below control at day 9 (Figure 16C). Combined exposure to elevated CO₂ and PFOS caused an overall drop in GPx activity below control levels, but a significant drop was only observed in 0.3% CO₂+ 200µg PFOS/L exposure group at day 6 (Figure 16 C).

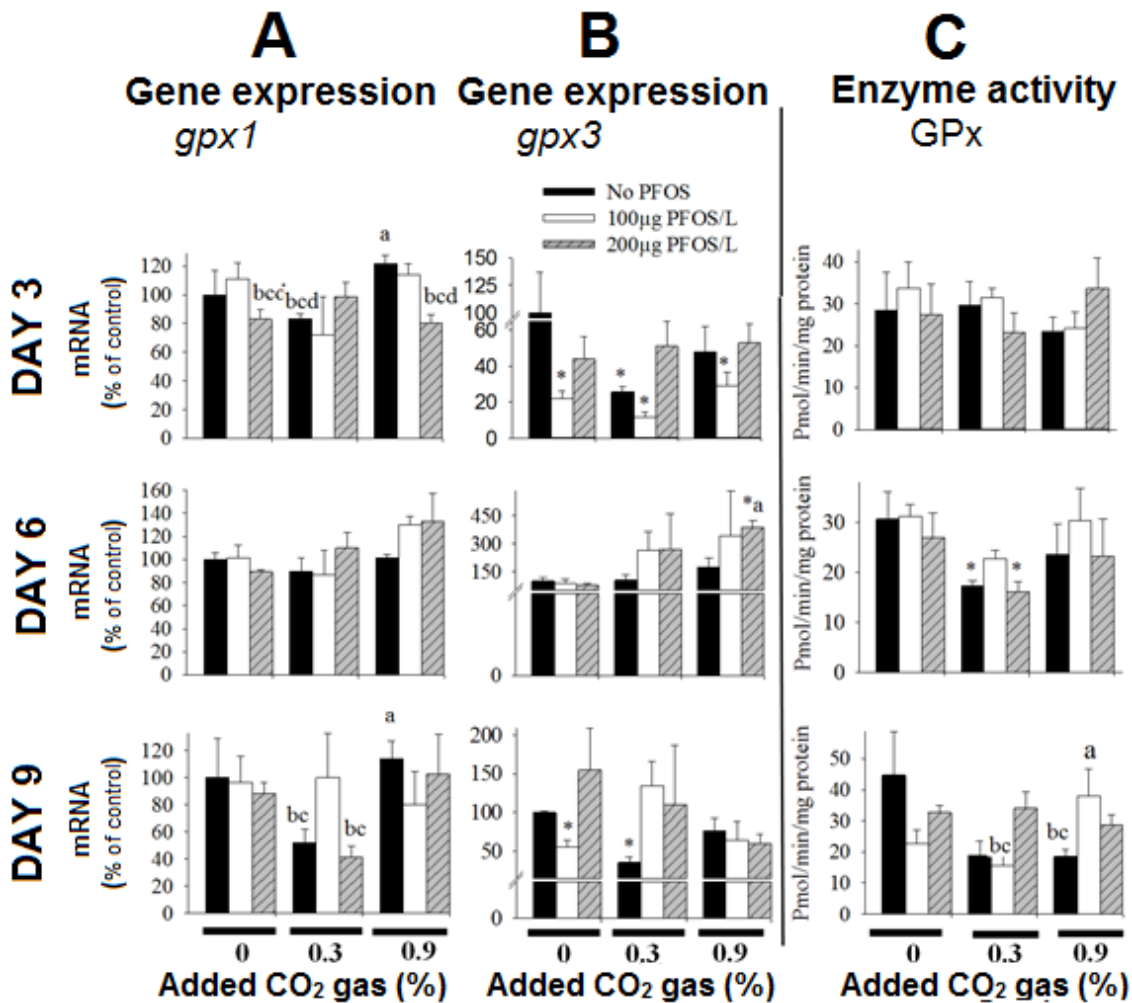


FIGURE 16: Changes in messenger RNA (mRNA) levels for **A:** *Glutathione peroxidase 1* (*gpx1*) expressed as percentage of control (n=3/4/5) ± standard mean of error (SEM), and **B:** *Glutathione peroxidase 3* (*gpx3*) expressed as percentage of control (n=3/4/5) ± standard mean of error (SEM). Changes in enzyme activity for *GPx* (Figure 12C) are expressed as pmol/minute/mg protein, with SEM (n=2/3). Juvenile Atlantic cod (*Gadus morhua*) were exposed to PFOS and elevated levels of dissolved CO₂, singly or in combination. Transcriptional changes were analyzed with quantitative RT-PCR using gene specific primer pairs, and enzyme activity was measured spectrophotometrically. Asterisks denote significant differences between exposure groups and control, while different letters indicate significant differences between exposure groups (one-way ANOVA with Tukey's post-hoc test (p < 0.05) for *gpx1* day 6+9, and *Gpx3* day 3, Games-Howell post hoc test (p < 0.05) for *gpx1* day 3 and *gpx3* day 6+9 and Kruskal-Wallis nonparametric one-way ANOVA (p < 0.05), followed by Dunn's nonparametric post hoc test for *gpx1* day 6 and enzyme assays).

3.5.6 GLUTATHIONE REDUCTASE (GR)

At day 3, exposure to PFOS alone caused an apparent PFOS-concentration dependent reduction in mRNA levels for *glutathione reductase* compared to control (though not significant), however the impact of PFOS exposure on the transcription of this gene was weak at further days of the experiment (Figure 17A). With the exception of the significant decrease in the 0.9% CO₂ alone exposure group at day 6, the overall changes in the transcript levels for *glutathione reductase* weakly differed from control levels following exposure to elevated CO₂ alone (Figure 17A). Apparently, combined exposure to elevated CO₂ and PFOS caused differential regulation of *glutathione reductase* at mRNA level.

Apparently, exposure to PFOS alone resulted to differential regulation GR activity (Figure 17B). An apparent biphasic response of GR activity was observed upon exposure to elevated CO₂ levels alone or in combination with PFOS. This is based on the observation that an insignificant increase in GR activity above control that was observed earlier on in the experiment (day 3) was reversed toward control levels at day 6 and followed by further decline below control levels at day 9 (Figure 17 B). Note that the negative impact observed at day 9 was only significant in fish exposed to low CO₂ (0.3% CO₂) alone or in combination with low PFOS concentrations (0.3%CO₂ +100µg PFOS/L) (Figure 17 B).

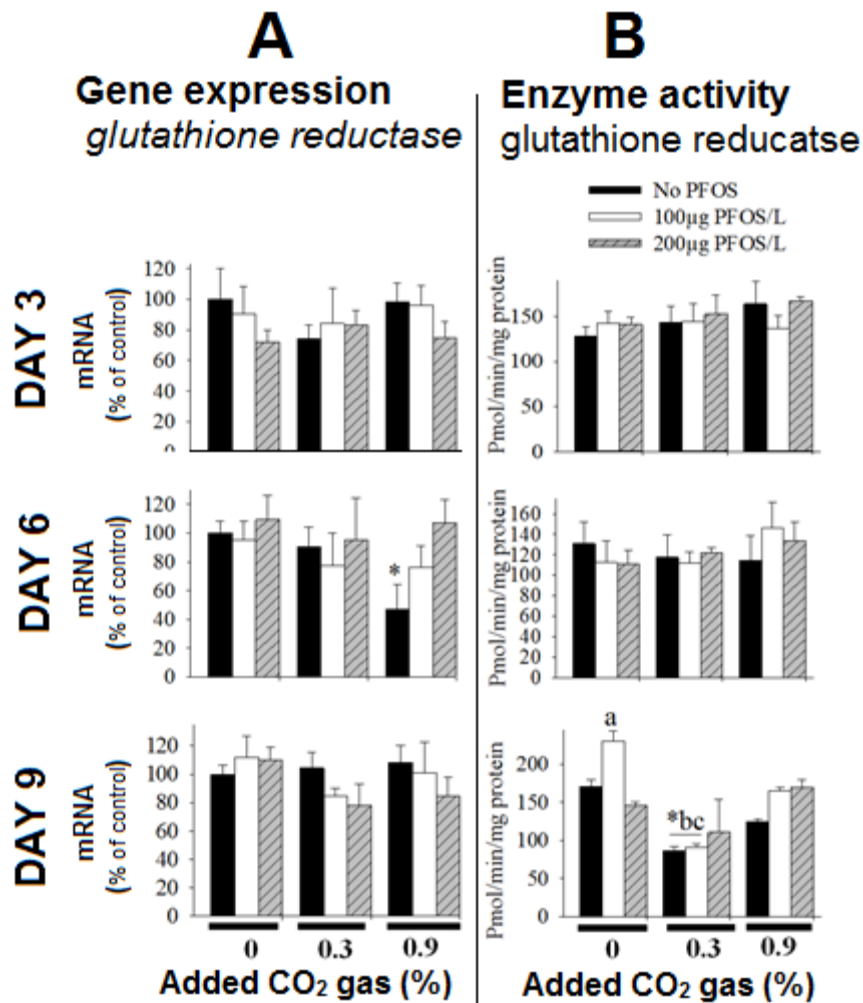


FIGURE 17: Changes in messenger RNA (mRNA) levels for **A:** *Glutathione reductase* (*GR*) expressed as percentage of control ($n=4/5$) \pm standard mean of error (SEM), and **B:** enzyme activity for *Glutathione reductase* (*GR*) expressed as pmol/minute/mg protein, with SEM ($n=2/3$). Juvenile Atlantic cod (*Gadus morhua*) were exposed to PFOS and elevated levels of dissolved CO₂, singly or in combination. Transcriptional changes were analyzed with quantitative RT-PCR using gene specific primer pairs, and enzyme activity was measured spectrophotometrically. Asterisks denote significant differences between exposure groups and control, while different letters indicate significant differences between exposure groups (one-way ANOVA with Tukey's post-hoc test ($p < 0.05$) for *GR* mRNA levels at day 9, and Kruskal-Wallis nonparametric one-way ANOVA ($p < 0.05$), followed by Dunn's nonparametric post hoc test for *GR* mRNA levels at day 3+6 and enzyme assays).

3.5.7 GLUTATHIONE S-TRANSFERASE (GST)

At day 3 and 6, weak changes in GST activity were observed after exposure to PFOS alone compared to control, however, enzyme activity increased to levels above control at day 9 (though not significant) (Figure 18). Upon exposure to elevated CO₂, GST activity generally differed weakly from enzyme activity levels in the unexposed groups. An insignificant increase in GST activity above control levels was observed following combined exposure to high CO₂ and high PFOS levels (0.9%CO₂+200µg PFOS/L) at day 3 and 6, however this effect was reversed to levels below control at day 9 (though not significantly) (Figure 18).

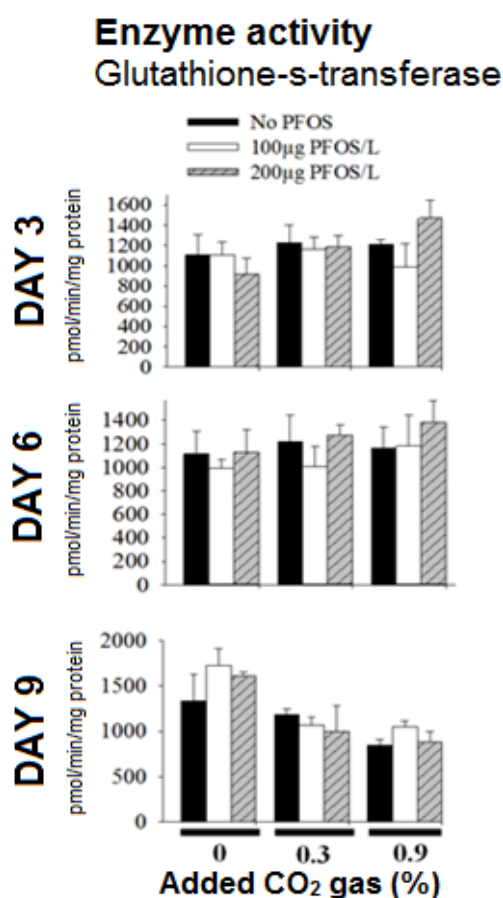


FIGURE 18: Changes in enzyme activity for *Glutathione S-transferase* (GST) expressed as pmol/minute/mg protein, with SEM (n=2/3). Juvenile Atlantic cod (*Gadus morhua*) were exposed to PFOS and elevated levels of dissolved CO₂, singly or in combination, and enzyme activity in the gills was measured spectrophotometrically. Asterisks denote significant differences between exposure groups and control, while different letters indicate significant differences between exposure groups (Kruskal-Wallis nonparametric one-way ANOVA (p < 0.05), followed by Dunn`s nonparametric post hoc test).

3.5.7 NON-ENZYMATIC ANTIOXIDANTS

In some few instances pooled samples were used in the measurements of cellular content of reduced glutathione and in thiobarbituric acid (TBARS) assay, a consequence of which was the inability to estimate variation within some exposure groups, hence the lack of error bars in the respective groups (Figure 19 and 20).

Reduced glutathione (GSH)

An apparent overall decline in GSH levels compared to control was observed after single exposure to PFOS or elevated CO₂ (0.3% and 0.9%) (Figure 19). However, differential changes in GSH content were observed upon combined exposure to PFOS and elevated CO₂ levels (Figure 19).

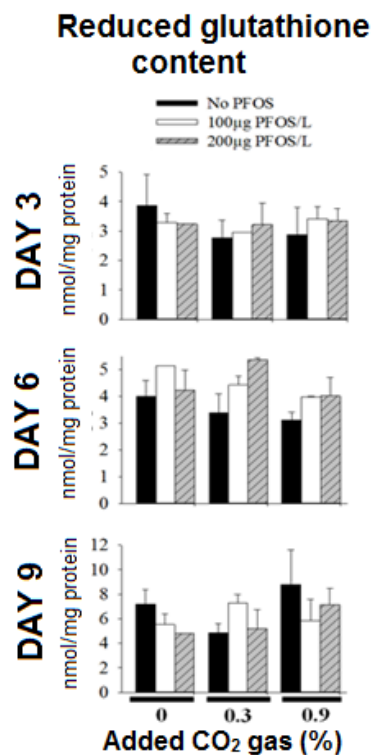


FIGURE 19: Changes in levels of reduced Glutathione (GSH) expressed as nmol/minute/mg protein, with SEM (n=1/2). Juvenile Atlantic cod (*Gadus morhua*) were exposed to PFOS and elevated levels of dissolved CO₂, singly or in combination, and glutathione levels in the gills were measured spectrophotometrically. Asterisks denote significant differences between exposure groups and control, while different letters indicate significant differences between exposure groups (Kruskal-Wallis nonparametric one-way ANOVA ($p < 0.05$), followed by Dunn`s nonparametric post hoc test).

3.6 EFFECTS ON LIPID PEROXIDATION

3.6.1 MALONDIALDEHYDE (MDA)

Apparently, an overall increase in MDA levels above control was observed in fish exposed to PFOS alone (Figure 20). At day 3, exposure to elevated CO₂ levels alone led to an apparent CO₂-level dependent increase in MDA levels (though not significant). This observation should be considered with caution due to the large standard deviation values for these exposure groups. The malondialdehyde response to hypercapnia was biphasic in nature since the apparent increase in MDA levels earlier on (day 3) was leveled back to control levels at day 6, and followed by a decline well below control levels at day 9 (though not significant) (Figure 20). A similar development of events was observed after combined exposure to both stressors, where an apparent increase in MDA levels observed at day 3 was followed by an apparent time-dependent decline at later days of the experiment, though none of the effects could be proved statistically (Figure 20).

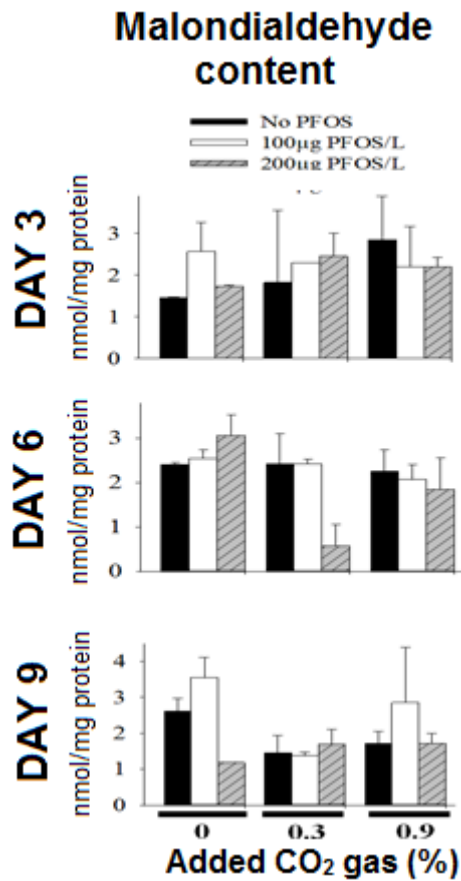


FIGURE 20: Changes in levels of reduced *Malondialdehyde* (MDA) expressed as pmol/minute/mg protein, with SEM (n=1/2). Juvenile Atlantic cod (*Gadus morhua*) were exposed to PFOS and elevated levels of dissolved CO₂, singly or in combination, and malondialdehyde levels in the gills were measured spectrophotometrically. Asterisks denote significant differences between exposure groups and control, while different letters indicate significant differences between exposure groups (Kruskal-Wallis nonparametric one-way ANOVA ($p < 0.05$), followed by Dunn's nonparametric post hoc test).

4.0 DISCUSSION

Several studies have associated the toxicity of PFOS and other high profile PFCs such as PFOS and PFOA in fish with the induction of oxidative stress (Arukwe and Mortensen, 2011, Wåggbø et al., 2012, Lorentzen, 2013)). Induction of oxidative stress under hypercapnic conditions has also been suggested by some studies (Denicola and Rafael, 2005, Rafael et al., 2001). However, there are very few studies that have investigated the potential toxic effects of PFOS on fish in a continuously changing aquatic environment driven by global climate change. This raises great concern given the reportedly increasing accumulation of anthropogenic CO₂ into aquatic environment (IPCC, 2013) and the global distribution of PFCs (PFOS) (Renner, 2001). The present study reports the effects of single or combined exposure to an emerging POP (PFOS) or elevated CO₂ levels (representative of ocean acidification) on oxidative stress responses in the gills of juvenile Atlantic cod.

4.1 ANALYTICAL METHODS

4.1.1 EVALUATION OF real-time PCR PROCEDURES

The success of a two-step real-time PCR (reverse transcription followed by quantitative PCR) as an analytical method for gene expression is greatly dependent on the quality of early upstream processes such as RNA isolation and complementary DNA (cDNA) synthesis (Fleige and Pfaffl, 2006). This is because errors introduced at these early steps could significantly compromise the efficiency, sensitivity and accuracy of real-time PCR, thereby increasing the risk of providing erroneous results (Invitrogen, 2008). Collection of high quality RNA (pure and intact) is important for the efficiency of reverse transcription step (RT) in which the template for real-time PCR process is generated. Well aware that RNA quality could be readily compromised by intracellular nucleases and/or different components of body fluids such as blood and bile, all tissue samples used in this study were embedded in TRIzol® reagent and snap frozen in liquid nitrogen. An RNA-purity check was performed with the help of nanodrop, and A260/A280 ratio of above 1.8 was registered for all samples. This was an indication of “clean” RNA samples (Pfaffl, 2004), which were thereafter converted to cDNA.

The downside of the nanodrop method is its insensitivity to degraded RNA and hence the inability to check for RNA integrity. The presence of intact RNA in extracts was verified through gel electrophoresis on randomly chosen RNA samples, with single band for 18S rRNA and 28S rRNA observed for each sample.

Because errors introduced at the cDNA synthesis stage are likely to be amplified in downstream PCR steps, thoughtful planning and execution of this procedure is extremely important for the success of real-time PCR and the reliability of derived results (Bustin and Nolan, 2004). High quality starting material was used for cDNA synthesis in the present study with A260/A280 > 1.8 and RNA concentration > 100 ng/ μ L just as recommended (Bustin and Nolan, 2004, Pfaffl, 2004). For maximum coverage of cellular RNA content, oligo-dT primers rather than sequence specific primers were used for cDNA synthesis.

Specificity, efficiency and accuracy of quantitative real-time PCR (qPCR) are greatly dependent on primers. Primers should be specific for the gene of interest (with high selectivity for cDNA rather than genomic DNA), and less likely to form primer-dimers or secondary intramolecular structures (Invitrogen, 2008). This is why primer functionality was tested before proceeding to qPCR procedures. This was done by using gene specific primer-pairs in PCR amplification of a cDNA pool collected from Atlantic cod, followed by separation of PCR product by gel electrophoresis, the observation of only one band per well indicated presence of a single PCR product and hence verification of primer functionality.

Due to the use of gene-specific high quality primers, only one amplification product is expected at the end of each qPCR assay. Because each PCR product has specific properties such as size, GC content, and melting point, the specificity of qPCR products is verified through dissociation curve analysis (Pfaffl, 2004, Bustin, 2000). Performance of this analysis revealed that all amplification products in each qPCR assay peaked at the same melting point, thereby indicating the presence of a single amplification product. Further verification was done by separation of qPCR products from randomly chosen samples on agarose gel electrophoresis, which also revealed single bands of expected size.

4.1.2 NORMALIZATION OF qPCR DATA

Experimental inconsistencies introduced at the different stages including RNA isolation, reverse transcription and qPCR amplification are among the sources of variability in qPCR. If not eliminated this variability could potentially lead to erroneous interpretation of the data and misleading conclusions (Invitrogen, 2008). The effects of variability can be neutralized through normalization of the data, which can be done via two strategies; relative or absolute. Under the relative strategy, qPCR data is normalized to a normalizer gene (also known as reference gene or “housekeeping gene”). However, use of this this method requires unregulated expression of the reference gene under different exposure conditions, which has been demonstrated not to be the case for those genes that have so far been employed including β -actin, glyceraldehyde-6-phosphshate dehydrogenase and others (Arukwe, 2006, Bustin, 2000). If normalizer genes are to be used, then one has to prove their constant expression under the exposure conditions in question. Under the absolute strategy, the data is normalized to a pre-made standard curve. A dilution series is made from known concentrations of linear plasmid containing the amplicon of interest, and then qPCR amplified simultaneously with test samples. A standard curve is generated in which each of the plasmid concentrations are plotted against a specific C_t value. The unknown sample C_t values are normalized to this standard curve, to determine the number of mRNA copies initially present in the samples (Pfaffl, 2004). Normalization to standard curves is widely considered to be a sufficient and accurate method for determination of the copy number of mRNA for the gene of interest. In this study, all qPCR data was normalized to a standard plot that was created from plasmids containing the *cyp19* (*aromatase*) gene.

4.1.3 MALONDIALDEHYDE AND THIOBARBITURIC ACID (TBARS)

Due to its cheapness and relative ease, the TBARS test is widely used for the measurement of cellular content of malondialdehyde (MDA) a well-known product of lipid peroxidation. In this procedure, thiobarbituric acid is added to the test samples and heated at low pH, the resultant pink chromogen (MDA) is measured spectrophotometrically. However, precaution should be taken when using data on MDA levels derived from TBARS test as an indicator of oxidative stress-mediated peroxidation of lipid systems. This is mainly because the TBARS test has been criticized for being relatively unreliable and has been associated with the risk of

providing inaccurate signals. This is because this test has been considered non-specific since it can detect other aldehydes in addition to MDA and also the fact that most, if not all of the MDA measured is a product of decomposition of lipid peroxides, which are produced during the acid-heating stage. Peroxide decomposition generates radicals which could in turn initiate lipid peroxidation processes, hence potentially causing undesired amplification of the measured signal (Barry and Susanna, 1993).

4.1.4 EVALUATION OF STATISTICAL ANALYSIS

Statistically significant differences between the means of different exposure groups are more likely to be detected by parametric tests such as one-way ANOVA compared to non-parametric tests, this is due to their larger statistical power. However, their stringent assumptions such as normality of dataset, which are often difficult to meet, allow for the application of less stringent but also less robust non-parametric test. The probability of detecting statistically significant group mean differences is diminished upon application of non-parametric tests. Statistical analysis is also influenced by sample number (direct relationship), and variation among individuals (inverse relationship). High variability can reduce statistical power during hypothesis testing. Nonetheless, variation between individuals is common in biological systems due to individual differences in response to different conditions. In addition to biological variation, technical variations are inevitably introduced by the operator at different phases of the experiment such as tissue extraction, RNA isolation, reverse transcription and PCR amplification (Invitrogen, 2008). In this study, statistical significance was largely not proved probably due to small sample size ($n = 2-5$), relatively high variation within some exposure groups, and occasional used of non-parametric tests. However, a lack of significant does not necessarily mean that the difference/effect does not exist (Gunnar, 2005, Helmut, 2008), or lack of biological significance, for this reason statistically insignificant results were also discussed, though more emphasis was put on statistically significant results.

Further analysis of the data was performed with Principle component analysis (PCA) method in order to find possible patterns in oxidative stress responses and the different exposure regimes that could be associated with them. PCA analysis was performed on normalized real-

time PCR data and data for enzyme activity as well as content of MDA and glutathione-and the data was analyzed in groups based on the sampling days (3, 6 and 9). All PCA models had poor predictive properties since their goodness of prediction (Q^2X) value was low-ranged from (0.8% to 19.9%). In addition, observations from the score and loading plots showed no clustering of the variables and samples. Because of the poor predictive properties of the PCA models and the absence of clustering of variables and samples, PCA analysis seemed not to provide any useful information-therefore, a decision was made not to include the PCA results in this thesis.

4.2 EXPERIMENTAL SETUP

4.2.1 PFOS EXPOSURE, UPTAKE AND BIOCONCENTRATION

The uptake of water-borne PFOS by fish may be influenced by several confounding factors, with this in mind, exposure to PFOS was done under normocapnic conditions before initiation of CO₂ exposure in order to avoid any influence that dissolved (saturated) CO₂ could potentially have on PFOS uptake by the fish. This would also allow us to investigate PFOS toxicity following its bioconcentration, and how this toxicity may change under hypercapnic conditions. The rationale behind the short-term experimental design was to allow for bioaccumulation of PFOS by exploiting its high bioconcentration rate, and poor elimination from the exposed organism (Zhang et al., 2009, Kannan et al., 2003). Values of measured body PFOS burden show that substantial levels of PFOS were accumulated after exposure to both high and medium nominal PFOS concentrations (100 and 200 µg/L), since all concentrations were well above the detection limit (10 ng/g wet weight). Several field studies have reported the presence of high PFOS levels in fish from industrialized and/or heavily populated areas: 1100 ng/g PFOS was detected in the liver of tilapia (*oreochromis sp*) and Japanese seaperch (*Lateolabrax japonicus*) in two heavily polluted rivers (nam-kan and tour-chyan) in Taiwan (Tseng et al., 2006). Average PFOS concentrations of 3673ng/g was detected in the bile of mullet (*mugil incilis*) at an industrialized site in Colombia- Cartagena bay (Olivero-Verbel et al., 2006). Put in context of the high PFOS burden detected in fish and fish-eating animals in industrialized and/or highly populated areas, the high body PFOS burden used in the present study is realistic.

4.2.2 DISSOLVED CO₂ LEVELS IN EXPERIMENTAL TANKS

Field studies on ocean acidification have reported hydrogen ion concentration to be more than 30% higher than it was for 200 years ago (Potera, 2010). Ocean acidification has been predicted to continue and ocean pH has been projected to fall by 0.3-0.5 units within the next century and 0.8-1.4 units by 2300 (Caldeira and Wickett, 2005). In the present study, saturation of experimental water with moderate and high CO₂ levels resulted to a drop in pH ranging from 0.4 to 0.9 units. Seen in light of the projected drop in ocean pH mentioned above, the pH values measured in the current study can be considered realistic.

4.3 EFFECTS ON PEROXISOMAL- β OXIDATION

The mechanisms through which high profile perfluoro-alkyl acids such as PFOS exert their toxicity are yet to be fully understood. Nevertheless, PFOS toxicity has been associated with PPAR mediated peroxisomal proliferation in several species including rodents, monkeys, fish and humans (Takacs and Abbott, 2007b, Sohlenius et al., 1993, Ikeda et al., 1987). However, sensitivity of PPARs and their target genes towards PFCs may be dependent on PPAR isoform and the organism in question. Generally, PPAR β response to PFOS has been suggested to be weaker compared to PPAR α and PPAR γ across several species including mouse, rat and humans (Takacs and Abbott, 2007b, Seacat et al., 2003, Sohlenius et al., 1993), and similar tendencies have also been suggested for several fish species. (Wåggbø et al., 2012, Hoff et al., 2003a).

Additionally, conflicting results have been reported about the effect of PFCs on the expression of Acyl-CoA oxidase-: Oakes and colleagues (2005) reported a moderate increase in ACOX1 activity in five different fish species; fathead minnow (*pimehales promelas*), rainbow trout (*oncorhynchus mykiss*), creek chub (*semotilus atromaculacus*), spottail shiner (*notropishudsonius*), and white sucker (*catostomus commersoni*) in a short-term PFOS exposure (3 mg/L) experiment. In other studies, exposure of fish to PFOSA-a precursor for PFOS or perfluorododecanoic acid showed no significant effect on ACOX enzyme activity or gene transcription (Wåggbø et al., 2012, Liu et al., 2008).

In the present study, exposure to PFOS alone generally caused rather minimal and insignificant changes in gill mRNA levels for *ppar β* and its downstream target gene-*acox1*, compared to unexposed group. It is possible that this apparently weak response could be attributed to the fact that PPAR β is ubiquitously/abundantly expressed in most organs (Michalik et al., 2006), and probably involved in basic cellular processes such as cell proliferation, differentiation and membrane turnover (Braissant and Wahli, 1998). It is therefore arguable that further induction following exposure to PFOS was difficult to detect due to the high base-line transcript levels of *ppar- β* .

Alternatively, the fish used in this study were starved throughout the experiment and starvation has been associated with increased utilization of lipid stores for energy production (Li et al 2007). Due to its reported involvement in the regulation of global lipid metabolism, it is possible that *ppar- β* was expressed at relatively high levels throughout this short experiment to allow increased β -oxidation of fatty acid as an adaptive response to starvation, and hence making it difficult to detect any transcriptional alterations upon further stimulation by activating agents such as PFOS.

It could also be speculated that the weak responses of peroxisomal- β oxidation related genes observed in gills of juvenile Atlantic cod following exposure to PFOS alone could have been a potential mechanism for dealing with water-borne xenobiotic compounds. This speculation is based on the fact that fish gills are in intimate first contact with aqueous external environment that usually contains a mixture of numerous water-borne compounds, several of which are potential activators of pleiotropic transcriptional factors including PPAR β . Since activated-PPAR β has been suggested to be involved in the regulation of several cellular processes, it could be arguable that the weak responses to water-borne PFOS may have been a potential mechanism of avoiding unnecessary perturbation of different cellular processes that are direct or indirect downstream targets for PPAR β .

This apparently weak effect of PFOS on *ppar β* and its target gene (*acox*) appears to be in agreement with the suggestion of a general low sensitivity of fish species towards peroxisome proliferators (Hoff et al., 2003a, Pretti et al., 1999). Additionally, after exposure of PFOS (2ppm) to juvenile Thicklip grey mullets (*chelon labrosus*) for 2 and 16 d, it was concluded that PFOS did not behave as a typical peroxisome proliferator (Bilbao et al., 2010). On the contrary, this observation is in conflict with studies that have demonstrated peroxisome-

proliferation activity of PFOS in several fish species (Arukwe and Mortensen, 2011, Oakes et al., 2005). Possible explanations for this discrepancy could be differences in experimental setup (exposure dosage and duration), and study-tissue (due to the possibility of tissue specific responsiveness to PFOS).

Despite the minor transcriptional changes of *pparβ* following exposure to elevated CO₂ levels compared to normocapnia (control), a drop in *acox* mRNA levels to levels below control (though not significant) was generally observed under hypercapnic conditions (0.3% or 0.9% CO₂). This apparent reduction effect of hypercapnia on peroxisomal-β oxidation observed in this study is in agreement with previous studies that have reported an association between an overall metabolic depression and hypercapnia in marine organisms (Langenbuch, 2002, Kenneth et al., 2011, Portner et al., 1998).

On the other hand, combined exposure to elevated CO₂ and PFOS caused an insignificant increase in *pparβ* transcription as seen in different exposure groups; 200µg PFOS/L+0.3% CO₂, 100µg PFOS/L+0.9% CO₂ and 0.9% CO₂+PFOS at day3 and 6, respectively. Although not statistically proven, this observation appears to suggest that gill *pparβ* was more responsive when the stressors were given in combination rather than singly. Note that the apparently negative effect of hypercapnia on the transcription of *acox* was also reversed in the presence PFOS, however, this occurred predominantly under high CO₂ levels where *acox* mRNA levels were either restored back to control levels (day 9) or slightly but insignificantly increased above control (day 3 and 6). This observation is in agreement with observations made in a similar study recently done in our laboratory showing that combined exposure to PFOS and elevated CO₂ (at identical levels like in the current study) caused an increase in mRNA levels of hepatic *pparβ* and its target gene, Acyl-CoA dehydrogenase (*acod*) in juvenile Atlantic cod (Lorentzen, 2013)

It is possible to consider the observed increase in transcript levels for *pparβ* and *acox* (though not significant) upon exposure to PFOS under hypercapnic conditions as an adaptive response to increase in energy demand required to deal with the stress created by both stressors. This apparent hypercapnia-related modification of fish sensitivity to PFOS is in agreement with the general view in toxicology that environmental factors including; pH, ambient temperature,

and salinity may influence toxicokinetic and toxicodynamic properties of pollutants, and could also potentially alter their toxicities (Doris et al., 2007)

4.4 EFFECTS ON ANTIOXIDANT SYSTEMS

Antioxidant responses are commonly used in assessment of biological effects of environmental pollutants in several organisms. This is achieved through measurement of variations of transcriptional expression of several antioxidant and detoxification genes as well as the functional activity of the gene products (enzyme activity) (Regoli et al., 2011). However, antioxidant responses could be difficult to elucidate or predict, with inconsistent and/or contradictory results commonly arising between variations in transcript expression of genes and catalytic activity of the gene products (Giuliani et al., 2013). Nevertheless, transcriptional changes are considered to be more sensitive to contamination, hence their utilization as biomarkers of exposure, while biochemical responses such as enzyme activity are considered to function more efficiently as biomarkers of effect (Giuliani et al., 2013, Regoli et al., 2011).

Generation of ROS is considered an obligatory outcome of the expression/activity of fatty acid β -oxidation related genes such as PPARs and ACOX, therefore measures of oxidative stress are commonly used in the evaluation of whether toxicity of a given pollutant is attributed to oxidative stress-related damage arising from peroxisomal proliferation (Oakes et al., 2005). However, as already mentioned, conflicting results have been reported about fish sensitivity to typical mammalian peroxisome proliferators such as PFOS, hence making it debatable if PFOS related oxidative stress responses should be attributed to peroxisomal or extra-peroxisomal sources.

Exposure to PFOS alone generally caused differential changes in the expression of *ppar β* and *acox*, as well as all antioxidant enzymes (SOD, CAT, GPX and GR). Although unclear, the alterations in expression of antioxidant enzymes could be considered as an adaptive response to oxidative stress, however, it is likely that sources of free radicals may be extra-peroxisomal rather than peroxisomal.

Alternative intracellular sources of ROS include autoxidation reactions and the “leakage” of electrons from the electron-transport chains to oxygen (Gary, 1990). Generation of superoxide

anions in association with PFOS exposure may be attributed the ability of PFOS to disrupt phospholipid bilayers (Lehmler et al., 2006, Hu et al., 2000, Hu et al., 2002a, Takacs and Abbott, 2007b). Upon interaction with several of its components, PFOS can disrupt the electron transport chain (ETC) located in the mitochondrial inner membrane which may be followed by leakage of partially reduced oxygen intermediates (ROS) into cytosol, hence generation of oxidative stress (Starkov and Wallace, 2002). This mitochondrial respiratory dysfunction and the resultant oxidative stress has been associated with the induction of mitochondrial membrane potential transition (MMPT), and cellular necrosis or apoptosis (Sokol et al., 2001). Generally, the transcriptional expression and activity of cytosolic antioxidants (SOD and GPx) following exposure to PFOS alone was differential (with the exception of *gpx3*). Nevertheless, these observations may indicate transient generation of intracellular ROS upon PFOS exposure.

There could be several explanations for this unclear response all of which are speculative; for instance, it could be speculated that the impact of PFOS could be tissue specific. In a 14 d *in vivo* experiment where juvenile Atlantic salmon were forced-fed with 0.2mg/kg PFOS, organ specific changes in peroxisomal β -oxidation and oxidative stress responses were observed, with greater severity in kidney than in the liver (Arukwe and Mortensen, 2011). In another study, Oakes and colleagues (2005) demonstrated that exposure to 3mg PFOS/L for 14-28 d predominantly provoked hepatic compared to gonadal oxidative stress responses in female fathead minnow (*pimephales promelas*). Additionally, antioxidant responses were demonstrated to be generally higher in liver than gills of juvenile European eel (*Anguilla Anguilla*) exposed to moderately or highly polluted sediments (Regoli et al., 2011).

It may be possible that the observed ambiguous response to PFOS exposure in the gills might have been due to several tissue specific factors including; oxidative metabolic/biotransformation and bioconcentration capacity and cellular machinery (which is lower in fish gills). Additionally, fish gills are not only a site for uptake of water-borne toxicants, but also a major site of depuration of these compounds (Martin et al., 2003). It may be possible that a continuous flux of water-borne PFOS in and out of the gills could have made it difficult to allow accumulation of PFOS to sufficient concentrations needed to provoke a clear response in this tissue.

There are conflicting reports about the association of lipid peroxidation with PFOS exposure. In an *in vivo* 8d experiment where juvenile Atlantic cod were exposed to PFOS (0.2 mg PFOS/kg fish), hepatic malondialdehyde (MDA) levels significantly increased only at day 2 but no significant changes were observed on further days-day 5 and 8, while renal MDA levels hardly changed compared to the control (Arukwe and Mortensen, 2011). Additionally, in an *in vitro* study where hepatocytes from freshwater tilapia (*Oreochromis niloticus*) were exposed to 0,1,5,15 and 30 mg PFOS/L for 24 hours, no significant changes in MDA levels were observed (Liu et al., 2007). In this study, the measured levels of MDA appear to have generally increased (though not significantly) following exposure to PFOS alone, an indication of lipid peroxidation since MDA is a well-known product of this process. However, due to reasons already given concerning the TBARS test, this observation should be considered with precaution.

High intracellular CO₂ levels as is the case during hypercapnia could be associated with oxidative stress. Generation of ROS and RNS under hypercapnic conditions may occur either via peroxynitrite pathway (Denicola and Rafael, 2005), or Fenton reaction (Sipe and Murphy, 1991, Garrick and Garrick, 2009). The later scenario may seem to be less likely since fish have been reported to efficiently compensate for acid-base disturbances through trans-epithelial transfer of acid-base equivalents via their gills with the help of membrane ion-exchangers such as Na⁺/H⁺ exchangers, Cl⁻/HCO₃⁻ exchanger, and Na⁺/K⁺ ATPase (Towle and Weihrauch, 2001). In other words, oxidative stress associated with hypercapnia may most likely arise from actual intracellular elevation of CO₂ levels rather than hypercapnia-related changes in pH.

The reaction yielding peroxynitrite has been reported to occur at a higher rate compared to SOD mediated dismutation of superoxide anions. Indeed, nitric oxide has been reported as the only known biological molecule produced at substantially high levels under pathological/stressful conditions to out-compete endogenous SOD for superoxide anions (Beckman and Koppenol, 1996). An example of the stressful conditions under which high levels of nitric oxide is produced is hypercapnia: In a 48 h *in vitro* study, Lang and colleagues (2000) demonstrated that more nitric oxide was produced by rat alveolar epithelial cells under hypercapnic conditions (5% or 15% CO₂) via increased activity of inducible nitric oxide synthase (iNOS). Reference to these findings should however be done with caution due to the huge differences in hypercapnic levels and test organisms.

Apparently, an overall decrease in SOD activity was observed following exposure to elevated CO₂ (0.3% and 0.9%), although this could not be proven statistically. The decrease in SOD activity could be associated with a decline in intracellular superoxide anion levels, and hence a subsequent reduction in the need for SOD. A partial explanation for the low superoxide anion levels could be their high consumption during formation of peroxynitrite—a process that is fast ($k = 6.7 \times 10^9 \text{ M}^{-1} \cdot \text{S}^{-1}$) (Rafael et al., 2001, Vesela and Wilhelm, 2002), and probably favored under hypercapnic conditions as mentioned above.

Generally, the transcriptional expression of *gpx3* and GPx activity decreased after exposure to elevated CO₂, though this effect was only significant at 0.3% CO₂. This drop in transcriptional expression and activity of glutathione peroxidase could indicate presence of low concentrations of hydrogen peroxide in the cytosol, and could be associated with the observed low SOD activity since hydrogen peroxide is a major product of SOD mediated dismutation of superoxide anions (Gary, 1990).

ROS and RNS generated via the peroxynitrite pathway under hypercapnic conditions could lead to oxidative damage of several biomolecules among others lipid components of cellular membranes (lipid peroxidation). At day 3, an apparent CO₂-level dependent insignificant increase in MDA levels above control was observed following exposure to elevated CO₂ alone (0.3% or 0.9%). This could indicate occurrence of lipid peroxidation during hypercapnia. However, this observation should be considered with precaution due to high the relatively big standard deviation values. However, this effect was reversed at further days of the experiment in an apparently time-dependent manner. The reason for the fall in MDA levels is unknown, but could be linked to the fact that MDA molecules are reactive electrophilic species and therefore cytotoxic, so they may have been eliminated via oxidation to CO₂ by aldehyde dehydrogenases (Siu and Draper, 1982, Draper et al., 1986)

A direct consequence of increased expression of peroxisomal β -oxidation related genes (particularly *acox*) observed after combined exposure to PFOS and hypercapnia is the generation of hydrogen peroxide. A corresponding increase in expression of catalase (peroxisomal scavenger of hydrogen peroxide) was also expected. Although transcriptional changes for *catalase* were generally differential, an apparent increase in mRNA levels in 0.3%CO₂+200 μ g PFOS/L and 0.9%CO₂+100 μ g PFOS/L exposure groups at day 3 and 0.9%CO₂+ PFOS exposure groups at day 6 is noteworthy. Although not significant, this

increase in transcription of *catalase* could be considered as an adaptive response to increased intracellular levels of hydrogen peroxide. Therefore, it could be arguable that exposure to PFOS under hypercapnic conditions could have possibly caused increased generation of energy via peroxisomal fatty acid β -oxidation, which in turn generated ROS.

Clear (not differential) changes in CAT activity occurred only after relatively durable exposure (day 9), where the enzyme activity dropped below control (only significant in the 0.3%CO₂+100 μ g PFOS/L group). This apparent time-dependent decrease in enzyme activity could be an indication that this antioxidant system could have been overwhelmed by huge amounts of hydrogen peroxide. This result seems to further support the suggested improvement of responsiveness of fish to PFOS (as a peroxisome proliferator) under hypercapnic conditions compared to normocapnia, hereby indicating that PFOS toxicity may most likely be ROS-mediated under hypercapnia. However, given the fact that the observed effects were largely not statistically proven and the existence of only a handful of similar studies (Lorentzen, 2013), more studies need to be done for the verification of this suggested positive effect of hypercapnia on the peroxisome proliferator activity of PFOS in fish.

The apparent CO₂ dependent increase in SOD activity upon combined exposure to high PFOS concentration (200 μ g PFOS/L) and elevated CO₂ at day 9 could indicate the presence of high cytosolic levels of superoxide anions, hence the augmentation of this adaptive mechanism responsible for elimination of these radicals.

An increase in SOD activity is expected to be followed by a corresponding increase in hydrogen peroxide levels. Glutathione peroxidase scavenges extra-peroxisomal hydrogen peroxide, and therefore the expression of the different isoforms of the *gpx* gene is expected to increase as an adaptive response to increased intracellular levels of hydrogen peroxide (Winston and Di Giulio, 1991, Arthur, 2000). Transcriptional regulation of *gpx1* and *gpx3* at day 6 seems interesting; mRNA levels of both isoforms increased following combined exposure to both stressors in an apparently CO₂ dependent manner, although this effect was clearer in the high PFOS+ elevated CO₂ exposure groups (200 μ g PFOS/L+ CO₂), and was statistically proven only for *gpx3*. This increase in transcriptional levels for *gpx* could be considered as an adaptive response to increased intracellular levels of hydrogen peroxide.

However, the observed increase in mRNA levels of *gpx1* and *gpx3* at day 6 appears not to have been translated into a corresponding increase in enzyme activity. On the contrary, GPx

activity dropped below control levels upon combined exposure to both PFOS and elevated CO₂, with a significant drop observed in the 200µg PFOS/L+ 0.3%CO₂ exposure group. A decrease in enzyme activity was also observed in the same exposure groups at day 9 (though not significant). This could indicate an inability to produce functional enzymes and most probably a compromised capacity of the cellular hydrogen peroxide scavenging systems upon combined exposure to both stressors.

ROS and RNS apparently generated upon combined exposure to PFOS and elevated CO₂ could be associated with occurrence of lipid peroxidation. At day 3, the levels of MDA increased (though not significantly) following combine exposure to both stressors (Figure 16), thereby indicating the occurrence of lipid peroxidation. However, for reasons already mentioned this effect was reversed in an apparently time-dependent manner at further days of the experiment.

4.4.1 EFFECTS ON GLUTATHIONE BASED ANTIOXIDANT RESPONSES

Generally, intracellular levels of reduced glutathione dropped below control (though not significantly) upon single exposure to PFOS or hypercapnia, while differential changes were observed following combined exposure to both stressors. The generally low levels of reduced glutathione could probably be attributed to its high consumption during direct or indirect (enzyme mediated) elimination of free radicals (ROS, RNS and reactive intermediates of lipid peroxidation) generated under the different exposure conditions. However, the capacity to replenish cellular GSH and therefore maintenance of a reduced redox-state in the gill cells appears to have been relatively weakened under hypercapnia alone or in combination with PFOS. This is due to the reduction in enzyme activity for glutathione reductase observed under the above-mentioned conditions especially at day 9.

Upon exposure to PFOS alone, weak changes in GST activity were observed at day 3 and 6 followed by an increase at day 9 (though not significant). This could imply that the involvement of GST in PFOS elimination might have occurred at later rather early stages of exposure. This “postponed” response might have been an attempt to avoid unnecessary

consumption of GSH (which is costly to produce) at earlier stages of chemical insult. The increased GST activity following combined exposure to high levels of both stressors (200µg PFOS/L+0.9 CO₂) observed at day 3 and 6 may indicate increased GST mediated elimination oxidative stress products. However, the reversal of this effect to levels well below control at day 9, coupled with the apparent CO₂ dependent drop in activity in groups exposed to elevated CO₂ levels alone observed at the same day, might have been due to overwhelming of this detoxification pathway by oxidative stress products generated under the respective exposure conditions.

Note that with the exception of SOD activity in the high PFOS+ elevated CO₂ exposure groups (200µg PFOS/L+CO₂), an overall decrease in enzyme activity of all antioxidants was observed at day 9 especially in groups exposed to hypercapnia alone or in combination with PFOS. It is possible that this apparent time-dependent decline in antioxidant enzyme activity may be attributed to oxidative impairment related to oxidative stress or overwhelming of the antioxidant enzymes (Giuliani et al., 2013). This result is an indication of a possibility of compromised capacity of antioxidant defenses following exposure to hypercapnia alone or in combination with PFOS, a consequence of which is an imbalance between pro-oxidants and antioxidants-oxidative stress-hence occurrence of oxidative stress.

Several vital biological molecules are potential targets for oxidative damage under oxidative stress conditions, whose damage could result into numerous deleterious consequences for the affected organism (Storey, 1996). Introduction of single or double strand breaks in DNA or oxidative modification of the DNA bases by ROS or RNS can cause loss-of-function mutations resulting into deleterious effects not only for the victim such as increased risk of cancer development but also for future generations if germ cells are affected (Anthony and Murphy, 1995). Upon oxidative attack, the structure of proteins could be modified which may potentially compromise their functionality (Hyslop et al., 1988), and thereby disrupting several vital protein-dependent cellular processes.

Several important cellular processes are dependent on properly functioning intact membranes (plasma membrane and intracellular organelle membranes), these include; different extra-cellular signal transduction pathways by components of plasma membrane (Campbell et al., 2008), mitochondrial-based energy production (Bruce et al., 2007) and compartmentalization of otherwise cytotoxic substances in specific organelles (Clark, 2010). Lipid peroxidation can

alter membrane integrity and structure, consequently resulting into impairment several of the above-mentioned membrane functions. Many organisms are able to deal with oxidative stress by hindering or mitigating several of oxidative stress related damages. However, allocation of huge amounts of energy to antioxidant defenses and/or containment of oxidative stress related damage (repair or elimination of damaged substances) may leave less energy available for vital processes including; reproduction, growth, hence a potential reduction in the fitness of the organism (Heugens et al., 2001).

Taken together, the results in this study indicate that generation of oxidative stress occurred under all exposure conditions in the gills of Atlantic cod, however, this effect was clearer upon exposure to elevated CO₂ levels alone or in combination with PFOS.

4.5 EFFECTS ON MEMBRANE PHOSPHOLIPID HOMEOSTASIS

A noticeable but insignificant increase mRNA levels for both *pemt* and *pisd* at day 9 was observed following exposure to high PFOS concentrations under normocapnia compared to control. Additionally, an increase in mRNA levels for *pemt* occurred only after exposure to high CO₂ levels alone or in combination with PFOS (Figure 9). There is a discrepancy between these results and those reported in a similar study (with identical experimental setup as in the current study) (Lorentzen, 2013). In this study, no significant effects were observed in hepatic *pemt* and *pisd* after single or combine exposure to elevated CO₂ (0.3% and 0.9%) and PFOS (100µg or 200µg PFOS/L), and this was attributed to the organisms' choice not to invest energy in unnecessary metabolic processes. This discrepancy could be attributed to differences in test tissue. Unlike the liver, the gills were in direct contact with the exposure-medium, which was saturated with CO₂ or also contained dissolved membrane active compounds (PFOS). It could be speculated that phospholipid composition of membranes in gill cells is likely to change as the exposed organisms attempt to maintain the membrane functionality in gill cells.

5.0 CONCLUSION

Taken together, these results indicate that PFOS and hypercapnia might induce oxidative stress in fish-although the observed changes in the expression of antioxidant genes were generally unclear (differential) in fish singly exposed to PFOS or elevated CO₂. Generally, single exposure to PFOS or elevated CO₂ levels had a weak effect on the transcription of peroxisomal β -oxidation related genes (*ppar- β* and *acox*). This raises some questions about the extent to which peroxisomal fatty acid β -oxidation pathway contributes to intracellular oxidative stress. However, *ppar- β* and *acox* were more responsive to PFOS under hypercapnic conditions, as mRNA levels of these genes generally increased above control (though not significantly) in fish exposed to a combination of both stressors. This was an indication that peroxisomal fatty acid β -oxidation pathway might be involved in the induction of oxidative stress under such conditions. An increase in extra-peroxisomal ROS generation was also suggested to have occurred following combined high PFOS (200 μ g) and elevated CO₂ levels. This was due to the apparent CO₂ dependent increase in mRNA levels of *gpx1*, *gpx3* at day 6 and SOD activity at day 9 observed in fish exposed to a combination of high PFOS (200 μ g) and elevated CO₂ levels.

The apparent positive interactive effect of water-borne PFOS and seawater hypercapnia on oxidative stress responses observed in this study may serve as a warning signal about the potentially huge environmental challenges faced by several aquatic organisms given the widespread distribution of PFOS and the increasing release of anthropogenic CO₂ into atmosphere which is in turn absorbed by aquatic environment.

6 FUTURE PERSPECTIVES

In order to get an extensive understanding of how aquatic organisms may be impacted by combined exposure to PFOS and environmental hypercapnia, more studies need to be done on several aquatic organisms, especially those that dwell at the surface of oceans since most of the anthropogenic CO₂ in the atmosphere is absorbed by ocean surface waters.

References

- ABBOTT, B. D., J. WOLF, C., DASA, K. P., ZEHRA, R. D., JUDITH E. SCHMIDA, LINDSTROMB, A. B., STRYNARB, M. J. & LAUA, C. 2009. Developmental toxicity of perfluorooctane sulfonate (PFOS) is not dependent on expression of peroxisome proliferator activated receptor-alpha (PPAR) in the mouse. *Reproductive Toxicology*, 27, 258–265.
- AHMAD, T. H., FATIMA, M., CHAND, H. S., JAIN, S. K., ATHAR, M. & RAISUDDIN, S. 2000. Induction of hepatic antioxidants in freshwater catfish (*Channa punctatus* Bloch) is a biomarker of paper mill effluent exposure. *Biochim. Biophys. Acta*, 1523, 37–48.
- ANTHONY, P. B. & MURPHY, J. A. 1995. Reactions of oxyl radicals with DNA. *free radic biol Med*, 18, 1033-1077.
- ARTHUR, J. R. 2000. The glutathione peroxidases. *CMLS, Cell. Mol. Life Sci*, 57, 1825–1835.
- ARUKWE, A. 2006. Toxicological Housekeeping Genes: Do They Really Keep the House? *Environ. Sci. Technol*, 40 (24), 7944–7949.
- ARUKWE, A. & MORTENSEN, A. S. 2011. Lipid peroxidation and oxidative stress responses of salmon fed a diet containing perfluorooctane sulfonic- or perfluorooctane carboxylic acids. *Comparative Biochemistry and Physiology, Part C*, 154, 288–295.
- BALLANTYNE, A. P., C. B. ALDEN, MILLER, J. B., TANS, P. P. & WHITE, J. W. C. 2012. Increase in observed net carbon dioxide uptake by land and oceans during the last 50 years. *Nature*, 488, 70–72.
- BARRY, H. & SUSANNA, C. 1993. Lipid peroxidation: its mechanism, measurement, and significance. *Am J Clin Nutr*, 52, 715-725.
- BARRY, M., FORMAN, JASMINE, C. & RONALD, M. E. 1997. Hypolipidemic drugs, polyunsaturated fatty acids, and eicosanoids are ligands for peroxisome proliferator-activated receptors alpha and delta. *Proc. Natl. Acad. Sci. USA*, 94, 4312–4317.
- BECKMAN, J. S. & KOPPENOL, W. H. 1996. Nitric oxide, superoxide, and peroxynitrite: the good, the bad, and the ugly. *Am J Physiol* 271, C1424-C1437.
- BERNARD, M., SAMUEL, P. D. V. & SASON, S. 2004. Mechanism of Oxidation Reactions Catalyzed by Cytochrome P450 Enzymes. *Chem. Rev*, 104, 3947–3980.
- BIJLAND, S., RENSEN, P. C. N., PIETERMAN, E. J., MAAS, A. C. E., HOORN, J. W. V. D., VAN, M. J., ERK, L. M. H., DIJK, K. W. V., CHANG, S.-C., EHRESMAN, D. J., BUTENHOFF, J. L. & PRINCEN, H. M. G. 2011. Perfluoroalkyl Sulfonates Cause Alkyl Chain Length–Dependent Hepatic Steatosis and Hypolipidemia Mainly by Impairing Lipoprotein Production in APOE*3-Leiden CETP Mice. *TOXICOLOGICAL SCIENCES*, 123(1), 290–303.
- BILBAO, E., RAINGEARD, D., DE CERIO, O. D., ORTIZ-ZARRAGOITIA, M., RUIZ, P., IZAGIRRE, U., ORBEA, A., MARIGOMEZ, I., CAJARAVILLE, M. P. & CANCIO, I. 2010. Effects of exposure to Prestige-like heavy fuel oil and to perfluorooctane sulfonate on conventional biomarkers and target gene transcription in the thicklip grey mullet *Chelon labrosus*. *Aquatic Toxicology* 98, 282–296.
- BIOTEKINSTRUMENTSINC 2006. The Importance of the 240 nm Absorbance Measurement - The A260/A280ratio just isn't enough anymore (Winooski, VT, USA).

- BJORK, J. A. & WALLACE, K. B. 2009. Structure-Activity Relationships and Human Relevance for Perfluoroalkyl Acid-Induced Transcriptional Activation of Peroxisome Proliferation in Liver Cell Cultures. *TOXICOLOGICAL SCIENCES*, 111(1), 89–99.
- BJORKA, J. A., BUTENHOFFB, J. L. & WALLACEA, K. B. 2011. Multiplicity of nuclear receptor activation by PFOA and PFOS in primary human and rodent hepatocytes. *Toxicology*, 288, 8– 17.
- BLOBEL, G. & POTTER, V. R. 1967. Studies on free and membrane-bound ribosomes in rat liver: I. Distribution as related to total cellular RNA. *Journal of Molecular Biology* 26, 279-292.
- BOELSTERLI, U. 2009. Mechanistic Toxicology: Toxicology: The Molecular Basis of How Chemicals Disrupt Biological Targets. 2nd edn (New York: Informa Healthcare). 325, pp. 117-168.
- BRAISSANT, O. & WAHLI, W. 1998. Differential expression of peroxisome proliferator-activated receptor- α , - β , and - γ during rat embryonic development. *Endocrinology*, 139, 2748–2754.
- BRUCE, A., ALEXANDER, J., JULIAN, L., MARTIN, R., KEITH, R. & PETER, W. 2007. *Molecular Biology of the Cell*, 270 madisson avenue, New York, USA, Garland Science.
- BUSTIN, S. A. 2000. Absolute quantification of mRNA using real-time reverse transcription polymerase chain reaction assays. *Journal of molecular endocrinology*, 25(2), 169-193.
- BUSTIN, S. A. & NOLAN, T. 2004. Pitfalls of quantitative real-time reverse-transcription polymerase chain reaction. *Journal of biomolecular techniques* :, *JBT*, 15, 155-166.
- CALDEIRA, K. & WICKETT, M. E. 2005. Ocean model predictions of chemistry changes from carbon dioxide emissions to the atmosphere and ocean. *110(C09S04)*
- CAMPBELL, N., REECE, J., URRY, L., CAIN, M., WASSERMAN, S., MINORSKY, P. & JACKSON, R. 2008. *Biology*, San Fransisco, CA, USA: Pearson Benjamin Cummings.
- CHIRGWIN, J. M., PRZYBYLA, A. E., MACDONALD, R. J. & RUTTE, W. J. 1979. Isolation of biologically active ribonucleic acid from sources enriched in ribonuclease. *Biochemistry* 18, 5294-5299.
- CHOMCZYNSKI, P. & SACCHI, N. 2006. The single-step method of RNA isolation by acid guanidinium thiocyanate-phenol-chloroform extraction: twenty-something years on. *nature protocols*, 1, 581-585.
- CLAIBORNE, J. B., EDWARDS, S. L. & MORRISON-SHETLAR, A. I. 2002. Acid-Base Regulation in Fishes: Cellular and Molecular Mechanisms. *JOURNAL OF EXPERIMENTAL ZOOLOGY*, 293, 302–319.
- CLARK, D. P. 2010. *Molecular Biology*, Update edition edn (Elsevier Inc.). pp 101-102, 655-666.
- COHEN, D. M., LNADA, T., LWAMOTO, T. & SCIALABBA, N. 1990. Gadiform fishes of the world. *Food and Agriculture Organization of the United Nations* 10.
- COX, R. A. 1968. The use of guanidinium chloride in the isolation of nucleic acids. In *Methods in Enzymology*. L. Grossman, K. Moldave, ed. (Academic Press), 12, 120-129.
- CROCKETT, E. L. & SIDELL, B. D. 1993. Substrate selectivities differ for hepatic mitochondrial and peroxisomal beta-oxidation in an Antarctic fish, *Notothenia gibberifrons*. . *The Biochemical journal of Cell Science*, 289 (Pt 2), 427-433.
- DENICOLA, A. & RAFAEL, R. 2005. peroxynitrite and drug-dependent toxicity. *Toxicology* 208 (2005) 208, 273–288.
- DESVERGNE, B. & WAHLI, W. 1999. Peroxisome proliferator-activated receptors: nuclear control of metabolism. *Endocr. Rev.* , 20, 649–688.
- DONGMEI, X., CHANDAN, L., YUEZHONG, W. & WEIPING, L. 2013. Antioxidant defense system responses and DNA damage of earthworms exposed to Perfluorooctane sulfonate (PFOS). *Environmental Pollution* 174, 121-127.
- DORIS, S., BRITA, S., JAMES W, R. & ROBIE W, M. 2007. Interactions between climate change and contaminants. *Marine Pollution Bulletin* 54 1845–1856.

- DORTSA, J., PATRICK, K., PIERRE-ANDRÉ, M., WENDY, D. H., MARIE-LAETITIA, T., MARTINE, R. & FRÉDÉRIC, S. 2011. Ecotoxicoproteomics in gills of the sentinel fish species, *Cottus gobio*, exposed to perfluorooctane sulfonate (PFOS). *Aquatic Toxicology* 103 1–8.
- DOULL, J. & CASARETT 2013. *Casarett and Doull's Toxicology: The Basic Science of Poisons*, New York, McGraw-Hill Education.
- DRAPER, H. H., MCGIRR, L. G. & HADLEY, M. 1986. The Metabolism of Malondialdehyde. *LIPIDS* 21, 305-307.
- DREYER, C., KREY, G., KELLER, H., GIVEL, F., HELFTENBEIN, G. & WAHLI, W. 1992. Control of the peroxisomal β -oxidation pathway by a novel family of nuclear hormone receptors. *Cell* 68, 879–887.
- DRINKWATER, K. F. 2005. The response of Atlantic cod (*Gadus morhua*) to future climate change. *Ices journal of marine science*, 62(7), 1327-1337.
- ESCHER, P., BRAISSANT, O., BASU-MODAK, S., MICHALIK, L., WAHLI, W. & DESVERGNE, B. 2001. Rat PPARs: quantitative analysis in adult rat tissues and regulation in fasting and refeeding. *Endocrinology* 142, 4195–4202.
- ESTERBAUER, H., STRIEGL, G., PUHI, H. & M., R. 1989. Continuous monitoring of in vitro oxidation of human low density lipoprotein. *Free Radic Res Commun* 6, 67-75.
- EVANS, D. H. 1987. The Fish Gill: Site of Action and Model for Toxic Effects of Environmental Pollutants. *Environmental Health Perspectives*, 71, 47-58.
- FATIMA, M., AHMAD, I. I., SAYEED, I. I., ATHAR, M. & RAISUDDIN, S. 2000. Pollutant-induced over-activation of phagocytes is concomitantly associated with peroxidative damage in fish tissues. *Aquat. Toxicol.*, 49, 243–250.
- FLEIGE, S. & PFAFFL, M. W. 2006. RNA integrity and the effect on the real-time qRT-PCR performance. *Molecular Aspects of Medicine* 27, 126–139.
- FORMAN, B. M., JASMINE, C. & RONALD, M. E. 1997. Hypolipidemic drugs, polyunsaturated fatty acids, and eicosanoids are ligands for peroxisome proliferator-activated receptors alpha and delta. *Proc. Natl. Acad. Sci. USA*, 94.
- FORMAN, H. J., FUKUTO, J. M. & TORRES, M. 2004. Redox signaling: thiol chemistry defines which reactive oxygen and nitrogen species can act as second messengers. *Am J Physiol cell physiol*, 287, C246-C256.
- GARRICK, M. D. & GARRICK, L. M. 2009. Cellular iron transport. *Biochimica et biophysica acta* 1790, 309-325.
- GARY, W., WINSTON 1990. OXIDANTS AND ANTIOXIDANTS IN AQUATIC ANIMALS. *Camp. Biochem. Physiol*
- GIULIANI, M. E., REGOLI, F., MAURA, B. & AUGUSTINE, A. 2013. Transcriptional and catalytic responses of antioxidant and biotransformation pathways in mussels, *Mytilus galloprovincialis*, exposed to chemical mixtures. *Aquatic Toxicology* 134– 135, 120–127.
- GULICK, T., CRESCI, S., T, C., MOORE, D. D. & KELLY, D. P. 1994. The peroxisome proliferator-activated receptor regulates mitochondrial fatty acid oxidative enzyme gene expression. *Proc Natl Acad Sci USA*, 91.
- GUNNAR, G. L. 2005. *Statistikk for universiteter og høyskoler*, Oslo, Universitetsforlaget As.
- GUTTERIDGE, J., M.C. 1995. Lipid Peroxidation and Antioxidants as Biomarkers of Tissue Damage. *CLIN. CHEM.* , 41/12, 1819-1 828
- HARADA, K., KOIZUMI, A., SAITO, N., INOUE, K., YOSHINAGA, T., DATE, C., FUJII, S., HACHIYA, N., HIROSAWA, I., KODA, S., KUSAKA, Y., MURATA, K., J, K. O., SHIMBO, S., TAKENAKA, K., TAKESHITA, T., TODORIKI, H., WADA, Y., WATANABE, T. & IKEDA, M. 2007. Historical and

- geographical aspects of the increasing perfluorooctanoate and perfluorooctane sulfonate contamination in human serum in Japan. *Chemosphere*, 66, 293–301.
- HASHIMOTO, F. & HIDENORI, H. 1987. Significance of catalase in peroxisomal fatty acyl-CoA beta-oxidation. *Biochimica et Biophysica Acta* 921 142-150.
- HAUKÅS, M., BERGER, U., HOP, H., GULLIKSEN, B. & GABRIELSEN, G. W. 2007. Bioaccumulation of per- and polyfluorinated alkyl substances (PFAS) in selected species from the Barents Sea food web. *Environ. Pollut.*, 148, 360–371.
- HELMUT, F. V. E. 2008. *Statistics for Terrified Biologists*, Oxford, UK, blackwell publishing Ltd.
- HEUGENS, E. H. W., HENRIKS, A. J., DEKKER, T., VAN STRAALLEN, N. M. & ADMIRAAL, W. 2001. A review on the effects of multiple stressors on aquatic organisms and analysis of uncertainty factors for use in risk assessment. *Critical Review in Toxicology* 31, 247–284.
- HOFF, P. T., DONGEN, W. V., ESMANS, E. L., BLUST, R. & COEN, W. M. D. 2003a. Evaluation of the toxicological effects of perfluorooctane sulfonic acid in the common carp (*Cyprinus carpio*). *Aquatic Toxicology*, 62, 349-359.
- HOFF, P. T., VIJVER, K. V. D., DONGEN, W. V., EDDY.LESSMANS, BLUST, R. & WIM.M.DECOEN 2003b. PERFLUOROCTANE SULFONIC ACID IN BIB (*TRISOPTERUS LUSCUS*) AND PLAICE (*PLEURONECTES PLATESSA*) FROM THE WESTERN SCHELDT AND THE BELGIAN NORTH SEA: DISTRIBUTION AND BIOCHEMICAL EFFECTS. *Environmental Toxicology and Chemistry*, 22, 608–614.
- HOTTA, K., USTAFSON, T. A., YOSHIOKA, S., ORTMEYER, H. K., BODKIN, N. L. & HANSEN, B. C. 1998. Relationships of PPAR α and PPAR β mRNA levels to obesity, diabetes and hyperinsulinaemia in rhesus monkeys. *Int J Obes Relat Metab Disord*, 22, 1000–1010.
- HOUDE, M., MARTIN, J. W., LETCHER, R. J., SOLOMON, K. R. & MUIR, D. C. G. 2006. Biological Monitoring of Polyfluoroalkyl Substances: A Review. *ENVIRONMENTAL SCIENCE & TECHNOLOGY*, 40, 3463-3473.
- HU, W.-Y., JONES, P. D., DECOEN, W., KING, L., FRAKER, P., NEWSTED, J. L. & GIESY, J. P. 2002a. Alterations in cell membrane properties caused by perfluorinated compounds. *Comp. Biochem. Physiol.*, 135, 77–88.
- HU, W.-Y., JONES, P. D., UPHAM, B. L., TROSKO, J. E., LAU, C. & GIESY, J. P. 2002b. Inhibition of gap junctional intercellular communication by perfluorinated compounds in rat liver and dolphin kidney epithelial cell lines in vitro and Sprague-Dawley rats in vivo. *Toxicol. Sci.*, 68, 429–436.
- HU, W., JONES, P. D., CELIUS, T. & GIESY, J. P. 2005. Identification of genes responsive to PFOS using gene expression profiling. *Environmental Toxicology and Pharmacology*, 19, 57–70.
- HU, W., KING, L. E., JONES, P. D. & GIESY, J. P. 2000. Measurement of effects of perfluorinated compounds on cell membrane fluidity by flow cytometry. *Presented at SETAC North America, 21th annual meeting, Nashville, Tennessee*, 12-16.
- HYSLOP, P. A., HINSHAW, D. B. & HALSEY, W. A. I. 1988. Mechanisms of oxidant-mediated cell injury: the glycolytic and mitochondrial pathways of ADP phosphorylation are major intracellular targets inactivated by hydrogen peroxide. *J Biol Chem*, 263, 1665-75.
- IKEDA, T., FUKUDA, K., MORI, L., ENOMOTO, M., KOMAI, T. & SUGA, T. 1987. Peroxisomes in Biology and Medicine. *Springer, New York.*, 304-308.
- INVITROGEN 2008. REAL-TIME PCR: FROM THEORY TO PRACTICE. *Invitrogen corporation*, 3-72.
- IPCC 2011. Workshop Report of the Intergovernmental Panel on Climate Change Workshop on Impacts of Ocean Acidification on Marine Biology and Ecosystems [C. B. Field, V. Barros, T. F. Stocker, D. Qin, K. J. Mach, G.-K. Plattner, M. D. Mastrandrea, M. Tignor and K. L. Ebi (eds.)]. *IPCC Working Group II Technical*

Support Unit, Carnegie Institution, Stanford, CA, USA.

- IPCC, F. A. R. 2013. Climate Change 2013 (AR5) Chapter 3: Ocean acidification.
- ISSEMANN, I. & GREEN, S. 1990a. Activation of a member of the steroid hormone receptor superfamily by peroxisome proliferators. *Nature*, 347, 645–650.
- ISSEMANN, I. & GREEN, S. 1990b. Activation of a member of the steroid hormone receptor superfamily by peroxisome proliferators. *Nature*, 347, 645–650.
- JEON, J., LIM, H. K., KANNAN, K. & KIM, S. D. 2010. Effect of perfluorooctanesulfonate on osmoregulation in marine fish, *Sebastes schlegeli*, under different salinities. *Chemosphere*, 81, 228–234.
- JOHNSON, J. D., GIBSON, S. J. & OBER, R. E. 1984. Cholestyramine enhanced fecal elimination of carbon-14 in rats after administration of ammonium [¹⁴C]perfluorooctanoate or potassium [¹⁴C]perfluorooctanesulfonate. *Appl. Toxicol*, 4, 972-976.
- JONATHAN, D., TUGWOOD, ISABELLE, I., ROSEMARY, G., ANDERSON, KENNETH, R., BUNDELL, WILLIAM, L., MCPHEAT & STEPHEN, G. 1992. The mouse peroxisome proliferator activated receptor recognizes a response element in the 5' flanking sequence of the rat acyl CoA oxidase gene. *The EMBO Journal*, 11, 433-439.
- JURGEN, M. L., STEVEN, A. K., SCOTT, S. S., JONES, S. A., PETER, J. B., WISELY, G. B., CECILIA, S. K., PALLAVI, D., WALTER, W., TIMOTHY, M. W., LENHARD, J. M. & 1997. Fatty acids and eicosanoids regulate gene expression through direct interactions with peroxisome proliferator-activated receptors alpha and gamma. *Proc. Natl. Acad. Sci. USA*, 94, 4318–4323.
- KANNAN, K., CORSOLINI, S., FALANDYSZ, J., OEHME, G., FOCARDI, S. & GIESY, J. P. 2002. Perfluorooctanesulfonate and related fluorinated hydrocarbons in marine mammals, fishes, and birds from coasts of the Baltic and the Mediterranean Seas. *Environmental science & technology*, 36, 3210-3216.
- KANNAN, K. & JOHN, P. G. 2001. Global Distribution of Perfluorooctane Sulfonate in Wildlife. *Environ. Sci.*, 25, 1339-1342.
- KANNAN, K., TANIYASU, S., HORII, Y., HANARI, N. & YAMASHITA, N. 2003. A survey of perfluorooctane sulfonate and related perfluorinated organic compounds in water, fish, birds, and humans from Japan. *Environmental science & technology*, 37, 2634-2639.
- KELLY, B. C., IKONOMOU, M. G., BLAIR, J. D., SURRIDGE, B., HOOVER, D., GRACE, R. & GOBAS, F. A. P. C. 2009. Perfluoroalkyl contaminants in an Arctic marine food web: trophic magnification and wildlife exposure. *Environmental science & technology*, 43(11), 4037-43.
- KENNETH, D., JAMES R, C., STEINER, N., PO'RTNER, H.-O. & NOJIRI, Y. 2011. Potential impacts of future ocean acidification on marine ecosystems and fisheries: current knowledge and recommendations for future research. *ICES Journal of Marine Science* 68(6), 1019–1029.
- KHATIWALA, S. 2013. Global ocean storage of anthropogenic carbon. *Biogeosciences*, 10, 2169–2191.
- KIKKAWA, T. & KITA, J. A. I. 2004. Comparison of the lethal effect of CO₂ and acidification on red sea bream (*Pagrus major*) during the early developmental stages. *Marine Pollution Bulletin* 48, 108-110.
- KIM, J. J. & MIURA, R. 2004. Acyl-CoA dehydrogenases and acyl-CoA oxidases. Structural basis for mechanistic similarities and differences. *European journal of biochemistry /FEBS* 271, 483-493.
- KLEYPAS, J. A., RICHARD A. FEELY, FABRY, V. J., CHRIS LANGDON & LISA L. ROBBINS 2006. Impacts of Ocean Acidification on Coral Reefs and Other Marine Calcifiers: A Guide for Future Research. *NOAA/Pacific Marine Environmental Laboratory*, 2897.

- KRØVEL, A. V., SØFTELAND, L., TORSTENSEN, B. & OLSVIK, P. A. 2008. Transcriptional effects of PFOS in isolated hepatocytes from Atlantic salmon *Salmo salar* L. *Comparative Biochemistry and Physiology, Part C*, 148, 14-22.
- LANGENBUCH, M. & PÖRTNER, H. O. 2003. Energy budget of hepatocytes from Antarctic fish (*Pachycara brachycephalum* and *Lepidonotothen*) as functions of ambient CO₂: pH-dependent limitations of cellular protein biosynthesis. *The Journal of Experimental Biology* 206, 3895-3903.
- LANGENBUCH, M. P. H. O. 2002. Changes in metabolic rate and N excretion in the marine invertebrate *Sipunculus nudus* under conditions of environmental hypercapnia: identifying effective acid-base variables. *Journal of Experimental Biology* 205, 1153-1160.
- LEHMLER, H.-J. 2005. Synthesis of environmentally relevant fluorinated surfactants—a review. *Chemosphere*, 58, 1471–1496.
- LEHMLER, H. J., XIE, W., BOTHUN, G. D., BUMMER, P. M. & B.L, K. 2006. Mixing of perfluorooctanesulfonic acid (PFOS) potassium salt with dipalmitoyl phosphatidylcholine (DPPC). *Colloids Surf B Biointerfaces*, 51(1), 25–9.
- LESSER, M. P. 2006. OXIDATIVE STRESS IN MARINE ENVIRONMENTS: Biochemistry and Physiological Ecology. *Annu. Rev. Physiol*, 68, 253–278.
- LIU, C., YU, K., SHI, X., WANG, J., LAM, P. K. S., WU, R. S. S. & ZHOU, B. 2007. Induction of oxidative stress and apoptosis by PFOS and PFOA in primary cultured hepatocytes of freshwater tilapia (*Oreochromis niloticus*). *Aquatic Toxicology*, 82, 135-143.
- LIU, Y., WANG, J., YANHONG, W., HONGXIA, Z., MUQI, X. & JIAYIN, D. 2008. Induction of time-dependent oxidative stress and related transcriptional effects of perfluorododecanoic acid in zebrafish liver. *Aquatic Toxicology* 89, 242–250.
- LOPEZ-TORRES, M., PEREZ-CAMPO, R., CADENAS, S., ROJAS, C. & BARJA, G. 1993. A COMPARATIVE STUDY OF FREE RADICALS IN VERTEBRATES--II. NON-ENZYMATIC ANTIOXIDANTS AND OXIDATIVE STRESS. *Comp, Biochem. Physiol*, 105B, 757-763.
- LORENTZEN, K. 2013. *Cellular Lipid Homeostasis and Oxidative Stress Responses in the Liver of Atlantic Cod (Gadus morhua) Exposed to a Quantifiable Measure of Climate Change (CO₂) and Perfluorooctane Sulfonate (PFOS)*. master, Norwegian University of Science and Technology.
- MANDARD, S., MÜLLER, M. & KERSTEN, S. 2004. Peroxisome proliferator-activated receptor alpha target genes. *CMLS, Cell. Mol. Life Sci*, 61, 393–416.
- MANGELSDORF, D. J., THUMMEL, C., BEATO, M., HERRLICH, P., SCHIIT, G., UMESONO, K., BLUMBERG, B., KASTNER, P., MARK, M., CHAMBON, P. & EVAN, R. M. 1995. The Nuclear Receptor Superfamily: The Second Decade. *cell*, 83, 835-839.
- MANNAERTS, G. P. & VAN VELDHOVEN, P. P. 1993. Metabolic role of mammalian peroxisomes. In: Gibson G, Lake B (eds) *Peroxisomes: Biology and Importance in Toxicology and Medicine*. Taylor & Francis, London, 19–62.
- MARTIN, J. W., MABURY, S. A., SOLOMON, K. R. & MUIR, D. C. G. 2003. Bioconcentration and tissue distribution of perfluorinated acids in rainbow trout (*oncorhynchus mykiss*). *Environmental Toxicology and Chemistry*, 22, No. 1, 196–204
- MARTIN, J. W., MUIR, D. C. G., MOODY, C. A., ELLIS, D. A., KWAN, W. C., SOLOMON, K. R. & MABURY, S. A. 2002. Collection of Airborne Fluorinated Organics and Analysis by Gas Chromatography/Chemical Ionization Mass Spectrometry. *Anal. Chem*, 74, 584-590.
- MICHALIK, L., JOHAN, A., JOEL, P. B., KRISHNA, C., V, CHRISTOPHE, R. K. G., FRANK, J. G., PAUL, A. G., TAKASHI, K., MITCHEL, A. L., STEPHEN, O. R., COLIN, N. A. P., JORGE, P., JANARDAN, K. R.,

- BRUCE, M. S., BART, S. & WALTER, W. 2006. International Union of Pharmacology. LXI. Peroxisome
- Proliferator-Activated Receptors. *Pharmacol Rev*, 58, 726–741.
- MITCHELL, B. R., CHRISTOPHER, L. & CHRISTOPHER, J. C. 2009. Does Exposure to Perfluoroalkyl Acids Present a Risk to Human Health? *TOXICOLOGICAL SCIENCES*, 111(1), 1–3.
- MIZUKAMI, J. & TANIGUCHI, T. 1997. The antidiabetic agent thiazolidinedione stimulates the interaction between PPAR gamma and CBP
Biochem Biophys Res Commun 240, 61–64.
- MORTENSEN, A. S., ROBERT, J. L., MARIA, V. C., SHAOGANG, C. & AUGUSTINE, A. 2011. Tissue bioaccumulation patterns, xenobiotic biotransformation and steroid hormone levels in Atlantic salmon (*Salmo salar*) fed a diet containing perfluoroactane sulfonic or perfluorooctane carboxylic acids. *Chemosphere* 83 1035–1044.
- NELSON, D. L. & COX, M. M. 2008. *Lehninger Principles of Biochemistry*, New York: W.H. Freeman.
- NOYES, P. D., MCELWEE, M. K., MILLER, H. D., CLARK, B. W., VAN TIEM, L. A., WALCOTT, K. C., ERWIN, K. N. & LEVIN, E. D. 2009. The toxicology of climate change: Environmental contaminants in a warming world. *Environment international*, 35(6), 971-986.
- OAKES, K. D., SIBLEY, P. K., MARTIN, J. W., MACLEAN, D. D., SOLOMON, K. R., MABURY, S. A. & VAN DER KRAAK, G. 2005. Short-term exposures of fish to perfluorooctane sulfonate: acute effects on fatty acyl-CoA oxidase activity, oxidative stress, and circulating sex steroids. *Environ. Toxicol. Chem*, 24, 1172–1181.
- OECD 2002. Co-operation on existing chemicals — hazard assessment of perfluorooctane sulfonate and its salts. Environment Directorate Joint Meeting of the Chemicals Committee and the Working Party on Chemicals, Pesticides and Biotechnology (ENV/JM/RD(2002)17/FINAL). *Organisation for Economic Cooperation and Development, Paris*.
- OLIVERO-VERBEL, J., TAO, L., JOHNSTON-RESTREPO, B., GUETTE-FERNANDEZ, J., BALDIRIS-AVILA, R., O'BYRNE-HOYOS, I. & KANNAN, K. 2006. Perfluorooctanesulfonate and related fluorochemicals in biological samples from the north coast of Colombia. *Environ. Pollut.*, 142, 367–372.
- OLSVIK, P. A., LIE, K. K., GOKSOYR, A., MIDTUN, T., FRANTZEN, S. & MAAGE, A. 2009. Are Atlantic cod in Store Lungegardsvann, a seawater recipient in Bergen, affected by environmental contaminants? A qRT-PCR survey. *Journal of toxicology and environmental health Part A*, 72, 140-154.
- OSMUNDSEN, H., BREMER, J. & PEDERSEN, J. I. 1991. Metabolic aspects of peroxisomal betaoxidation. *Biochimica et biophysica acta* 1085, 141-158.
- PABON, M. & CORPART, J. M. 2002. Fluorinated surfactants: synthesis properties effluent treatment. *Journal of Fluorine Chemistry*, 114, 149–156.
- PARIHAR, M. S., DUBEY, A. K., TARANGINI, J. & PREM, P. 1996. Changes in lipid peroxidation, superoxide dismutase activity, ascorbic acid and phospholipid content in liver of freshwater catfish heteroz'neustes i; ossilis exposed to elevated temperature. *J. rherm. Biol*, 21, 323-330.
- PAUL, A. G., JONES, K. C. & SWEETMAN, A. J. 2008. A First Global Production, Emission, And Environmental Inventory For Perfluorooctane Sulfonate. *Environ. Sci. Technol*, 43, , 386–392.
- PAWERT, M., MOILER, E. & TRIEBSKORN, R. 1998 Ultrastructural changes in fish gills as biomarker to assess small stream pollution. *Tissue & Cell*, 30 (6) 617-626.
- PFAFFL, M. V. 2004. Quantification strategies in real-time PCR. In A-Z of quantitative PCR. S.A. Bustin, ed (La Jolla, CA, USA: International University Line), pp. 87-112.

- PORTNER, H. O., LANGENBUCH, M. & REIPSCHLÄGER, A. 2004. Biological Impact of Elevated Ocean CO₂ Concentrations: Lessons from Animal Physiology and Earth History. *Journal of Oceanography*, 60, 705-718.
- PORTNER, H. O., REIPSCHLÄGER, A. & HEISLER, N. 1998. ACID-BASE REGULATION, METABOLISM AND ENERGETICS IN SIPUNCULUS NUDUS AS A FUNCTION OF AMBIENT CARBON DIOXIDE LEVEL. *The Journal of Experimental Biology* 201, 43-55.
- PORTNER, H. O., BERDALB, B., BLUSTC, R., BRIXB, O., COLOSIMOD, A., WACHTERC, B. D., GIULIANID, A., JOHANSENE, T., FISCHERA, T., KNUSTA, R., LANNIGA, G., NAEVDALE, G., NEDENESB, A., NYHAMMERE, G., SARTORISA, F. J., SERENDEROA, I., P. SIRABELLAD, THORKILDSEN, S. & ZAKHARTSEV, M. 2001. Climate induced temperature effects on growth performance, fecundity and recruitment in marine fish: developing a hypothesis for cause and effect relationships in Atlantic cod (*Gadus morhua*) and common eelpout (*Zoarces viviparus*). *Continental Shelf Research* 21, 1975-1997.
- POTERA, C. 2010. Will Ocean Acidification Erode the Base of the Food Web? *Environmental Health Perspectives*, 118, A157.
- PRETTI, C., SIMON, N., LONGO, V. & GERVASI, P. G. 1999. Effect of clofibrate, a peroxisome proliferator, in sea bass (*Dicentrarchus labrax*), a marine fish. *Environ. Res.*, 80 294-296.
- RAES, M., MICHIELS, C. & REMACLE, J. 1987. Comparative study of the enzymatic defense systems against oxygen-derived free radicals: the key role of glutathione peroxidase. *Free radical biology & medicine*, 3, 3-7.
- RAFAEL, R., GONZALO, P., MARÍA, N. A., MERCEDES, N. & ALFONSO, C. 2001. Unraveling peroxynitrite formation in biological systems. *Free Radical Biology & Medicine* 30, 463-488.
- RAJNAUTH, J. 2013. A Proposed Workflow for Disposal of Carbon Dioxide using Carbon Dioxide Hydrate *The Journal of the Association of Professional Engineers of Trinidad and Tobago* 41, No.1, 18-22.
- REGOLI, F., GIULIANI, M. E., BENEDETTI, M. & ARUKWE, A. 2011. Molecular and biochemical biomarkers in environmental monitoring: a comparison of biotransformation and antioxidant defense systems in multiple tissues. *Aquatic Toxicology* 105, 56-66.
- REIPSCHLAGER, A. & PÖRTNER, H. O. 1996. METABOLIC DEPRESSION DURING ENVIRONMENTAL STRESS: THE ROLE OF EXTRACELLULAR VERSUS INTRACELLULAR PH IN SIPUNCULUS NUDUS. *The Journal of Experimental Biology* 199, 1801-1807.
- RENNER, R. 2001. Growing evidence of toxic effects and environmental impacts has sent researchers scrambling to obtain more data. *ENVIRONMENTAL SCIENCE & TECHNOLOGY*, 154A-160A.
- SABINE, C. L. 2004. The oceanic sink for anthropogenic CO₂. *Science*, 305, 367-371.
- SEACAT, A. M., THOMFORD, P. J., HANSEN, K. J., CLEMEN, L. A., ELDRIDGE, S. R., ELCOMBE, C. R. & BUTENHOFF, J. L. 2003. Sub-chronic dietary toxicity of potassium perfluorooctane sulfonate in rats. *Toxicology*, 183, 117-131.
- SIES, H. 1997. OXIDATIVE STRESS: OXIDANTS AND ANTIOXIDANTS. *Experimental Physiology*, 82, 291-295.
- SIPLE, D. M. & MURPHY, R. F. 1991. Binding to Cellular Receptors results in Increased Iron Release from Transferrin at Mildly Acidic pH. *The Journal of Biological Chemistry*, 266, 8002-8007.
- SIU, G. M. & DRAPER, H. H. 1982. Metabolism of malonaldehyde in vivo and in vitro. *Lipids* 17, 349-355.

- SOHLENIUS, A. K., ERIKSSON, A. M., HOGSTROM, C., KIMLAND, M. & DEPIERRE, J. W. 1993. Perfluorooctane sulfonic acid is a potent inducer of peroxisomal fatty acid beta-oxidation and other activities known to be affected by peroxisome proliferators in mouse liver. *Pharmacol. Toxicol.*, 72, 90-93.
- SOKOL, R. J., STRAKA, M. S., DAHL, R., DEVEREAUX, M. W., YERUSHALMI, B. & GUMPRICH, E. 2001. Role of oxidant stress in the permeability transition induced in rat hepatic mitochondria by hydrophobic bile acids. *Pediatr. Res*, 49, 519-531.
- SQUADRITO, G. L. & PRYOR, W. A. 1998. oxidative chemistry of nitric oxide: the roles of superoxide, peroxynitrite, and carbon dioxide. *Free Radical Biology & Medicine*, 25, 392-403.
- STARKOV, A. A. & WALLACE, K. B. 2002. Structural determinants of fluorochemical-induced mitochondrial dysfunction. *Toxicol. Sci.*, 66, 244-252.
- STOREY, K. B. 1996. Oxidative stress: animal adaptations in nature. *Brazilian journal of medical and biological research*, 29, 1715-1733.
- TACHIBANA, K., KOBAYASHI, Y., TANAKA, T., TAGAMI, M., SUGIYAMA, A., KATAYAMA, T., UEDA, C., YAMASAKI, D., ISHIMOTO K & SUMITOMO, M. 2005. Gene expression profiling of potential peroxisome proliferator-activated receptor (PPAR) target genes in human hepatoblastoma cell lines inducibly expressing different PPAR isoforms. *Nuclear Receptor* 3 3.
- TAKACS, M. L. & ABBOTT, B. D. 2007a. Activation of Mouse and Human Peroxisome Proliferator-Activated Receptors (a, b/d, c) by Perfluorooctanoic Acid and Perfluorooctane Sulfonate. *TOXICOLOGICAL SCIENCES*, 95(1), 108-117.
- TAKACS, M. L. & ABBOTT, B. D. 2007b. Activation of Mouse and Human Peroxisome Proliferator-Activated Receptors (a, b/d, c) by Perfluorooctanoic Acid and Perfluorooctane Sulfonate. *Toxicological sciences* 95(1), 108-117
- TANAKA, T., YAMAMOTO, J., IWASAKI, S., ASABA, H., HAMURA, H., IKEDA, Y., M, W., MAGOORI, K., IOKA, R. X. & TACHIBANA, K. 2003. Activation of peroxisome proliferator-activated receptor d induces fatty acid beta-oxidation in skeletal muscle and attenuates metabolic syndrome. *PNAS* 100, 15924-15929.
- TOMMY, G. T., BUDAKOWSKI, W., HALLDORSON, T., HELM, P. A., STERN, G. A., FRIESEN, K., PEPPER, K., TITTEMIER, S. A. & FISK, A. T. 2004a. Fluorinated organic compounds in an eastern Arctic marine food web. *Environmental science & technology*, 38(24), 6475-81.
- TOMMY, G. T., TITTEMIER, S. A., PALACE, V. P., BUDAKOWSKI, W. R., BRAEKEVELT, E., BRINKWORTH, L. & FRIESEN, K. 2004b. Biotransformation of N-ethyl perfluorooctanesulfonamide by rainbow trout (*Onchorhynchus mykiss*) liver microsomes. *Environmental science & technology*, 38(3), 758-62.
- TOWLE, D. W. & WEIHRAUCH, D. 2001. Osmoregulation by gills of euryhaline crabs: Molecular analysis of transporters. *American Zoologist*, 414, 770-780.
- TSENG, C. L., LIU, L. L., CHEN, C. M. & DING, W. H. 2006. Analysis of perfluorooctanesulfonate and related fluorochemicals in water and biological tissue samples by liquid chromatography-ion trap mass spectrometry. *J. Chromatogr, A*, 1105, 119-126.
- UNITED NATIONS STATISTICS DIVISION 2010. 2010 World Population and Housing Census Programme. . 300 East 42nd Street Room IN-927A New York, NY 10017, USA: United Nations.
- VESELA, A. & WILHELM, J. 2002. The role of carbon dioxide in free radical reactions of the organism. *Physiological research / Academia Scientiarum Bohemoslovaca* 51, 335-339.
- VIDAL-PUIG, A., JIMENEZ-LINAN, M., LOWELL, B. B., A, H., HU, E., SPIEGELMAN, B., FLIER, J. S. & MOLLER, D. E. 1996. Regulation of PPAR γ gene expression by nutrition and obesity in rodents. *J Clin Invest*

97, 2553–2561.

WANIA, F. 2007. A Global Mass Balance Analysis of the Source of Perfluorocarboxylic Acids in the Arctic Ocean. *Environmental science & technology*, 41, 4529-4535.

WEI, Y., SHI, X., ZHANG, H., WANG, J., ZHOU, B. & DAI, J. 2010. Combined effects of polyfluorinated and perfluorinated compounds on primary cultured hepatocytes from rare minnow (*Gobiocypris rarus*) using toxicogenomic analysis. *Aquat Toxicol. Sci.*, 95, 27–36.

WENDELAAR, B. S. & LOCK, R. 2008. The osmoregulatory system. In: Di Giulio RT, Hinton DE, eds. *The toxicology of fishes.*, 401-406.

WINSTON, G. W. & DI GIULIO, R. T. 1991. Prooxidant and antioxidant mechanisms in aquatic organisms. *Aquatic Toxicology* 9, 137-161.

WÅGBØ, A. M., MARIA, V. C., NICOLA, C., ROBERT, J. L. & AUGUSTINE, A. 2012. Perfluorooctane Sulfonamide-Mediated Modulation of Hepatocellular Lipid Homeostasis and Oxidative Stress Responses in Atlantic Salmon Hepatocytes. *Chem. Res. Toxicol*, 25, 1253–1264.

ZHANG, X., CHEN, L., FEI, X.-C., MA, Y.-S. & GAO, H.-W. 2009. Binding of PFOS to serum albumin and DNA: insight into the molecular toxicity of perfluorochemicals. *BMC Molecular Biology*, 1-12.

Appendix

Appendix A: Reagents used for gel electrophoresis

Table A1: 10 x MOPS used in preparation of gels and buffers.

MOPS	41.86 g
EDTA	(0.2 M) 25 mL
DEPC-treated MilliQ water	475 mL
Adjusted to pH = 7.0 with NaOH	
Autoclaved (121°C, 20 min)	
<hr/>	
Total	500mL

Table A2: Sample buffer.

Deionized formamide	250 µL
10 x MOPS	50 µL
37% formaldehyde	83 µL
DEPC treated Milli-Q water	57 µL
Glycerol	50 µL
<hr/>	
Total	(490 µL)

Table A3: 1% agarose gel with formaldehyde

Agarose	1.0 g
10 x MOPS	10 mL
DEPC treated Milli-Q water	87 mL
Formaldehyde (37%)	5.1 mL
GelRed	10 μ L

Table A4: 1% agarose gel

Agarose	1.0 g
1 x TAE	100 mL
GelRed	10 μ L

Table A5: 50x TAE

Tris base	242 g
Glacial acetic acid	57.1 mL
EDTA (0.5 M, pH 8.0)	100 mL
MilliQ water	1 L
Autoclaved (121°C, 20 min)	

Total	(1 L)
-------	-------

Table A6: Running buffer

10 x MOPS	20 mL
DEPC-treated MilliQ water	225 mL
Formaldehyde (37%)	5 mL

Total	250mL
-------	-------

Appendix B: Reagents used for biochemical analysis

Reagents (and their recipes) used in assays for enzyme activity and total content of glutathione and malondialdehyde are given in table B1.

Table B1: Reagents used in biochemical assays

<u>Reagent</u>	<u>Recipes</u>
Bacitracin	100 mg/mL Dissolve 100 mg bacitracin in 1 mL dH ₂ O
CDNB, 50 mM	Dissolve 0.0506 g CDNB in 5 mL methanol
CHP, 200 mM	Add 37 μ L CHP 5.2 M to 963 mL methanol
DTNB, 20 mM	Dissolve 0.07962 g DTNB in 10 mL methanol
DTT 100 mM	Dissolve 0.01542 g DTT in 1 mL methanol
EDTA, 100 mM	Dissolve 3.7224 g EDTA in 100 mL dH ₂ O

GSH, 100 mM	Dissolve 0.0307 g GSH in 1 mL dH ₂ O
GSSG, 10 mM	Dissolve 0.006566 g GSSG in 1 mL dH ₂ O
H ₂ O ₂ , 1.2 M	Add 100 μL H ₂ O ₂ 12 M to 900 μL dH ₂ O
Homogenizing buffer	100 mL Tris-HCL buffer, 100 μL 100 mM PMSF, 100 μL 100 mg/mL bacitracin, and 1.8 g NaCl
K-phosphate buffer, 100 mM	Dissolve 1.36 g KH ₂ PO ₄ in 100 mL dH ₂ O. Adjust pH.
NaCl, 1.8 %	Dissolve 1.8 g NaCl in 100 mL buffer
NADPH, 1 mg/mL	Dissolve 1 mg NADPH in 1 mL dH ₂ O
NADPH, 4 mg/mL	Dissolve 4 mg NADPH in 1 mL dH ₂ O
NADPH, 20 mg/mL	Dissolve 2 mg NADPH in 100 μL dH ₂ O
PMSF, 100 mM	Dissolve 0.174 g PMSF in 10 mL methanol
Tris-HCL buffer, 100 mM	Dissolve 1.211 g C ₄ H ₁₁ NO ₃ in 100 mL dH ₂ O, adjust pH.

Appendix C: Real-time PCR calibration curve

The calibration curve used for normalization of real-time PCR data was prepared by making a dilution series of plasmids containing *gadus morhua cyp19* gene followed by PCR amplification. $Y = -4.372 \cdot \log(X) + 13.09$, was derived from standard curve.

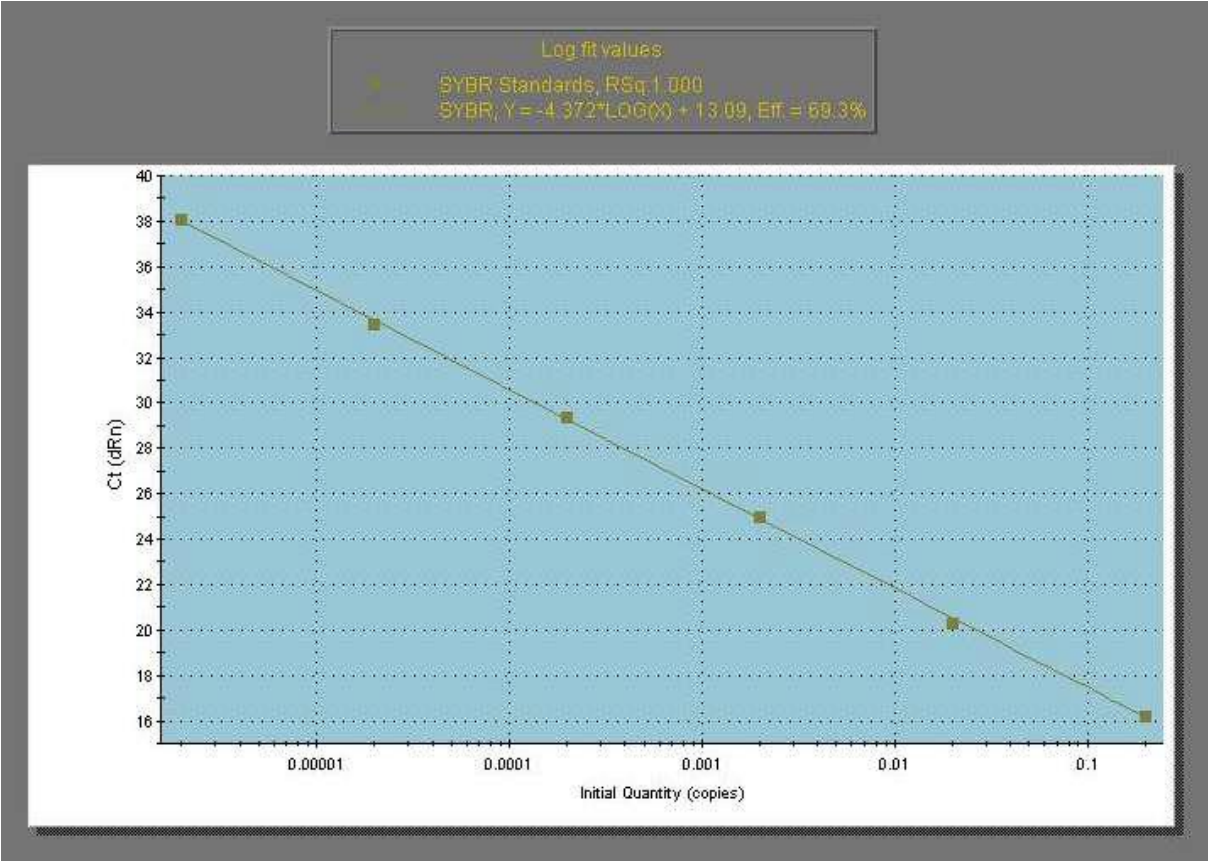


Figure C1: Calibration curve for normalization of real-time PCR data.